Available online at www.sciencedirect.com

ScienceDirect

Surface Science Reports 69 (2014) 325–365

surface science reports

www.elsevier.com/locate/surfrep

The debate on the dependence of apparent contact angles on drop contact area or three-phase contact line: A review

H. Yildirim Erbil

Gebze Institute of Technology, Department of Chemical Engineering, Gebze 41400, Kocaeli, Turkey

Received 28 April 2014; received in revised form 31 August 2014; accepted 10 September 2014

Abstract

A sessile drop is an isolated drop which has been deposited on a solid substrate where the wetted area is limited by the three-phase contact line and characterized by contact angle, contact radius and drop height. Although, wetting has been studied using contact angles of drops on solids for more than 200 years, the question remains unanswered: Is wetting of a rough and chemically heterogeneous surface controlled by the interactions within the solid/liquid contact area beneath the droplet or only at the three-phase contact line? After the publications of Pease in 1945, Extrand in 1997, 2003 and Gao and McCarthy in 2007 and 2009, it was proposed that advancing, receding contact angles, and contact angle hysteresis of rough and chemically heterogeneous surfaces are determined by interactions of the liquid and the solid at the three-phase contact line alone and the interfacial area within the contact perimeter is irrelevant. As a consequence of this statement, the well-known Wenzel (1934) and Cassie (1945) equations which were derived using the contact area approach are proposed to be invalid and should be abandoned. A hot debate started in the field of surface science after 2007, between the three-phase contact line and interfacial contact area approach defenders. This paper presents a review of the published articles on contact angles and summarizes the views of the both sides. After presenting a brief history of the contact angles and their measurement methods, we discussed the basic contact angle theory and applications of contact angles on the characterization of flat, rough and micropatterned superhydrophobic surfaces. The weak and strong sides of both three-phase contact line and contact area approaches were discussed in detail and some practical conclusions were drawn.
© 2014 Elsevier B.V. All rights reserved.

Keywords: Contact angles; Wenzel equation; Cassie equation; Contact area; Three-phase contact line

Contents

E-mail address: yerbil@gyte.edu.tr

http://dx.doi.org/10.1016/j.surfrep.2014.09.001
0167-5729/© 2014 Elsevier B.V. All rights reserved.

1. Introduction

Wetting refers to the study of macroscopic manifestations of intermolecular interactions between contacting liquids and solids. Wetting usually deals with the three phases of materials: solid; liquid and gas. A liquid drop forms at the solid/liquid/gas (or immiscible another liquid) interline having a contact angle (θ) as a result of the balance of the intermolecular interactions between solid and liquid [1–5]. If the cohesive forces between the liquid molecules are stronger than the adhesive forces between the solid and liquid molecules, then the liquid balls up and tend to avoid contact with the surface. Conversely, if the solid/liquid adhesion is much stronger than the cohesion within the liquid molecules, then no drop forms and the liquid spreads on the surface.

Contact angle is the tangent of the drop profile at the triple point (three-phase contact point) where the liquid–gas interface meets the solid–liquid interface as seen in Fig. 1 and it provides an inverse measure of wettability. A contact angle less than 90° indicates that wetting of the surface with the liquid is favorable, and if $\theta < 10^\circ$ then the liquid will spread over a large area of the surface, however if $\theta > 90^\circ$, it means that wetting of the surface is unfavorable. The use of contact angles and quantification of the wetting phenomena is pertinent to chemical, food, cosmetics industries, life sciences, soil, botany and nanotechnology [1–5].

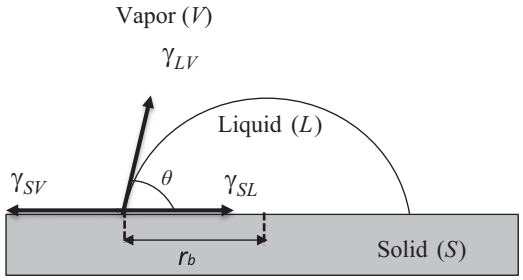

Fig. 1. Profile of a drop of liquid on a solid surface. Contact angle, contact radius and three interfacial tensions, γ, between solid, liquid, vapor phases.

The value of a contact angle on an ideal surface which is atomically flat and chemically homogenous was described in quantitative terms by Young's equation which was given in 1805 without proof [6], relating the contact angle to the three interfacial tensions involved: solid/vapor, liquid/vapor, and solid/liquid. The well-known relation of contact angle to the "work of adhesion" was developed by Dupré in 1869 [7], on the basis of the earlier work of Young. The units of interfacial tension is N/m (force per unit length) and interfacial free energy is J/m^2 (energy per unit area) and most of the surface scientists have been taught that these units and concepts can be used interchangeably although this is not the case in strict thermodynamic terms [4]. There would be no problem with the duality of force per unit length and energy per unit area units if the contact angles are determined on ideal surfaces where perfect spherical cap geometry is obeyed, however finding such an atomically flat and chemically homogenous ideal surface is nearly impossible and all the practical surfaces deviate from ideality. Actually, when a sessile droplet is placed on a substrate the solid/liquid interface advances to a certain area and the three-phase contact line advances to a certain length rapidly and stops with an apparent contact angle that depends on the roughness, chemical heterogeneity of the surface and also on the chemical, physical properties of the liquid. However, one of the most fundamental questions which remain unanswered in the surface science still holds: is wetting controlled by interactions through the total solid/liquid contact area or only at the three-phase contact line (solid/liquid/gas) formed around the droplet?

Surface free energy is always related with the contact area, but Young did not know this concept because it was not invented during his time. Lord Rayleigh noted that Gauss was

the first to introduce the surface energy concept. Gauss proposed that the existence of attractive forces leads of necessity to a term in the expression of the potential energy proportional to the surface area of the liquid so that a liquid surface tends always to contract and exercises a tension [8]. Boltzmann showed that if a liquid can be deformed without change in the total area of a surface, the potential energy necessarily remains unaltered; but if there is a change of the total area, the variation of potential energy must be proportional to such change [9]. However, some scientists objected to the surface area–energy relationship in old days: Lord Kelvin pointed out that we usually interpret the contraction of a liquid droplet into spherical shape is the sole result of the specific surface area minimization process however, it may be possible that the final spherical form is the result of the parts (molecules) to get as near to one another by the action of cohesive forces since this also resulted in a spherical shape by close packing of molecules [8,10]. Although original, this view cannot be improved into a working theory and was forgotten.

One hundred and forty years passed after Young's equation without a dispute on the choice of the use of contact area or contact line to determine the value of contact angles and a debate started on this matter with the pioneering publication of Pease in 1945 [11]. Later, Extrand in 2003 [12] and McCarthy and co-workers in 2007 [13] published two important papers on the subject and they proposed that (force per unit length) gives a much more intuitive meaning and contact angle behavior (advancing, receding contact angles, and contact angle hysteresis) is determined by interactions of the liquid and the solid at the three-phase contact line alone and the interfacial area within the contact perimeter is irrelevant. McCarthy paper was specifically designed to present an experimental proof of the problem [13]. Later, a hot debate was started between the surface scientists on the validity and use of the well-known Wenzel [14,15] and Cassie [16,17] equations which were derived using the solid/liquid contact area approach and around 300 papers were published on this matter after 2007 to date resulting in more than 2000 citations. Unfortunately, still there is no universal agreement on the underlying physicochemical mechanisms of contact angles although wetting has been studied for more than 200 years. However, it is important to clarify this problem before progressing in the surface science since the superhydrophobic and superolephobic surfaces are very popular subjects in both industry and academia in the last decade and the characterization of these surfaces by using contact angles is especially problematic since the presence of the air pockets on irregular rough surfaces (or specific patterns) cause very high contact angle values. The application of contact angles to nano-rough surfaces is another recent issue in nanotechnology area awaiting clarification which is directly related with the above contact area/line problem.

This review will present the up-to-date publications on this topic and summarize the views of the both sides, i.e. three-phase contact line and solid/liquid contact area defenders. A brief history of contact angles, summary of contact angle measurement methods, industrial and academic applications of contact angles and the importance of the McCarthy publication in 2007 [13] will be given in Section 1. The classical contact angle theory including the derivation of Young's equation from the vectorial balance of interfacial tension forces and also from interactions between solid/liquid interfacial area; contact angle hysteresis; solid surface tension calculations from contact angles; and line tension concept are given in Section 2. The debate on this problem after 2007 will be given by reviewing the publications in chronological order which support the three-phase contact line approach in Section 3; and interfacial contact area approach in Section 4. Finally, the validity of Wenzel and Cassie–Baxter equations (and states) will be discussed in Section 5 without considering the chronology or priority matters. The weak and strong sides of both the contact line and contact area approaches were discussed in detail and some practical conclusions were drawn on applications of contact angles for the characterization of flat, rough, heterogeneous and superhydrophobic surfaces.

1.1. Brief history of contact angles

Probably Galileo was the first to recognize the wetting phenomena who noticed that when a dense flat, thin solid was floating on water, the top of the solid was below the surface level of water and comment on spreading and wetting in 1612 [18]. Contact angle equation on ideal surfaces was first introduced by Young in 1805 (he expressed his equation clearly in words without proof) [6], and Dupré gave the Young equation in his book, in relation with work of adhesion in 1869 [7]. Worthington was the first to investigate the shape of pendant drops in 1881 by using an Argand lamp (a home lighting oil lamp) and the magnified image of the drop was thrown by a lens upon a piece of white paper fixed on the wall of the room and the profile of the drop was recorded with a finely-pointed lead pencil for further use [19]. He pointed out that Guthrie's work inspired him who examined the effect of density, nature of liquid and dropping solid on the size of the final drops in 1864 [20]. Worthington did not directly measure the contact angles by forming tangents on the drop profile for his calculations, instead he applied Laplace curvature approach to analyze the drop profiles.

Quincke was the first to report the experimentally measured contact angle results in a series of papers from 1877 to 1898 [21]. Lord Rayleigh investigated contact angles in terms of surface forces and referred to contact angle hysteresis for the first time while he was examining a liquid drop to advance over or recede from a solid surface in 1890 [8]. The “tilting plate” method of measuring contact angles was first described by Huntington in 1906 [22] where a flat plate is dipped into a liquid, the surface of the liquid as it approaches the plate will curve upward or downward to establish the angle of contact required by the several interfacial surface tensions. As the plate is tilted the curvatures will change to maintain the contact angle, the curvature of the liquid surface on the underside of the plate becoming less and less and finally disappearing altogether. At this point, where the water surface is flat and horizontal right up to the line of contact with the plate on one side, the angle to which the plate is tilted measures the contact angle. Similar and more developed “tilting

plate" methods were employed by a number of other researchers in different forms [23–26].

Sulman explained the mechanism of floating of dense solids on water using contact angles in 1920. He introduced a new tilting plate method to measure advancing and receding contact angles to calculate the contact angle hysteresis (CAH) and pointed out that CAH is a fact of considerable importance in flotation [27]. Wark used contact angles for air bubbles in water in flotation studies in 1933 [28]. Methods depending upon visual observation of the image of a drop, bubble or meniscus in a thin tube projected on a screen or photographic plate was developed from 1929 to 1932 [29–31]. Bartell and Hatch [32] and later Mack [33] calculated contact angles from the height and diameter of small drops of a liquid resting upon a plane solid surface using trigonometric [$\tan\theta/2 = h/r_b$] equation by assuming spherical geometry, where h is the height of the drop, and r_b is the base radius of the drop. Kneen measured contact angles by drawing tangents to the profile of drop images in 1937 [34]. He obtained the magnified profile image of the drop on a white paper fixed on the wall of the room similar to the lamp method of Worthington.

Wenzel was the first to relate the contact angles with the roughness of a surface via liquid/solid interfacial area approach in 1936 [14]. He defined wetting as a thermodynamic process, and the magnitude of the free energy change involved determines whether or not wetting will proceed spontaneously. He proposed that a greater amount of actual surface is wetted under it if the surface of the solid is rough than if it is smooth. Consequently, there is a greater net energy decrease to induce spreading for the process involving the rough surface, and the rough surface is wetted more rapidly. He then defined the geometric roughness factor, r^W as the ratio of actual area to the plan area and derived the well-known Wenzel equation [14] which will be discussed in Section 4. In a subsequent paper, Wenzel pointed out that the surface roughness which modifies the wetting characteristics is a ratio of surface areas only and has no relation to the root mean square of deviations from mean elevation, derived from a profile of the surface in 1949 [15].

Bangham and Razouk proposed in 1937 that the solid surface tension (γ_{SV}) is in equilibrium with the vapor of the drop liquid during contact angle measurements and is different from solid surface tension under vacuum (γ_{S^o}) by the expression [$\gamma_{S^o} - \gamma_{SV} \equiv \pi_e$], where π_e, is the "equilibrium film pressure" or "spreading pressure" of the vapor on the solid surface [35]. They proposed that during contact angle measurements, liquid molecules evaporate and then condense onto the polymer next to the liquid drop, thus creating a tiny layer of liquid film of unknown thickness or extent creating the π_e factor. However, Good [36] and Fowkes [37] suggested that π_e is negligible in cases of a finite contact angle especially on low energy surfaces. Some researchers have objections against this proposal and some supported it and there is a controversy on the subject till today [38–50].

Cassie and Baxter extended Wenzel's analysis to porous surfaces by considering the interfacial area fractions of solid and air pockets on a solid contacting with the drop liquid and derived an equation to calculate the apparent contact angle on a porous surface from these area fractions in 1944 [16]. They tested their approach using the wires of a grating which were coated with a thin film of paraffin wax and also using water repellent textile yarns and reported that the agreement between the calculated and observed contact angle values was good. Cassie extended this analysis to rough and chemically heterogeneous surfaces using the same interfacial area fraction approach in 1948 [17] (see Section 4.1).

On the other hand, Pease published a paper on the significance of contact angles and presented strong objection against to Wenzel and Cassie–Baxter approaches in 1945 [11]. He proposed that the work of adhesion between the solid and the drop liquid cannot be calculated from advancing, receding and equilibrium contact angles since the junction of the air-liquid interface with the solid surface (three-phase contact line) is fundamentally a one-dimensional system. This line of junction can occupy various possible parallel positions on the plane of the solid surface, and different positions allow different mean works of adhesion depending upon the configuration of the different chemical groups exposed on the solid surface [11] (see Section 3.1). The importance of this paper was overlooked by many scientists until it was cited by Johnson and Dettre in 1964 [51], Extrand in 1997, 2003 [52,12] and Gao–McCarthy in 2007 [13].

After the Second World War, contact angle studies on solids (especially on polymers) gained a high momentum. Zisman and co-workers improved the method of direct contact angle measurement from a drop profile by using a telescope equipped with a goniometer eyepiece from 1946 to 1954 and published high quality papers on the subject [53–57]. In practice, a primary small droplet was placed on a surface and small amounts of additional liquids were added to this droplet until the advancing contact angle did not change with successive increases in the size of the drop. Two crosshairs which could be independently rotated were mounted as a diameter of the telescope in a plane perpendicular to the telescope axis and contact angles of drops were measured by rotating one of these crosshairs parallel to surface on which the drop rested, and the other was adjusted until it was tangent to the drop at the triple point [53]. Later, Fort and Patterson developed a new contact angle measurement method based on the reflection of light from the drop in a dark room in 1963 [58]. The arm carrying the light source rotated parallel to the drop axis and the arm was elevated until a bright star of light reflected from the drop surface appears at the viewpoint, and then lowered until the star just disappears from the view. The angles of appearance and disappearance (within 1°) were recorded as the contact angle. However, this simple but very practical method has some limitations: A dark room is required and only $\theta < 90^\circ$ can be measured [58]. Later, Neumann and Good reviewed the techniques of measuring contact angles in a book chapter in 1979 [59]. Some recent books also summarize contact angle measurement methods [3–5].

On the other hand, the validity of Young equation was also questioned: Johnson proposed that Young equation is valid in terms of surface tension and not surface free energies in 1959 [60]. He stated that many researchers proposed that the

free surface energy of the system should be minimum at constant temperature and volume by misconception, however actually the total free energy of the system must be minimum. He added that the surface tension cannot be interpreted as a "compressive force" in a surface. Referring to Gibbs, he pointed out that the "superficial interfacial tension" (ζ_{SL}) indicates the ability of the solid to modify the tendency of the liquid to contract [60]. All the thermodynamic as well as practical matters on contact angles up to 1963 were collected in a symposium book edited by Fowkes and published by American Chemical Society in 1964 [61].

In the same book, Adamson and Ling discussed the derivation of Young's equation and pointed out that the question of the physical definitions of these terms were under question [62]. Surface free energy approach may have better rational quantity than the surface forces if all the surfaces involved in the treatment be well defined thermodynamically. However, the thermodynamic derivation is suspicious since Harkins and Livingston [39] showed that the equilibrium of the liquid phase with the adjacent solid/vapor interface may not be hold. A stretching tension for solids should be present unlike the case of a drop on an immiscible liquid. Adamson and Ling proposed that most solids are incapable of adjusting to equilibrium conformations and their surface structure is usually a frozen-in record of an arbitrary past history [62]. Moreover, Herring showed that solid surfaces (even crystalline) will not usually display those faces demanded by the macroscopic minimizing of surface free energy [63]. In conclusion, the average contact angle will then reflect the topology of surface heterogeneities and surface free energy based thermodynamic equations cannot be successfully applied for such a case [62] (see also Sections 2.2, 3.1 and 5).

Meanwhile, Bikerman proposed that the proofs of Young's equation via the surface free energy or force considerations were both wrong due to the absence of any contractile tendency of solid surfaces which means that solid surfaces do not obey area minimization process when a liquid drop is placed on them [64]. This view was not supported by many scientists. For example, Neumann and Good investigated the capillary rise of a liquid in contact with a strip-wise heterogeneous surface thermodynamically using surface free energy approach and they concluded that the hysteresis of the contact angle is a function of surface heterogeneity and when the strip widths are less than 100 nm, then the amplitude of periodic contortion of the three phase contact line is less than 1 nm and it is indistinguishable from a straight line [65]. Neumann, Good and co-workers extended their analysis to energetically homogeneous and rough solid surfaces in 1975 [66] where the capillary rise of a liquid on a sawtooth rough surface was examined and the possible contact angle values on a tilted sawtooth plate were analyzed theoretically including the effect of gravity. They concluded that the slope of the asperities is an important factor to determine the resultant equilibrium contact angles [66].

Jameson and del Cerro opposed to the surface free energy approach and presented an alternative derivation of the Young's equation in 1976 [67]. The authors assumed that the contact angle itself is caused by molecular interactions near the contact line and the contact angle, wetting and adhesion are strongly influenced by the nature of the molecules near the three-phase contact line. All atoms and molecules possess excess free energy because of proximity to adjacent phases near the contact line. They considered that Young's equation was only an approximation and that if one wishes to derive an equation for mechanical equilibrium as Young did, the forces acting along the infinity of rays passing through the contact line should be considered and not just the rays which coincide with the surface between phases. Alternatively, if one wishes to argue along thermodynamic lines, it is not permissible to assume that interfacial free energy exists only in those atoms or molecules immediately adjacent to the surface. Equilibrium can be established by minimizing the total interphase free energy, not just that part which is ascribed to surfaces. In this important paper, an alternative method of finding the equilibrium contact angle has also been described, based on minimizing the configurational free energy of the contact line. Their theory predicted that the surface tensions in the vicinity of the contact line differ from those at infinity and the contact angle was found as the solution of a simple equation which involved only the solid–liquid and liquid–liquid Hamaker constants [67].

The relationship of contact angles with the roughness of a surface via the interfacial area approach was also an important research topic after Wenzel [14,15] and Cassie [16,17] by several scientists: Bikerman reported the effect of surface roughness of stainless steel plates on the siding behavior of water drops by reporting the length, width of the drop profile and contact areas from the plan view in 1950 [68]. Good derived a thermodynamic form of Wenzel's modification of the Young equation using surface free energy approach in 1952 [69]. Bartell and Shepard tested Wenzel's equation experimentally and found that it could not be applied to water and glycerol contact angles on rough paraffin surfaces in 1953 [70,71].

Johnson and Dettre published a series of theoretical papers on this subject in 1964–1965: they investigated contact angle hysteresis on idealized sinusoidal rough [72], and idealized heterogeneous surfaces by applying free energy approach [51]. They also compared their contact angle results on actual rough surfaces [73] and on actual heterogeneous surfaces [74] with their approach. They concluded that surface roughness leads to a large number of metastable configurations where each of them is separated from an adjacent state by an energy barrier. When the energy barriers become smaller, then the contact angle hysteresis becomes less. They assumed that advancing and receding angles are determined by a balance between the macroscopic vibrational energy of the drop and the heights of the energy barriers. They noted that they were not implying that surface roughness is the only or even the most important cause of contact angle hysteresis, it may only be a common source of CAH [72]. Johnson and Dettre prepared actual rough surfaces by spraying paraffin and fluorocarbon wax onto glass slides and these surfaces were made progressively smoother by heating in an oven. They stated that the theoretical derivation

for an idealized rough surface agrees well with that of real surfaces. However, the reasoning for this conclusion is questionable because they did not measure the roughness factor of their samples and reported only the number of heat treatments in their plots. They used the experimental data of Bartell and Shepard [70,71] for the application of their theory in their paper, however they only compared the general trends and did not report a good fit with the experimental data [73].

In addition, Johnson and Dettre investigated contact angle hysteresis on idealized heterogeneous surfaces by applying surface free energy approach to check the validity of Cassie equation using a simple idealized geometry of flat surfaces in 1964 [51]. They postulated that a liquid drop is at rest on a solid surface consisting of alternating circular bands of different surface energy (concentric ring model) where the boundary is assumed contributes no surface energy to the system and there is an energy barrier between each two positions of the metastable equilibrium. The drop periphery moves over the barrier regions and this model provides for an infinitely sharp transition between regions of different surface tensions. Both the values of these surface free energies of the regions and free energy barriers control the contact angle hysteresis of the system, since free energy barriers hinder the attainment of a minimum free energy. They stated that advancing contact angle is insensitive to coverage by the high contact angle (low free energy) regions once the coverage is above 40%. Conversely, at the low coverage of low free energy regions, the advancing angle is sensitive to coverage and receding angle insensitive to coverage. They concluded that the actual contact angle in a real system will depend on the energy barrier heights and on the ability of a drop to cross over these barriers [51]. For comparison of their theory with the experiments, Johnson and Dettre measured contact angles on actual heterogeneous surfaces where titania was partially coated on glass slides and compared these results with their theoretical approach [74]. Electron micrographs indicated that titania was present on the glass surface in discrete patches (however no image was given). They assumed that the coverage of titania increased with the number of dip coating of the slides into the titanate solutions and they reported the change of contact angles with the change of titania percentage. Water and methylene iodide contact angle curves was suggested to agree qualitatively with those obtained from the computer study of an idealized heterogeneous surface and the effects observed are attributed to primarily to variations in coverage by high- and low-contact-angle regions and that surface roughness has at most, a second-order effect [74].

Huh and Mason distinguished between microscopic and macroscopic contact angles and investigated the effect of surface roughness on the contact angles [75]. They obtained the relation between the true (or microscopic) equilibrium contact angle at the three-phase contact line and the apparent (or macroscopic) contact angle observed at the geometrical contour plane of the solid by calculating the equilibrium shape of a liquid drop resting on a rough surface with concentric grooves. Although the hysteresis in contact angle and drop shape cannot be evaluated by their method, the apparent contact angle and the local contact line positions are approximately predicted when the surface roughness has the form of cross grooves, hexagonal grooves, and radial grooves [75]. Schwartz and Garoff determined that contact angle hysteresis is a strong function of the details of the "patch" structure rather than only fractional coverage by modeling the capillary rise of a liquid on a vertical surface having a periodic wettability pattern [76]. Israelachvili and Gee pointed out that Cassie implicitly assumed that the surface is composed of well separated and distinct patches or domains of either type 1 or 2 for the derivation of his Cassie equation, but this is not the case for practical surfaces [77].

Marmur investigated the dependence of the highest and lowest possible contact angles on the volumes of the drops placed on a smooth but periodically heterogeneous solid surface and found that the dependence can be described by an oscillatory curve [78]. Later, Swain and Lipowsky made a thorough mathematical analysis of Young, Cassie and Wenzel equations by applying a novel minimization technique on the free energy of a three-dimensional liquid drop which is sitting on a rough and chemically heterogeneous substrate under the presence of gravity while keeping account of line tension terms [79]. They described the chemical heterogeneities within the surface in terms of interfacial and contact line tensions which are position-dependent. They pointed out that the anisotropy of the solid substrate will lead to a line tension which depends on the orientation of the contact line, however, they ignore this anisotropy and treated the surface of the solid as a structure less wall. They showed that the states should be defined in order to average individual contact angles on a heterogeneous surface to arrive Cassie equation or on a rough surface to derive Wenzel equation but there may be three different states: (a) if the solid is rough and heterogeneous, the drop can be investigated at a certain position on the surface and move along its contact line and the contact angle will vary; (b) different positions for the drop can be considered, however, the contact line contour and the contact angles at that contour will, in general, change if we require the state of the drop to be a local minimum of its free energy resulting in a prohibitively difficult calculation process; and (c) instead of considering the states of the drop, one could instead choose for those of the contact line then average over all contact line contours which pass through a specific point and correspond to the states of the droplet which are local minima of the free energy is carried out. Swain and Lipowsky choose the method (c) and ignored the dependence of the contact angle on the shape of the drop and assumed that all locations of the droplet were equally likely in order to derive Cassie and Wenzel equations. However, they did not discriminate between the contact area or contact line approaches in their complex analysis, instead they tried to include all the possible affecting parameters into a single equation [79].

1.2. Methods of measuring contact angles

Contact angle measurement appears to be quite easy when first encountered. However, this simplicity is misleading and

the accurate measurement of a contact angle requires considerable efforts. If the substrate is not prepared properly; if very pure liquids are not used while forming drops and if some important practical issues during the measurement such as drop evaporation; the location of the needle in the drop; and maintaining of a sharp image in the video image are not considered, then a wrong and generally useless contact angle value is obtained, which can be used as an evidence for false physical or thermodynamical conclusions [3,4,59].

Many different methods have been developed for the measurement of contact angles such as from drop dimensions [32,33,80,81], tilting plate [22–26], interference microscopy [82], capillary rise at a vertical plate [83,84], reflection from a drop [58,85], liquid rise in a capillary tube [59], capillary rise in a vertical plate [86,87], captive-bubble [88], axisymmetric drop shape analysis-profile (ADSA-P) [89–91], axisymmetric drop shape analysis-diameter (ADSA-D) [92–94], but only two methods are most popular today: (i) the dynamic contact angle measurement method by tensiometry which involves measuring the forces of interaction, while a dynamic (moving) flat solid plate is immersed to or withdrawn from a test liquid [95–103], and (ii) the measurement of contact angle of a sessile drop formed on a solid by means of a needle and syringe, and using a goniometer or video camera for image capture [29–31,53–57,104,105]. We will only discuss the details of the sessile drop contact angle method in this review since it is most suitable to explain the contact area/contact line issues.

In the sessile drop method, the contact angle of a drop resting on a solid surface is measured usually with the aid of a video camera equipped with a suitable magnifying lens and interfaced to a computer having an image analysis software to determine the tangent value precisely on the captured image. A suitable cold light source, and a sample stage whose elevation can be controlled by high precision are also required to apply this technique (Formerly, the drop profile was photographed for this purpose and then a tangent with the sessile drop profile at the three-phase contact point is drawn on the photo-prints to determine the contact angle value.). In most of the published papers, a single value of contact angle is reported by simply putting a drop of liquid on the surface and removing the needle and calling this angle as the "static" or sometimes "equilibrium" contact angle where the results are somewhat dependent on the experience of operator. However, the measurement of a single static contact angle to characterize a solid surface is not adequate, because in practice, there is no single "*equilibrium contact angle*", θ_e, on a solid surface: While deriving the Young's equation, we assume that the substrate is an ideal solid which is chemically homogeneous, rigid, and flat at an atomic scale. However, there is no such a solid surface, because all the practical solid surfaces have surface imperfections and are also heterogeneous to a degree. Thus, there may be a range of static contact angles, depending on the location of the drop edge and the application type of the measurement.

In order to obtain reliable contact angles, two types of measurement techniques are standardized: When a liquid drop is formed by injecting the liquid from a needle connected to a syringe, on a substrate surface, it is allowed to advance on the fresh solid surface and the measured angle is said to represent the "*advancing contact angle*", θ_a. For each drop/solid system, there is a maximum value of θ_a before the three-phase line is broken (it should be noted that the needle must be kept in the middle of the drop during the θ_a measurement and if the needle is made of stainless steel, it is better to coat it by paraffin wax in order to prevent climbing of some strongly adhering liquids such as water; or plastic needles such as Teflon or polypropylene may also be used with water). The other contact angle type is the "*receding contact angle*", θ_r and it can be measured when a previously formed sessile drop on the substrate surface is contracted by applying a suction of the drop liquid through the needle. The liquid is withdrawn from the drop by means of a micrometer syringe to measure θ_r. However, there is a strong influence of the rate of liquid removal from the drop on θ_r values during measurement [104]. The precise measurement of θ_r is more difficult than θ_a. It is expected that θ_a approaches to a maximum value and θ_r to a minimum value ($\theta_a > \theta_r$). Alternately, both advanced and receded angles are measured when the stage on which the solid is held, is tilted to the point of incipient motion of the liquid drop, however, the reproducibility of this method is usually poor [104].

Some researchers do not measure θ_a or θ_r, they only measure the observed angle of the freely standing drop after removing the needle, (an unknown period passes after the drop formation) by calling it "*static*" or "*equilibrium contact angle*", θ_e. θ_e values are between θ_a and θ_r and often nearer to θ_a. Since it does not represent the initial contact angle formed on the fresh surface, such an angle is of a lower degree of scientific usefullness than will a true θ_a or θ_r. Some researchers use θ_e as the arithmetic mean value of θ_a and θ_r, but this approach is thermodynamically wrong [18,59]. Both θ_a and θ_r depends on the surface roughness (detailed shapes and configurations of the patches or strips) and also on the surface chemical heterogeneity. The direct determination of θ_a within $\pm 2^\circ$ is easy but it is difficult to reduce the relative error to $\pm 0.5^\circ$. This is so because the direction of a liquid profile rapidly changes with the distance from the 3-phase contact point. The difference between θ_a and θ_r gives the "*contact angle hysteresis*", $\mathrm{CAH} \equiv \theta_a - \theta_r$ which can be quite large, around 5–20° in the conventional measurements (or 20–60° in some exceptional cases) [18] (see Section 2.3).

Historically, Zisman and co-workers used the tip of a fine platinum wire to bring a droplet to the surface and detach it from the wire in 1950s. More liquid was added, in successive droplets from the wire and θ was measured after each addition by viewing through a goniometer-microscope and the limiting value of θ is taken to be θ_a. The receding angle was measured by stepwise removal of small increments of liquid by touching the tip of a fine glass capillary to the drop and withdrawing it to give θ_r. Many researchers started to introduce the liquid drop by means of a micrometer syringe with a fine stainless steel needle up to a drop contact diameter of 4 mm in 1960s. The liquid drop was held captive while additional liquid is added to the drop until a steady value of θ_a is obtained and the

addition of the liquid is stopped. The needle having usually a diameter of less than 1 mm must not be removed from the drop during measurement as this may cause mass and profile vibrations, which can decrease θ_a to some lower metastable state. Contact angles must be measured on both sides of the drop and reported separately, and also as an arithmetic mean value. Neumann and co-workers make a small hole in the flat substrate sample and first deposit a small drop on the substrate through a needle connected to this hole beneath the substrate. The size of the drop is then increased by feeding more liquid to the drop by means of this needle connected to a motorized syringe. This procedure prevents the drop oscillation and also the destruction of the drop axisymmetry [89,90]. By this way, they can control the rate of advance or retreat of the symmetrical sessile drop on the substrate to measure θ_a and θ_r precisely. They also developed a method to determine both the contact angle and surface tension of the liquid by applying digital image analysis to drop profiles and a computation method named "*axisymmetric drop shape analysis-profile*", (ADSA-P) [89–91]. An objective function is constructed which expresses the error between the physically observed profile in this method, and the theoretical Laplacian curve; the function is then minimized using an iterative procedure.

The inclusion of the gravity (g) correction into the Young–Laplace equation is feasible for large sessile liquid drops formed on solids. The wording of a "*large*" or a "*small*" drop can be done by simply comparing the contact diameter of the sessile drop with the capillary constant, $a = (2\ \gamma/\rho_L\ g)^{1/2}$ (m) of the liquid where ρ_L is the liquid density. If the contact diameter is much smaller (say more than 10 times) than the capillary constant, then the influence of gravitation can be neglected. When volatile liquid drops are formed, the measurements must be made in an enclosed chamber to prevent the drop evaporation by permitting the establishment of the equilibrium vapor pressure of the liquid. However, when high-boiling liquids are used such as water, glycerol, hexadecane, and if the measurement can be carried out rapidly, then there is no need such a closed chamber.

There are several advantages of sessile drop contact angle measurement method: It can be used for almost any solid substrate, as long as it has a relatively flat portion and can be fitted on the stage of the instrument. Testing can be done using very small quantities of liquid. However, this advantage is also the downside of this technique due to the higher risk/impact of local impurities. Shape distortions of drops can be monitored and data may be discarded by using two plan and horizontal cameras during the contact angle measurements [105]. However, there are some limitations of this method: Firstly, the conventional goniometry relies on the consistency of the operator in the assignment of the tangent line. The camera or imaging device will be focused on the largest meridian section, and hence reflect only the contact angle at the point in which the meridian plane intersects the three-phase line. This may lead to subjective error, especially significant when the contact angle results of multiple users are compared. The second problem is the varying liquid flow rates through the needle to increase the volume of the drop during the determination of θ_a; and the variable flow rates of withdrawal of the liquid during determination of θ_r [104]. The sessile drop method is not particularly well adapted to the quantitative measurement of the dependence of contact angle on the rate of advance or retreat, because a linear rate of change in drop volume does not correspond to a linear rate of motion of the drop front. An appropriate rate is of the order of 0.01–0.10 mm min^{-1} linear advance or retreat by using a motor-driven syringe. Also, it is best to specify the constant time allowed before measuring the contact angle after the motion stops, e.g. 1–10 s to dampen the drop oscillations formed in order to obtain more precise data. The third problem is the distortion of the drop surface caused by the needle. If the needle enters the drop at a point very close to the solid, it may obscure the drop profile. It is best to keep the needle at the center of the drop. If the needle passes through the upper surface of the drop, there will be some capillary rise of the liquid up the needle and distortion of the surface. (However, it has been claimed by some authors that this capillary rise does not perturb the liquid in the region of the contact line with the solid). Removing the needle from the drop does not help, because that makes it impossible to study CAH. Finally, objects other than flat, such as cylindrical fibers cannot be easily studied by the goniometry approach.

1.3. Industrial and academic applications of contact angles

Measurement of contact angles quantifies the interactions between solids and liquids which play a key role in understanding the chemical and physical processes in many industries. Contact angles are also used to calculate the surface free energy of solids as given in Section 2.4. Although it is a difficult task to measure the contact angle properly on solids, a large body of reliable data has been accumulated and a vast literature exists correlating contact angle data with the surface free energy of solids.

The determination of contact angles is very important in the adhesives, paints and coatings industries. The new preparation methods to obtain long-lasting adhesion between the coating and substrate surfaces (paper, metal, wood, plastic etc.) in automotive and building industries requires the optimization of the interfacial free energy and the measurement of the strength of interaction by the use of contact angles. The effectiveness of a coating formulation and related coating process, for example a car body coating can be accessed by measuring the hydrophobicity (i.e. the contact angle) of the lacquer surface. The advent of new environmentally friendly water-based inks and other types of coatings started new research in the paper industry to improve the ink performance. All the materials involved in an offset printing process need to have a certain surface free energy in order to obtain an optimum printing quality, so that contact angle measurements are required at many steps during the printing process.

Composite materials made of reinforcing fibers and polymeric (resin) matrix systems have replaced many of the traditional metals and other heavier and weaker materials and started to be used in a wide range of products in aerospace, automotive and sports industries. The adhesion between different composite structures (glass–metal, leather–fabrics, wood–paper) and the

wetting of an adhesive on a substrate can be accessed by contact angle measurements. It is also possible to optimize the adhesion between the fiber and resin matrix system and to find the right formulation of the resin matrix with proper wetting properties against the fiber. In the textile industry, everything from carpet fibers to surgical gowns involves surface treatments such as anti-static or anti-stain coatings applied to the textile materials providing protection. The wettability of single fibers or fabrics as well as their hydrophobicity can be checked by the contact angle measurements.

Flotation is used in the mining industry to separate various kinds of solid particles from each other. These particles are usually less than 100 μm in diameter and were obtained by crushing minerals and mixed with water to form a dispersion. Air bubbles are passed through the dispersion and the particles bind to bubbles by hydrophobic forces and removed as a froth from the top of the flotation pool. Contact angles are used to determine the wetting properties of these particles to improve the flotation efficiency.

Medical, pharmaceutical and cosmetic industries also use the contact angle measurements: biocompatibility is an important issue in medical and dental industries and can be assessed by contact angle measurements. Surface-modified biomaterials are being employed to create disposable contact lenses, catheters, dental prosthetics and biocompatible implants however they must be biocompatible, that is they should not be rejected by the human body. In the case of dental surgery, a good adhesion between the tooth and embodiment is required. The effectiveness of a cleaning solution formulation for contact lenses can be improved by optimizing the surface free energy of the lens and the solution. Meanwhile, applying special surface treatments can largely influence the distribution and dissolving behavior of a pharmaceutical powder. The dissolving behavior of an orally ingested pharmaceutical powder, tablet and capsule, or transdermally applied controlled-release drug product can be improved with the help of contact angle and surface tension measurements.

In cosmetic industry, the interactions between the ingredients of shampoos, cleaning solutions, suntans, body creams and lotions can be checked by measuring the contact angles. The superabsorbent personal hygiene products such as baby diapers have been developed in order to improve absorbency and provide protection against wetness with the application of contact angle measurements. The surface free energy of the pesticide or fertilizer formulations directly affects their spreading on plant leaves or in soil, which influence the environmental pollution. Similarly, oil polluted seas and lands can be treated by surfactant solutions, and the cleaning process can be followed by contact angle measurements on the treated samples. Recently, contact angle methods are used to assess the cleanliness of semiconductor surfaces in electronics industries.

Contact angle methods have also large potential in the newly developing nanotechnology field. Microfluidics is related with the flow of tiny amounts of fluids which is confined in micrometer dimensions. It becomes an important field of research for biological and analytical applications such as DNA and protein analysis. Chemical synthesis can also be carried out on a microchip (or "*lab-on-chip*"). Electrowetting is another new research field where contact angles are used to measure the adjustment of the extent of wetting properties of solids by applying electricity. In comparison with the other surface characterization techniques, contact angle methods can be accepted as complementary analytic techniques to provide supporting information to other expensive surface analysis methods such as ESCA, SIMS, SAXS, Raman, IR etc. In practice, a researcher in the surface field can be guided by the contact angle results in the right direction before doing a more elaborate surface analysis by using much more expensive surface characterization equipments.

1.4. Importance of the Extrand publication in 2003 and Gao–McCarthy publication in 2007

Extrand published a paper to disprove the Cassie equation experimentally for the first time in 2003 [12]. He investigated the contact angle behavior on considerably flat surfaces where single circular heterogeneous islands were formed. Extrand made up a circular lyophobic island made of polystyrene on a flat lyophilic Si wafer surface and conversely, a circular lyophilic island made by etching with sodium naphthalene complex on a lyophobic perfluoroalkoxy fluoropolymer film as seen in Fig. 2.

The root-mean-square-roughness of the surfaces varies between 1.4 and 32 nm, which were determined by atomic force microscopy. Contact angles and CAH were measured with water and hexadecane sessile drops. A small drop was deposited on the center of an island and liquid was sequentially added, eventually forcing the contact line to advance beyond the island perimeter onto the surrounding area. Drop volumes ranged between 1 and 100 μL. It was found that, even though the underlying contact area contained a mixture of lyophilic and lyophobic domains, the contact angles, both advancing and receding, were equal to the angles exhibited by the homogeneous periphery. No area averaging of the contact angles occurred and these findings suggest that interactions at the three-phase contact line, not the contact area, control wetting of heterogeneous surfaces.

As another test, Extrand injected air inside the water drops to create sessile bubbles sitting on the solid in the drop. Then, the contact area of the solid was converted into a heterogeneous form, consisting of interfaces that were both liquid/solid and gas/liquid. Here again, if the contact angle were determined by contact area fractions according to the Cassie equation, the air/liquid interface would have been expected to cause an increase in the apparent contact angles, but it did not. Extrand concluded that contact angles are determined by interactions at the contact line, and not by those within the interfacial contact area [12].

Later, Gao and McCarthy published a very important paper entitled "*How Wenzel and Cassie were wrong*" showing experimentally that three-phase contact lines and not contact areas are important in determining the advancing and receding contact angle values in 2007 [13]. The authors fabricated specific patterned surfaces and planned contact angle experiments to present an experimental proof of the contact line/area problem. They prepared three different surfaces using silicon wafers and photolitography, one flat, one rough with a specific pattern design

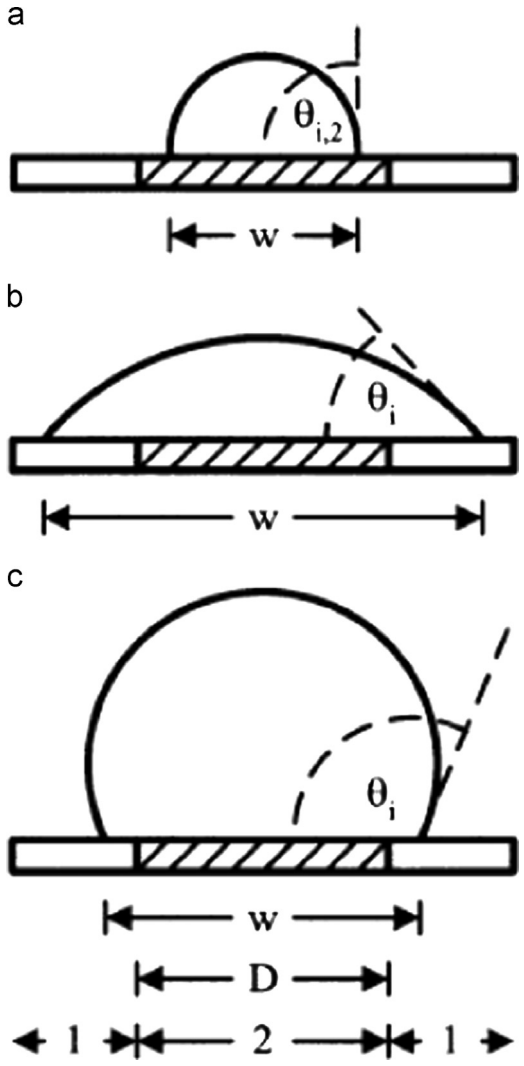

Fig. 2. Side views of a liquid drop on a heterogeneous surface. (a) A small liquid drop resides on a circular island of material 2; ($w < D$ and $f_2 = 1$). The drop exhibits an inherent contact angle of $\theta_{i,2}$. If additional liquid is added such that $w > D$, then the drop rests over a mixed surface, $f_2 < 1$. (b) If material 1 is more lyophilic than material 2, the apparent contact angle decreases, $\theta i < \theta_{i,2}$. (c) Otherwise, if material 1 is more lyophobic than material 2, the apparent contact angle increases, $\theta i > \theta_{i,2}$.
Reprinted with permission from Ref. [12] Copyright (2003) American Chemical Society.

but chemically homogeneous; and one flat but chemically heterogeneous in order to study the effect of different topographies and different chemistries on contact angles as seen in Fig. 3. Initially all the samples were coated with a hydrophobized layer of (heptadecafluoro-1,1,2,2-tetrahydrodecyl)dimethylchlorosilane by a vapor phase reaction. Then they formed hydrophilic spots on these surfaces by using concentrated sodium hydroxide droplets having a desired spot diameter which were located on the hydrophobized coatings. By this method, a hydrophilic circular spot was formed inside the hydrophobic flat sample; a rough circular spot was formed in the flat sample and a flat circular spot was formed in the rough sample. Then, ultra pure water drops with varying contact diameter were located on these samples where the authors put the drop in the spot in some cases, or out of the spot in the other cases and measured advancing and receding contact angles precisely.

Gao and McCarthy compared the contact angle results in two sets: flat homogeneous-flat heterogeneous and flat homogeneous-rough homogeneous. For the first case, the surface containing a hydrophilic spot inside the hydrophobic flat sample was used. Water contact angles on the flat hydrophobic surfaces were nearly the same, $\theta_a = 118–120^\circ$ and $\theta_r = 108–110^\circ$. Water contact angles on the flat hydrophilic surfaces were also nearly the same, $\theta_a = 33–35^\circ$ and $\theta_r = 9–11^\circ$. It is very interesting that when the size of the interfacial liquid/solid contact area increased with the increase in the water drop diameter, then the magnitude of the water contact angles did not change and were nearly the same in the range of $\theta_a = 118–120^\circ$ and $\theta_r = 108–110^\circ$ indicating that there was no effect of interfacial contact area on contact angles and this is a direct experimental proof showing that the Cassie equation is wrong.

For the second case, where the authors investigated the differences between the flat homogeneous and rough homogeneous case, they used two different patterned samples. The first one was obtained by forming a rough hydrophobic spot inside a hydrophobic flat sample. When the authors formed a large water drop which was located on the large hydrophobic flat sample, then the contact angles were nearly the same, $\theta_a = 118–120^\circ$ and $\theta_r = 108–110^\circ$, however when they form a small water drop on only inside the rough circular spot, then the contact angles increased very much up to $\theta_a = 165–168^\circ$ and $\theta_r = 132–134^\circ$. It is also very interesting that when the size of the interfacial liquid/solid contact area increased with the increase in the water drop diameter then the magnitude of the water contact angles did not change and were nearly the same in the range of $\theta_a = 118–120^\circ$ and $\theta_r = 108–110^\circ$ indicating that there was no effect of interfacial contact area of the rough substrates on contact angles and this is a direct experimental proof showing that the Wenzel equation is wrong.

Gao and McCarthy also formed a flat hydrophobic spot inside a rough hydrophobic sample to investigate the differences between the flat homogeneous and rough homogeneous surfaces. When they formed a large water drop which was located on the large hydrophobic rough sample, then the contact angles were nearly the same, $\theta_a = 167–168^\circ$ and $\theta_r = 131–132^\circ$, however when they form a small water drop on only inside the flat circular spot, then the contact angles decreased very much down to $\theta_a = 116–117^\circ$ and $\theta_r = 82^\circ$. In addition, when the size of the interfacial liquid/solid contact area increased with the increase in the water drop diameter, then the magnitude of the water contact angles did not change and were nearly the same in the range of $\theta_a = 167–168^\circ$ and $\theta_r = 131–132^\circ$ indicating that there was no effect of interfacial contact area of rough substrates on contact angles and this is also a direct experimental proof of the wrongness of the Wenzel equation.

Gao and McCarthy concluded that "All of the data presented in this paper indicate that contact angle behavior (advancing, receding, and hysteresis) is determined by interactions of the liquid and the solid at the three-phase contact line alone (force

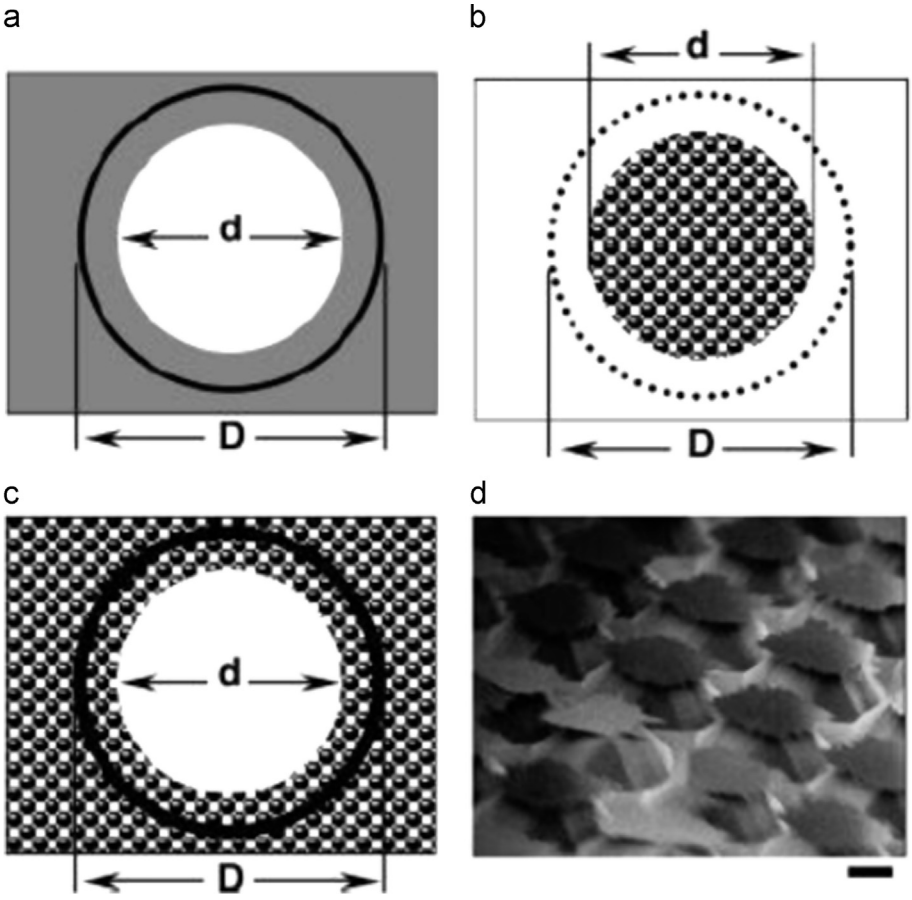

Fig. 3. Depictions of (a) a hydrophilic spot in a hydrophobic field, (b) a rough spot in a smooth field, and (c) a smooth spot in a rough field. (d) SEM indicating the topography of the rough regions in (b) and (c). *d* parameter in (a)–(c) indicates the spot diameter; *D* indicates the droplet diameter. The scale bar in (d) is 10 μm. Reprinted with permission from ref. [13] Copyright (2007) American Chemical Society.

per unit length) and that the interfacial area within the contact perimeter is irrelevant" [13]. It was expected that the disproof of Wenzel and Cassie equations would be confirmed by all the scientist working in the contact angle field after this publication. However, this was not the case, and a hot debate started after this publication, where we will examine the details of this debate in Sections 3 and 4.

2. Classical contact angle theory

2.1. Contact angle theory from vectorial balance of interfacial tension forces

The surface tension of solids, especially polymers having low surface tension cannot be measured directly because of the elastic and viscous restraints of the bulk phase, which necessitates the use of indirect methods. However, a solid surface does not usually display those faces demanded by the macroscopic minimizing of surface free energy. Most solids are incapable of adjusting to such equilibrium conformations and in practice their surface structure will be largely a frozen-in record of an arbitrary past history where some imperfections, humps and cracks are present. Thus, the laws of capillarity of liquids cannot be applied to solids and the only general method is to estimate the solid surface tension from

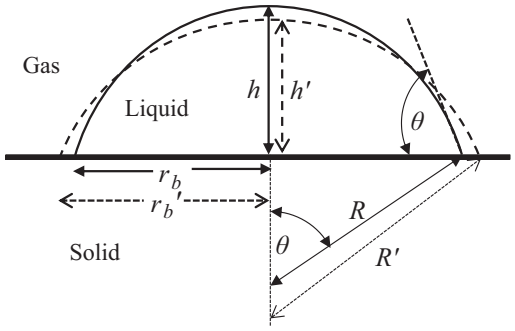

Fig. 4. Change of the sessile drop dimensions by the spreading of the liquid drop on a solid.

that of the contacting liquid. If we consider a liquid drop resting on a solid surface as seen in Fig. 1, the drop is in equilibrium by balancing three forces namely, the interfacial tensions between solid and liquid, γ_{SL}; that between solid and vapor, γ_{SV}; and that between liquid and vapor, γ_{LV}. As given above, the "*contact angle*", θ, is the angle formed by a liquid drop at the three-phase boundary where a liquid, gas and solid intersect and it is included between the tangent plane to the surface of the liquid and the tangent plane to the surface of the solid, at the point of intersection. Unless very volatile, any liquid having low viscosity can be used as the drop liquid. Low

values of θ indicate a strong liquid–solid interaction that the liquid tends to spread on the solid, or wets well, while high θ values indicate weak interaction and poor wetting. From microscopic point of view, if the solid has a low-energy surface, it attracts the molecules of the liquid with less force than the liquid molecules attract one another. Therefore, the molecules in the liquid next to the surface have a weaker force field than in the liquid surface, so that the liquid molecules at the interface are pulled more strongly into the bulk of the liquid than they are by the solid. There is a tension in the layer adjacent to the solid and the liquid molecules are somewhat separated, owing to the one-sided force field. (The situation is analogous to the behavior of a drop of one liquid on another immiscible liquid, the drop liquid having the higher surface tension that of the lower liquid, but not equivalent because of the mobility of surface molecules at the interphase region between two immiscible liquids.)

Young is the first to describe the contact angle equilibrium, in words, in 1805. The vectorial summation of forces at the three-phase intersection point (the so-called "*triple*" or "*three-phase contact point*") gives

$$\gamma_{SV} = \gamma_{SL} + \gamma_{LV} \cos\theta \tag{1}$$

where γ is the surface tension term. If, $[\gamma_{SV} > (\gamma_{SL} + \gamma_{LV})]$ which shows the presence of a high surface energy solid, then the Young's equation indicates ($\cos\theta = 1$), corresponding ($\theta = 0^\circ$), that means the complete spreading of the liquid on this solid. On the other hand, in order to complete the resolution of vector forces about the three-phase contact point, an "*up*" component, ($\gamma_{LV} \sin\theta$), should be present. This force is balanced with a ($-\gamma_{LV} \sin\theta$) force that corresponds to the strain field on the surface of the solid. It is shown that, this strain causes the formation of micro-humps on the surface of some soft polymers when a strongly interacting liquid drop (giving low θ values) sits on them [106–112].

2.2. Contact angle theory from interactions between solid/liquid interfacial area

It is also possible to derive Young's equation from thermodynamical considerations of the solid/liquid interfacial area [3]: If a drop which is placed on a solid spreads, then the contact radius of the drop at the solid/liquid interface, r_b increases by dr_b and the solid/liquid interfacial area on the solid surface would increase ($dA_{SL} = 2\pi r_b dr_b$) leading to a change in surface energy of $(\gamma_{SL} - \gamma_{SV})dA_{SL}$ as seen in Fig. 4.

The liquid/vapor interfacial area of the drop, A_{LV} also increases when the drop spreads. The total change in the Gibbs free energy can be written as

$$\begin{aligned} dG &= (\gamma_{SL} - \gamma_{SV})dA_{SL} + \gamma_{LV}dA_{LV} \\ &= 2\pi r_b(\gamma_{SL} - \gamma_{SV})dr_b + \gamma_{LV}dA_{LV} \end{aligned} \tag{2}$$

We need to find dA_{LV} parameter in dr_b terms in order to solve Eq. (2). Since, $A_{LV} = \pi(r_b^2 + h^2)$ is known from spherical cap geometry, where h is the height of the drop, then the change in A_{LV} can be calculated as

$$dA_{LV} = \left(\frac{\partial A_{LV}}{\partial r_b}\right)dr_b + \left(\frac{\partial A_{LV}}{\partial h}\right)dh = 2\pi r_b dr_b + 2\pi h dh \tag{3}$$

Since, the contact angle, θ, is of second order, it is not considered in the above treatment. However, r_b and h are dependent to each other because the volume of the drop is constant. (When r_b increases, then h decreases.) The volume of the drop, $V = (\pi/6)(3r_b^2 h + h^3)$ is given by spherical cap geometry and a small change in the drop volume can be calculated as

$$dV = \left(\frac{\partial V}{\partial r_b}\right)dr_b + \left(\frac{\partial V}{\partial h}\right)dh = \pi r_b h dr_b + \frac{\pi}{2}(r_b^2 + h^2)dh \tag{4}$$

Since the volume of the drop is constant, ($dV = 0$) then we have

$$\frac{dh}{dr_b} = -\frac{2r_b h}{r_b^2 + h^2} \tag{5}$$

In Fig. 4, we know from Pythagoras' law that $R^2 = r_b^2 + (R-h)^2$ where R is the radius of the spherical drop resulting in

$$\frac{dh}{dr_b} = -\frac{2r_b h}{2Rh - h^2 + h^2} = -\frac{r_b}{R} \tag{6}$$

When Eqs. (3) and (6) are combined one obtains

$$dA_{LV} = 2\pi r_b dr_b - 2\pi h\frac{r_b}{R}dr_b = 2\pi r_b\left(1 - \frac{h}{R}\right)dr_b \tag{7}$$

Since, $\cos\theta = (R-h)/R$ from trigonometry as seen in Fig. 4, then Eq. (7) becomes

$$dA_{LV} = 2\pi r_b \cos\theta dr_b \tag{8}$$

The Gibbs free energy change can be obtained by combining Eqs. (2) and (8)

$$dG = 2\pi r_b(\gamma_{SL} - \gamma_{SV})dr_b + 2\pi r_b \gamma_{LV} \cos\theta dr_b \tag{9}$$

When dG is negative, then the drop spreading will occur spontaneously and when dG is positive the drop will contract and $dG = 0$ at equilibrium, which is the energetically most favorable position. The extra interfacial area goes to zero at equilibrium, when $dG/dr_b = 0$, and Eq. (9) becomes

$$\gamma_{SV} - \gamma_{SL} = \gamma_{LV} \cos\theta \tag{10}$$

Eq. (10) is identical with the Young's equation, as given by Eq. (1).

Dupré combined the "*work of adhesion*", $[W_{12}^a = -\Delta G_{12}^a]$ concept with Young's equation to obtain the well-known Young–Dupré equation [6]. Work of adhesion is the reversible work at constant pressure and temperature conditions, per unit area, required to separate a column of two different liquids (or liquid/solid for this case) at the interface creating two new equilibrium surfaces of two pure materials, and separating them to infinite distance. The work of adhesion can be written as $[W_{12}^a = \gamma_1 + \gamma_2 - \gamma_{12}]$ in terms of surface tensions. For a solid–liquid interaction, it is rewritten as

$$-\Delta G_{SL}^a = W_{SL}^a = \gamma_{SV} + \gamma_{LV} - \gamma_{SL} \tag{11}$$

Young–Dupré equation can be written by combining Eqs. (1) and (11) as

$$-\Delta G_{SL}^a = W_{SL}^a = \gamma_{LV}(1 + \cos\theta) \tag{12}$$

Eq. (12) indicates that a contact angle is a thermodynamical quantity, which can be related to the work of adhesion and interfacial free energy terms. When θ values are small, the work of adhesion is high and a considerable energy must be spent to separate the solid from the liquid. If $\theta=0^\circ$, then $W_{SL}^a = 2\ \gamma_{LV}$; if $\theta=90^\circ$, then $W_{SL}^a = \gamma_{LV}$ and if $\theta=180^\circ$, then, $W_{SL}^a = 0$, which means that no work must be done to separate a completely spherical mercury drop from a solid surface, (or a water drop from a superhydrophobic polymer surface), and indeed these drops roll down very easily even with a 1° inclination angle of the flat substrate.

2.3. Contact angle hysteresis

Contact angle hysteresis is defined as the difference between the advancing and receding contact angles:

$$\mathrm{CAH} \equiv \theta_a - \theta_r \tag{13}$$

Young's equation is valid only on ideal solid surfaces which are chemically homogeneous, rigid, flat at an atomic scale and is not perturbed by chemical interaction or by vapor or liquid adsorption. If such an ideal solid surface is present, there would be a single, unique contact angle. Hysteresis of contact angle is due that the system under investigation do not meet the ideal conditions and it is common to measure CAH on practical surfaces, in the range of 10° or larger; and 50° or more of CAH was sometimes observed. There are two types of CAH, thermodynamic and kinetic. In the kinetic CAH, changes occur to the liquid/solid systems on a time scale comparable to the time of measurement so that the observed contact angles appear to change with time [113]. Solvent penetration into surface, solid swelling, or the rapid reorientation of surface chemical functionalities are the possible causes of kinetic CAH. In general, there appear to be four types of causes for the thermodynamic CAH: Surface roughness and the microscopic chemical heterogeneity of the solid surface are the most important ones and the others are the drop size effect and contamination of foreign materials [4].

If the surface of a substrate is rough, then the actual surface area is greater than the plan surface area and Wenzel proposed that the total liquid–solid interaction is larger on the rough surface than that of a flat surface for a given drop volume [14,15]. If the smooth material gives a contact angle greater than 90°, the presence of surface roughness increases this angle still further, but if θ is less than 90°, surface roughness decreases the angle. Wenzel assumed that the drop liquid fills up the grooves completely on a rough surface and related the surface roughness with the contact angle by a simple expression in 1936 [14]

$$r^W = \frac{\cos\ \theta_e^r}{\cos\ \theta_e^s} = \frac{A^r}{A^s} \tag{14}$$

where r^W is the ratio of the actual area of liquid/solid contact (A^r) to the apparent, macroscopic plan area of liquid/solid contact (A^s) and θ_e^r is the equilibrium contact angle on the real solid, and θ_e^s is the equilibrium contact angle on a flat, smooth surface of the same material. Wenzel suggested that the rough surface is more rapidly wetted since there is a greater net energy decrease to induce spreading. Later, Good derived a thermodynamic form of the Young's equation using surface free energy approach by applying Wenzel's equation [69]. Huh and Mason used a perturbation method of solving the Young–Laplace equation while applying Wenzel's equation for the surface texture in 1976 [75]. Their result can be reduced to Wenzel's equation for random roughness of small amplitude. They assumed that CAH was caused by nonisotropic equilibrium positions of the three-phase contact line, and its movement was predicted to occur in jumps. They obtained the relation between the true (or microscopic) equilibrium contact angle at the three-phase contact line and the apparent (or macroscopic) contact angle observed at the geometrical contour plane of the solid by calculating the equilibrium shape of a liquid drop resting on a rough surface with concentric grooves [75].

Wenzel's equation was found to be inapplicable to water contact angle data on rough paraffin surfaces [70,71]. Meanwhile, Pease opposed the use of Wenzel's equation [11]. He proposed that the work of adhesion between the solid and the drop liquid cannot be calculated from advancing, receding and equilibrium contact angles since the junction of the air-liquid interface with the solid surface (three-phase contact line) is a one-dimensional system and this line of junction can occupy various possible parallel positions on the plane of the solid surface, and different positions allow different mean works of adhesion depending upon the configuration of the different chemical groups exposed on the solid surface [11]. After 2003, Wenzel's relation was reported to be wrong [12,13] and also it was determined that it cannot be applied to the most of the published experimental contact angle data on superhydrophobic surfaces [114].

On the other hand, CAH is also seen on many flat substrates due to the presence of chemical heterogeneity on the surface. Some domains having different surface tensions exist on such heterogeneous surfaces which forms barriers to the motion of the three-phase contact line of drop. These domains represent areas with different contact angles. For example, when a water drop is formed on a heterogeneous surface, the hydrophobic domains will pin the motion of the contact line as the liquid advances, thus increasing the contact angles. When the water drop recedes, the hydrophilic domains will hold back the draining motion of the contact line thus decreasing the contact angle. The movement of the wetting front can give rise to CAH and the actual contact line movement can appear as "stick-slip" behavior, resulting in the slow movement of the triple-line on a heterogeneous surface. θ_a is more sensitive to the low-energy components of the surface, while θ_r is more sensitive to the high energy components of the surface. θ_a approaches to a maximum at high fractional coverage (along the contact line) of the lower energy components of a heterogeneous surface. Similarly, θ_r approaches to a minimum at high fractional coverage (along the contact line) of the high-energy component of a heterogeneous surface. At a microscopic level, the non-uniformity of the solid surface allows many metastable configurations for the fluid interface and the

energy barriers between them are the source of hysteresis. The range of hysteresis is dependent on the availability of energy to overcome such barriers [115]. It was proposed that the height of an energy barrier between successive metastable positions increases as the contact angle becomes closer to the stable equilibrium state.

Cassie and Baxter derived an equation describing contact angle hysteresis for composite smooth solid surfaces with varying degrees of heterogeneity in 1944 [16]

$$\cos\,\theta_e^r = \sum f_i\,\cos\,\theta_i \tag{15}$$

where f_i is the area fraction of the surface with a contact angle of θ_i. For a two-component surface, the above equation can be expressed as

$$\cos\,\theta_e^r = f_1\,\cos\,\theta_1 + f_2\,\cos\,\theta_2 = f_1\,\cos\,\theta_1 + \left(1-f_1\right)\,\cos\,\theta_2 \tag{16}$$

When air pockets are present on a rough surface, Cassie–Baxter equation can also be applied for the contact angle estimate of a water drop on such a surface: Since the contact angle of water in air equals to 180°, which corresponds to ($\cos\,\theta_2 = -1$), so that Eq. (16) becomes

$$\cos\,\theta_e^r = f_s\,(\cos\,\theta_s + 1) - 1 \tag{17}$$

where f_s is the area fraction of the solid component on a solid/air composite surface with a contact angle of θ_s on the flat solid surface. The Cassie–Baxter equation was found to be useful in the analysis of heterogeneous surfaces, however, it cannot explain the corrugation of the three-phase contact line and a wide scatter in contact angle data often observed for the heterogeneous systems which was attributed to the drop size (see Section 2.5).

Joanny and de Gennes proposed a model to explain CAH based on contact line pinning at solid surface defects in 1984 [116]. The authors assumed that the three-phase contact line is deformed by some weak external forces. For weak heterogeneities, the contact line becomes wiggly. The associated energy was described with a "*k*" parameter which was called as the spring constant of the contact line for localized perturbations. For stronger heterogeneities, the authors discussed the behavior of the contact line in the presence of a single, strong localized defect force on the contact line generating a Gaussian form and balancing elastic force to restore and bring the contact line to its initial position. Elastic force is the deformations which the contact line displays when it is subjected to arbitrary external forces. The authors showed that only two stable positions may exist for the contact line, obtained by a simple graphic construction of the above forces. The energy associated to a single defect is the sum of the elastic and defect energy. Minimization of this energy (at fixed nominal position of the contact line) gives back to the force balance and the absolute minimum of the energy determines the stable line conformation. Contact angle hysteresis shows up when the strength of the defect is above a certain threshold. Joanny and de Gennes obtained equations for the θ_a and θ_r on surfaces in terms of the distribution of defect strength and defect sharpness by extending their theory based on a single defect to a dilute system of defects. They suggested that their analysis was equally applicable to both physically rough and chemically heterogeneous surfaces [116].

On the other hand, solid surfaces usually have contamination of foreign substances during their manufacture or formation in the laboratory which also cause CAH. In addition, drop liquids may contain foreign substances to decrease their surface tensions affecting resultant contact angles. Thus, the rigorous cleaning of the solid surfaces and purification of drop liquids before the θ measurement is essential. If such a rigorous cleaning is not carried out and an oily contamination remains, it will result in smaller water θ_r because oil would be spread on the water surface and will give a different CAH value.

CAH arising from kinetic effects often occurs with the polymer surfaces due to molecular orientation and deformation under the influence of the contacting liquid. Kinetic CAH takes place especially if the polymer has polar or hydrogen bonding chemical groups in its structure [4,113]. "*Surface reconstruction*" or "*surface reorientation*" terms are also employed. In this process, the surface configuration of polymers (the spatial arrangement of atoms at the surface) changes in response to a change in the surrounding environment. As an example, hydroxyl groups in a polymer backbone chain is buried away from the air phase in the solid/air interface for a polymer which is kept in air, but when a water sessile drop is formed on the same polymer surface, then the hydroxyl groups turn over to form hydrogen-bonds with water. This movement results in reorientation of the surface under test and can be detected by the time-dependent change in contact angle. Another source for the kinetic CAH is the liquid adsorption on a surface causing a gradient of surface tension density, which will directly affect the horizontal component of force at the three-phase line resulting in CAH.

Recently, two review articles were published on CAH [117,118]. CAH is a well-known problem in immersion lithography, but it is an essential factor in fiber coatings, and inkjet printing [117]. There are mainly two different approaches to explain the dynamics of the moving contact line on the substrate: (i) hydrodynamic model assumes that the viscous dissipation in the bulk phase is dominant; and (ii) molecular-kinetic model relies on the adsorption–desorption processes between liquid and substrate molecules. However, full understanding on the CAH phenomenon on both smooth and chemically homogeneous surfaces cannot be achieved yet [117]. The question of whether the advancing and receding contact angles are determined by thermodynamics or contact line pinning still remains.

2.4. Solid surface free energy calculations from contact angles

Contact angles on solids can be used to estimate the surface tension of the solid. For this purpose, drops of a series of liquids are formed on the solid surface and their contact angles are measured. Calculations based on these measurements produce a parameter (critical surface tension, surface free

energy, etc.), which quantifies the characteristic of the solid surface and its wettability.

2.4.1. Critical surface tension of solids

Zisman and co-workers introduced an empirical organization of contact angle data on solids (especially on low energy polymers) in 1952 [119,120]. They measured θ_e of a series of liquids on the same solid sample and plotted ($\cos\theta_e$) versus surface tension (γ_{LV}) of the test liquids, and the graphical points fell close to a straight line (or collected around it in a narrow rectilinear band) which approaches $\cos\theta_e=1$ ($\theta_e=0$) at a given value of γ_{LV}. This value, called the "*critical surface tension of solid*", γ_c, can be used to characterize the solid surface under test. It often represents as the highest value of surface tension of the test liquid, which will completely wet the solid surface. The linear expression fitting the ($\cos\theta$) versus (γ_{LV}) plot is given as

$$\cos\theta = 1-\beta(\gamma_{LV}-\gamma_c) \tag{18}$$

where the slope of the line gives, $-\beta$ and the intercept gives ($\beta\gamma_c+1$) and both β and γ_c terms can be calculated from a single plot. β value was found to be approximately 0.03–0.04 for many polymers. This approach is most appropriate for low energy surfaces, which are being wetted by non-polar liquids. Zisman warned that ($\gamma_c \neq \gamma_{SV}$) and γ_c is only an empirical value characteristic of a given solid, however γ_{SV} is a thermodynamic quantity. Binary solutions such as water plus methanol must not be used to construct a Zisman plot since one of the components are selectively adsorbed on the solid surface and cause deviations in the contact angle value. There are objections to Zisman method because the value of γ_c is often uncertain since the extrapolation is quite long and considerable curvature of the empirical line is present for solids on which a wide range of liquids form non-zero contact angles [18]. It is generally believed that when dealing with liquids where van der Waals forces are dominant, γ_c of the polymeric solid is independent of the nature of liquid, and is a characteristic of the solid alone. However, when the polymer contains polar and hydrogen bonding chemical groups, which contribute to the polymer/liquid interactions, then the γ_c value may depend on both the nature of the liquids and the polymer.

2.4.2. Geometric-mean approach

Fowkes proposed that the work of cohesion, W_c, and the work of adhesion, W_a, can be separated to their dispersion, d; polar, p; induction, i; and hydrogen-bonding, h components [121–123]:

$$W_c = W_c^d + W_c^p + W_c^i + W_c^h + \ldots \tag{19}$$

$$W_a = W_a^d + W_a^p + W_a^i + W_a^h + \ldots \tag{20}$$

and the dispersion component of the work of adhesion between a solid and a liquid could be expressed as a geometric mean relation

$$W_a^d = \sqrt{(W_c^d)_{SV}(W_c^d)_{LV}} = 2\sqrt{\gamma_{SV}^d\gamma_{LV}^d} \tag{21}$$

Fowkes proposed that the interfacial tension for a solid–liquid system interacting by London dispersion forces only can be given as

$$\gamma_{SL} = \gamma_{SV}+\gamma_{LV}-2\sqrt{\gamma_{SV}^d\gamma_{LV}^d} \tag{22}$$

By combining Eq. (22) with the Young equation, he obtained the Young–Fowkes equation,

$$\gamma_{LV}\cos\theta_e = -\gamma_{LV}+2\sqrt{\gamma_{SV}^d\gamma_{LV}^d} \tag{23}$$

Then he expressed the equilibrium ideal contact angle, θ_e as

$$\cos\theta_e = -1+2\sqrt{\gamma_{SV}^d}\left(\frac{\sqrt{\gamma_{LV}^d}}{\gamma_{LV}}\right) \tag{24}$$

A plot of ($\cos\theta_e$) versus $\left(\gamma_{LV}^d/\gamma_{LV}\right)$ will give a straight line with origin at ($\cos\theta_e=-1$) and with a slope of $2\sqrt{\gamma_{SV}^d}$. Fowkes assumed that $\left(\gamma_{LV}^d=\gamma_{LV}\right)$ for all the non-polar liquids and then calculated (γ_{SV}^d) values of some non-polar polymers by using Eq. (24). He later evaluated $\left(\gamma_{LV}^d\right)$ values for polar liquids as a fraction of their total γ_{LV}, initially for water by using water–immiscible hydrocarbon liquid interactions. He used an empirical equation

$$\gamma_W^d = \frac{(\gamma_W+\gamma_O-\gamma_{WO})}{4\gamma_O^d} \tag{25}$$

where the subscript (W) denotes water and (O) denotes hydrocarbon. Fowkes assumed that $\left(\gamma_O^d=\gamma_O\right)$ for all non-polar hydrocarbons, and using interfacial tension data of eight hydrocarbons versus water, he found a value of $\gamma_W^d = 21.8\ \mathrm{mJ}/m^2$ for water, which is still in use. Next, he used the contact angle data of polar liquids on non-polar solids such as paraffin wax and polyethylene and by applying Eq. (25) he calculated $\left(\gamma_{LV}^d\right)$ values for polar liquids (it is impossible to find them by any direct method).

2.4.3. Surface free energy components approach

Owens and Wendt proposed a new expression in 1969, based on the Fowkes equation by assuming that the surface tension is the sum of two components, "*dispersion*", γ_i^d, and "*polar*", γ_i^p as given by [$\gamma_{SV}^{Tot}=\gamma_{SV}^d+\gamma_{SV}^p$] relationship [124]. They assumed that the free energy of adhesion of a polymer in contact with a liquid can be represented by a geometric mean equation containing both the dispersion and polar components

$$W_a = 2\left(\sqrt{\gamma_{SV}^d\gamma_{LV}^d}+\sqrt{\gamma_{SV}^p\gamma_{LV}^p}\right) \tag{26}$$

based on the assumption of

$$\gamma_{SL} = \gamma_{SV}+\gamma_{LV}-2\left(\sqrt{\gamma_{SV}^d\gamma_{LV}^d}+\sqrt{\gamma_{SV}^p\gamma_{LV}^p}\right) \tag{27}$$

and by combining Eq. (27) with the Young equation, they obtained

$$\gamma_{LV}(1+\cos\theta_e) = 2\left(\sqrt{\gamma_{SV}^d\gamma_{LV}^d}+\sqrt{\gamma_{SV}^p\gamma_{LV}^p}\right) \tag{28}$$

Owens and Wendt used only two liquids to form drops on solids in their experimental surface free energy determinations: Water, $\gamma_{LV}^d=21.8$ and $\gamma_{LV}^p=51.0$, and methylene iodide,

$\gamma_{LV}^d = 49.5$ and $\gamma_{LV}^p = 1.3\ \mathrm{mJ}/m^2$ values were used in their calculations. After measuring the contact angles of these liquid drops on solids (polymers), they solved Eq. (28) simultaneously for two unknowns of γ_{SV}^d and γ_{SV}^p, then they calculate the total surface free energy of the polymer by summing these two parameters. This easy method was used to calculate the surface free energy of copolymer surfaces [125]. Kaelble extended this approach and applied determinant calculations to determine γ_{SV}^d and γ_{SV}^p [126]. When the number of contact angle data is more than the number of equations, a non-linear programming method was introduced in 1988 [127–129].

Geometric-mean approach has been in constant use for more than four decades, even though many articles have been published proving it is incorrect for the cases where strong polar and hydrogen bonding interactions are part of the total solid/liquid interactions. Owens and Wendt equation falsely predicts ethanol and acetone to be as immiscible in water as benzene [130]. The main problem is the wrong assumption that all polar materials interact with all other polar materials as a function of their internal polar cohesive forces [$W_{SL}^p \neq 2\sqrt{\gamma_{SV}^p \gamma_{LV}^p}$]. Once it is realized that polar interactions are mostly electron donor–acceptor (acid–base) interactions and strong interfacial interactions occur only when one phase has basic sites and the other has acidic sites, otherwise there is no use of the polar surface free energy components, and the use of geometric mean approximation for polar interactions is meaningless.

2.4.4. Equation of state approach

Neumann and co-workers proposed that the solid–liquid interfacial tension was a function of the liquid and ideal solid surface tensions $\gamma_{SL} = f(\gamma_{SV}, \gamma_{LV})$ [131–133]. They assumed that the ideal solid surface to be smooth, homogeneous, rigid and non-deformable. Moreover, there is no dissolution of the solid in the liquid drop, nor is there any adsorption of any of the components from the liquid or gaseous phase by the solid. The semi-empirical equation of state approach was expressed as follows:

$$\gamma_{SL} = \frac{\left(\sqrt{\gamma_{SV}} - \sqrt{\gamma_{LV}}\right)^2}{\left(1 - 0.015\sqrt{\gamma_{SV}\gamma_{LV}}\right)} \tag{29}$$

Neumann and co-workers demonstrated that the minimum γ_{SL} is zero and could not be negative. Later they modified Eq. (29) as follows to avoid the discontinuity as the denominator goes to zero:

$$\gamma_{SL} = \left(\gamma_{SV} + \gamma_{LV}\right) - \left[2\left(\sqrt{\gamma_{SV}\gamma_{LV}}\right) \exp -\psi\left(\gamma_{LV} - \gamma_{SV}\right)^2\right] \tag{30}$$

where $\psi = 0.000115\ (\mathrm{m}^2/\mathrm{mJ})^2$. Combining Eq. (30) with the Young equation will yield

$$\cos\theta = -1 + 2\sqrt{\frac{\gamma_{SV}}{\gamma_{LV}}} \exp -\beta\left(\gamma_{LV} - \gamma_{SV}\right)^2 \tag{31}$$

The equation of state approach is very controversial in many respects and many papers were published to invalidate this approach [18,134,135]. First of all, it has been shown by Morrison to be based on erroneous thermodynamically [134]. Secondly, it was shown that there are gross experimental disagreement between predictions from Eq. (31) and observed interfacial tensions between water and organic liquids. Thirdly, Neumann and co-workers have tended to ignore any chemical contributions such as hydrogen-bonding or acid–base interactions to surface or interfacial tension calculations, treating all surface tensions similar to van der Waals interactions, even for water where the contribution of hydrogen-bonding to cohesive energy and surface tension is very large [18]. Lee showed the limitations of this approach by stating that without considering chemical interactions, this approach is incomplete and definitely not universal for interfacial tension calculations [136,137].

2.4.5. Acid–base approach (van Oss–Good method)

Based on the Lifshitz theory of the attraction between macroscopic bodies, van Oss, Good and Chaudhury developed a more advanced approach after 1987 to estimate the free energy of adhesion between two condensed phases [18,138,139]. They suggested that a solid surface consists of two terms, one is the "*Lifshitz–van der Waals interactions*", γ^{LW}, comprising "*dispersion*", "*dipolar*" and "*induction*" interactions and the other term is the "*acid–base*" interaction term, γ^{AB}, comprising all the electron donor–acceptor interactions, such as hydrogen-bonding. They proposed that the Lifshitz calculations yield γ^{LW}, that is the consequence of all the electromagnetic interactions taken together whether due to oscillating temporary dipoles (γ^d), or permanent dipoles (γ^p) or induced dipoles (γ^i). *LW* also includes the interactions of pairs, triplets, quadruplets, etc. of molecules within each phase, in all the actual configurations that are taken on when they are interacted. Then, the corresponding components of work of adhesion are

$$-W_a = \Delta G_{SL} = \Delta G_{SL}^{LW} + \Delta G_{SL}^{AB} \tag{32}$$

the combining rule for the *LW* component in Eq. (32) is geometric mean and is given as

$$\Delta G_{SL}^{LW} = \sqrt{\Delta G_S^{LW} \Delta G_L^{LW}} \tag{33}$$

Eq. (33) is in concordance with the Fowkes approach for dispersion attractions. γ_{SL}^{LW} can now be written as

$$\gamma_{SL}^{LW} = \gamma_S^{LW} + \gamma_L^{LW} - 2\sqrt{\gamma_S^{LW}\gamma_L^{LW}} \tag{34}$$

or

$$\gamma_{SL}^{LW} = \left(\sqrt{\gamma_S^{LW}} - \sqrt{\gamma_L^{LW}}\right)^2 \tag{35}$$

However, van Oss–Good did not applied geometric mean combining rule to acid–base (AB) interactions: Since hydrogen bonds are sub-set of acid–base interactions and surfaces of a number of liquids possess only electron donor properties and have no electron acceptor properties or the reverse is true, one may consider the asymmetry for these interactions. Thus, van Oss–Good adopted Small's combining rule [140] for acid–base

interactions which is not a geometric-mean

$$-\Delta G_{SL}^{AB} = 2\left(\sqrt{\gamma_S^+\gamma_L^-} + \sqrt{\gamma_S^-\gamma_L^+}\right) \tag{36}$$

where γ_i^+ is the Lewis acid, and γ_i^- is the Lewis base component of surface tension. γ_{SL}^{AB} is now given as

$$\gamma_{SL}^{AB} = 2\left(\sqrt{\gamma_S^+\gamma_S^-} + \sqrt{\gamma_L^+\gamma_L^-} - \sqrt{\gamma_S^+\gamma_L^-} - \sqrt{\gamma_S^-\gamma_L^+}\right) \tag{37}$$

or

$$\gamma_{SL}^{AB} = 2\left(\sqrt{\gamma_S^+} - \sqrt{\gamma_L^+}\right)\left(\sqrt{\gamma_S^-} - \sqrt{\gamma_L^-}\right) \tag{38}$$

On the other hand, if *LW* interfacial free energy is written in conjunction with the Young–Dupré equation, we have

$$-\Delta G_{SL}^{LW} = \gamma_S^{LW} + \gamma_L^{LW} - \gamma_{SL}^{LW} \tag{39}$$

by combining Eqs. (34) and (39), one obtains

$$-\Delta G_{SL}^{LW} = 2\sqrt{\gamma_S^{LW}\gamma_L^{LW}} \tag{40}$$

Later by combining Eqs. (33), (36) and (39) one obtains for the total interfacial free energy of adhesion as

$$-\Delta G_{SL} = 2\left(\sqrt{\gamma_S^{LW}\gamma_L^{LW}} + \sqrt{\gamma_S^+\gamma_L^-} + \sqrt{\gamma_S^-\gamma_L^+}\right) \tag{41}$$

by combining Eq. (41) with the Young equation, the general contact angle equation is obtained:

$$\gamma_{LV}(1+\cos\theta) = 2\left(\sqrt{\gamma_S^{LW}\gamma_L^{LW}} + \sqrt{\gamma_S^+\gamma_L^-} + \sqrt{\gamma_S^-\gamma_L^+}\right) \tag{42}$$

In order to find the AB interactions of cohesion in a solid or liquid phase Eq. (36) is rewritten for a single phase

$$-\Delta G_i^{AB} = 4\sqrt{\gamma_i^+\gamma_i^-} \tag{43}$$

since, $(-\Delta G_i^{AB} = 2\gamma_i^{AB})$, then Eq. (43) becomes

$$\gamma_i^{AB} = 2\sqrt{\gamma_i^+\gamma_i^-} \tag{44}$$

If both γ_i^+ and γ_i^- are present to interact, the substance is termed as "*bipolar*". If one of them is not present (equals to zero), the substance is termed as "*monopolar*". If both γ_i^+ and γ_i^- are absent, the substance is termed as "*nonpolar*". Therefore, $\gamma_i^{AB} = 0$ for nonpolar and monopolar substances and γ_i^{AB} is present for only bipolar substances. The total interfacial tension can be given from the sum of Eqs. (35) and (38)

$$\gamma_{SL} = \left(\sqrt{\gamma_S^{LW}} - \sqrt{\gamma_L^{LW}}\right)^2 + 2\left(\sqrt{\gamma_S^+} - \sqrt{\gamma_L^+}\right)\left(\sqrt{\gamma_S^-} - \sqrt{\gamma_L^-}\right) \tag{45}$$

The most important consequence of Eq. (45) is that the contribution of acid–base interaction results in negative total interfacial tension in some circumstances. A solid–liquid system may be stable although it has negative γ_{SL}. This occurs if $(\gamma_L^+ > \gamma_S^+)$ and $(\gamma_L^- < \gamma_S^-)$ or, if $(\gamma_L^+ < \gamma_S^+)$ and $(\gamma_L^- > \gamma_S^-)$ and if $|\gamma_{SL}^{AB}| > |\gamma_{SL}^{LW}|$.

In order to apply Eq. (42) to contact angle data, we need a set of values of γ_L^{LW}, γ_L^+ and γ_L^- for reference liquids. Since, $\gamma_{LV}^{LW} = \gamma_{LV}$ for nonpolar liquids, the problem is to determine a set of γ_L^+ and γ_L^- values for dipolar or monopolar liquids. van Oss–Good introduced an arbitrary relation for water: They assumed that $\gamma_W^+ = \gamma_W^-$ for water and since $\gamma^{AB} = 51.0\ \mathrm{mJ/m^2}$ is known, they calculated $\gamma_W^+ = \gamma_W^- = 25.5\ \mathrm{mJ}/m^2$ from Eq. (44). The values of all acid–base parameters derived from are relative to those of water and finally they suggest a set of liquid surface free energy component data with these operational values. After having the reference liquid surface tension component values, there are two methods to calculate the polymer surface values of γ_S^{LW}, γ_S^+ and γ_S^-. In the first method, three forms of Eq. (42) are simultaneously solved by using the contact angle data of three different liquids with two of them being polar. In the second method, γ_S^{LW} can be determined first by using an non-polar liquid, then two other polar liquids are used to determine γ_S^+ and γ_S^-. Unfortunately, sometimes negative square roots of γ_S^+ and/or γ_S^- occurs which has not yet received a definitive explanation and cause much objection against this theory. It is recommended that if polar liquids are employed water should be used always, otherwise if only two polar liquids other than water are used (e.g. ethylene glycol and formamide) highly variable γ_S^+ and γ_S^- values may be obtained. This method was successfully applied to determine the surface free energy of copolymer surfaces [141].

van Oss–Good methodology was also successfully used to interpret the immiscible liquid–liquid interactions. In addition, it is somewhat successful in polymer solubility prediction in solvents, critical micelle concentration estimation of surfactants, polymer phase separation, microemulsion formation in chemistry; and cell adhesion, cell–cell, antigen–antibody, lectin–carbohydrate, enzyme–substrate and ligand–receptor interactions in biology [139].

2.5. Line tension

The advancing and receding contact angle values may decrease with the decrease in the drop size (or in the captive bubble method, with the size of the bubble). This decrease is more pronounced in θ_r values more than θ_a [142–147]. Since the gravity effects are neglected for small drops, the possible explanation is the presence of the negative "*line tension*" [142]. Gibbs is the first to postulate the line tension concept. He proposed that an additional free energy component (line tension) for a three-phase system (solid/liquid/vapor) is needed to provide a more complete description of the system. Similar to the atoms near the surface, those near the contact line have a different energy from those in the bulk. The line tension results from an excess free energy for molecules located at or close to the three-phase contact line and becomes increasingly important with decreasing drop size. By considering the line tension, Boruvka and Neumann modified the Young's equation as [147]

$$\gamma_{SV} - \gamma_{SL} = \gamma_{LV}\cos\theta + \gamma_{SLV}K_{gs} \tag{46}$$

where γ_{SLV} is the line tension and K_{gs} is the geodesic curvature of the three-phase contact line. Since, K_{gs} is equal to the reciprocal of the drop base radius for a spherical drop sitting on

a flat horizontal and homogeneous surface, Eq. (46) can be expressed as

$$\gamma_{SV}-\gamma_{SL}=\gamma_{LV}\ \cos\ \theta+\frac{\gamma_{SLV}}{r_b} \tag{47}$$

where r_b is the drop base radius. The line tension can be determined from the slope of a plot of ($\cos\theta$) versus ($1/r_b$) according to the dependence

$$\cos\ \theta=\ \cos\ \theta_\infty-\frac{\gamma_{SLV}}{r_b\gamma_{LV}} \tag{48}$$

where $\cos\ \theta_\infty=\left(\gamma_{SV}-\gamma_{SL}/\gamma_{LV}\right)$ is assumed and $\theta=\theta_\infty$ for $r_b\to\infty$. However, experimental line tension values were found to be 10^5–10^6 times greater than the values predicted from the theoretical calculations [148–150]. Due to the weakness of the line energy, its influence on surface phenomena was controversial. The inconsistency between the theory and experiment is attributed to the solid surface imperfections, heterogeneities and roughness. A new parameter, pseudo-line tension (γ^*_{SLV}) was also proposed which includes the effects of surface imperfections to replace the controversial thermodynamic line-tension parameter.

3. Publications directly supporting three-phase contact line approach

As given in Section 1.4, Gao and McCarthy published an important paper entitled "*How Wenzel and Cassie were wrong*" in 2007 and presented experimental proof that contact angle behavior is determined by interactions of the liquid and the solid at the three-phase contact line alone and the interfacial area within the contact perimeter is irrelevant [13]. In contrast with the normal expectations that all of the scientist working in the contact angle field would confirm this conclusion and abandon the use of Wenzel [14,15] and Cassie–Baxter [16,17] equations, a hot debate started after this publication on the conditions or possibilities of the use of Wenzel and Cassie equations. This is probably due to the fact that both Wenzel and Cassie equations have been given in the textbooks which are used in surface science education for long years and most of the surface scientists get used to think with these surface area concepts [1,3–5,151]. The publications defending the three-phase contact line approach will be given in Sections 3.1 and 3.2. Other publications defending interfacial contact area approach will be given in Sections 4.1 and 4.2 in chronological order in this review. Unfortunately, there is no universal agreement on this matter till today, although around 300 papers were published after 2007 to date resulting in more than 2500 citations.

3.1. Before Gao and McCarthy publication in 2007

Pease was the first to present strong objections against to Wenzel and Cassie–Baxter approaches in 1945 [11]. He proposed that the work of adhesion between the solid and the drop liquid cannot be calculated from advancing, receding and equilibrium contact angles since the junction at the three-phase contact line is fundamentally a one-dimensional system. This line of junction can occupy various possible parallel positions on the plane of the solid surface, and different positions allow different mean works of adhesion depending upon the configuration of the different chemical groups exposed on the solid surface [11]. Then any work of adhesion calculated from the contact angle will be a mean value of different tensions which are arranged linearly. The component parts of a simple water drop/solid system would include the works of adhesion of polar groups and non-polar groups applied over the relative linear distances or lengths each type of group occupied along the line of the three-phase line. The mean work of adhesion must be an expression of a minimal energy and is as low as the configuration of the solid surface allows, and the contact angle will tend to be large. These conditions will be realized when the three-phase junction line passes across the largest possible number of apolar groups, and avoids as many polar groups as possible. However, the three-phase line of junction might assume an infinite number of parallel positions on the solid surface and it could ordinarily cross a varying number of polar and non-polar groups, depending upon the particular surface configuration of the solid. Consequently, the equilibrium contact angle should be related directly to the line of least possible mean work of adhesion that the three-phase junction can assume. When advancing contact angles are considered, work must be applied to wet the solid surface and will have to overcome the greatest possible mean resistance which will be greatest when the mean work of adhesion is minimal. On the other hand, we are dealing with a wet surface when receding contact angles are considered, and the work must be applied to overcome the maximum mean work of adhesion since the receding contact angle is related directly to the line of greatest possible mean work of adhesion whereas the advancing contact angle is dependent upon the greatest possible amount of work necessary to wet the solid surface [11].

Bartell and Shepard tested Wenzel's equation experimentally and found that it could not be applied to water, 3 M calcium chloride solution, and glycerol drop contact angles on rough paraffin surfaces in 1953 [70,71]. In one set of experiments, they placed small drops of glycerol on a smooth paraffin surface and measured an advancing contact angle of 98°. A small area of the same paraffin surface was crosshatched to produce a rough surface then the glycerol contact angle on this roughened island was 148°. However, if more glycerol was added to advance the contact line onto the smooth periphery, the contact angle was 98° again, even though most of the liquid/solid interface covered the rough portion of the surface. They concluded that the contact angles and resultant drop shapes are determined at the line of contact of the solid–liquid–air interface and are not altered by surface irregularities beneath the bulk of the drop [70,71]. McNutt and Andes derived an equation for the total energy difference per unit length in relation with the condition of three-phase contact line when a liquid is contacted with a plane wall by capillary interaction. They also re-derived the Young equation different than that of given by Gibbs by applying the conditions of the

increase of liquid meniscus (height between liquid levels) in 1959 [152].

Adamson and Ling pointed out the difference between liquid/solid and liquid/immiscible another liquid surfaces. They stated that the derivation of Young equation was sound thermodynamically from free energies however there remains the question of the physical definitions of these terms in 1964 [62]. If the terms of Young equation as forces parallel to the solid surface then a stretching tension for solids should be present unlike the case of a drop on an immiscible liquid. Surface free energy approach may have better rational quantity than the surface forces if all the surfaces involved in the treatment be well defined thermodynamically. The liquid phase must be expected to be in equilibrium with the adjacent solid/vapor interface however as Harkins and Livingston [39] showed it may not be hold, and if this is the case then the thermodynamic derivation is suspicious [62]. Adamson and Ling stressed that Herring [63] showed that solid surfaces (even crystalline) will not usually display those faces demanded by the macroscopic minimizing of surface free energy. Most solids are incapable of adjusting to equilibrium conformations and their surface structure is usually a frozen-in record of an arbitrary past history [62]. However, a solid surface can come to a local equilibrium with molecules of an adjacent liquid phase (even though non-equilibrium in larger sense) in terms of van de Waals and chemical interactions. If the solid surface is largely heterogeneous, the local contact angles will be local equilibrium ones and different in quantity on various parts of the surface. Consequently, varying local curvatures will exist on the drop and there will a tendency for liquid to extend over low contact angle regions and to retreat from high contact angle ones. The average contact angle will then reflect the topology of surface heterogeneities and surface free energy based thermodynamic equations cannot be successfully applied for such a case [62].

Oner and McCarthy prepared micro-patterned silicone surfaces containing posts of different sizes, shapes, and separations which were prepared by photolithography and subsequent hydrophobization. They investigated the effect of topography length scales on contact angles and measured the force required to move a water droplet on the micro-patterned surfaces placed on a inclined plane and found that the structure of the three-phase contact line has a very important effect on contact angles and drop mobility in 2000 [153]. Contact angles were found to be independent of the post heights from 20 to 140 μm and also independent of the surface chemistry. Water droplets moved very easily on the surfaces containing square posts with dimensions of 2–32 μm and similar distances between the posts and rolled off of slightly tilted surfaces. However, when the post dimensions increased larger than 64 μm with similar distances between them, then these surfaces did not show ultrahydrophobic properties since water droplets were pinned on these surfaces and water intruded between the posts. Changing the shape of the posts from square to staggered rhombus, star, or indented square also increased the receding contact angles due to the more contorted contact lines that form on these surfaces. Oner and McCarthy concluded that the structure of three-phase contact line (shape, length, continuity, amount of surface contact) is very important to determine the θ_a and θ_r. They pointed out that Cassie's analysis did not take the three-phase contact line structure into account and θ_r's are higher for the cases where the three-phase contact lines are longer and more contorted. For example, when the spacings between the posts were increased, then the receding contact angles also increased [153].

As given in Section 1.4, Extrand was the first to publish a paper to disprove the Cassie equation experimentally in 2003 [12]. He formed circular lyophobic islands made of polystyrene on lyophilic Si wafers and conversely, circular lyophilic islands made by etching with sodium naphthalene complex on lyophobic perfluoroalkoxy fluoropolymer films. He forced the contact line to advance beyond the island perimeter onto the surrounding area with the increase of the sessile drop volume and then he was able to show that even though the underlying contact area contained a mixture of lyophilic and lyophobic domains, the contact angles, both advancing and receding, were equal to the angles exhibited by the homogeneous periphery as seen in Fig. 2. Thus, no area averaging of the contact angles occurred contrary to the expectations from the Cassie's equation and Extrand concluded that contact angles are determined by interactions at the three-phase contact line, and not by those within the interfacial contact area [12].

Later, Extrand developed a new contact line density criterion to estimate the suspension or collapse of liquid drops on patterned rough surfaces in 2002 [154] and applied this method to data of Oner–McCarthy [153]. The contact line density (Λ) was calculated as the product of the length of the asperity perimeter per unit area (p) with the area density of asperities (ζ), $\Lambda = p\zeta$. This approach takes into account of the interactions of all the asperity perimeters beneath the droplet and not only the asperities on the three-phase contact line of drop on the solid alone. Extrand concluded that the absolute magnitude of roughness does not determine the contact angle variations, but the slope of surface asperities and the linear fraction of the contact line [154]. Two years later, Extrand extended his contact line density approach by adding the asperity height criterion in 2004 [155]. He found that the surface forces acting around the perimeter of asperities must be greater than body forces and directed upward. Also, asperities must be tall enough that liquid protruding between them does not contact the base of the solid, causing the drop to collapse. He determined critical values of contact line density and asperity height for the conditions of drop collapse from properties of the liquid, solid and their interfacial interactions. In a subsequent paper, Extrand investigated the drop retention forces in terms of asperity shape, size, height and spacing to create surfaces that maintain their liquid repellency even after exposure to large hydrostatic pressures associated with liquid columns or impinging drops in 2006 [156]. He found that the contact angle hysteresis increases linearly with the increase in the linear fraction of contact line on the asperities which is the ratio of asperity width to spacing. He defined that any surface must create a suspension pressure that is greater than or equal to any downward directed hydrostatic pressures and

simultaneously decreasing the asperity size and spacing is the most effective way of maximizing suspension pressure that can withstand the magnitude of the applied external pressure. In addition, the asperities should be sufficiently tall such that external pressure does not force liquid to fill the spaces between asperities, to destroy repellency [156].

Gao and McCarthy published two papers showing the importance of the three-phase contact line and of the kinetics of contact line motion in 2006 [157,158]. In the first paper, the authors proposed that there are two reasons, one involving the kinetics of droplet movement, and one involving the thermodynamics (Laplace pressure) of wetting which introduces water repellency and self-cleaning by forcing water droplets to roll on them and these two reasons mainly affected by the two length scales of surface topography [157]. They measured advancing and receding contact angles on three different silicon wafer surfaces as seen in Fig. 5: one is a smooth silicon surface and the second contains staggered rhombus posts which are hydrophobized using a vapor-phase reaction with dimethyldichlorosilane and the third surface is prepared adding a nanoscopic topography of cross-linked, toluene-swollen methylsiloxane network formed on the staggered rhombus posts by reacting the top of the posts with methyltrichlorosilane in toluene solution with controlled amounts of water present in controlled-humidity air.

It was found that the smooth silicon wafer exhibited θ_a/θ_r of 104°/103°, and the rhombus-patterned surface θ_a/θ_r of 176°/156°. However, contact angles were measured as $\theta_a/\theta_r > 176°/> 176°$ with no apparent hysteresis on the third one having two length scales of topography [157]. The authors also showed that the events happening during the advancement of a droplet is different than that of a receding droplet as seen in Fig. 5: During drop advancement on a surface, the discontinuous contact line does not move, but, instead, sections of the liquid–vapor interface descend onto the next posts to be wet. Since the droplet is at $\theta_a = 176°$ on the staggered rhombus posts and the tops of the next posts exhibit a low contact angle of $\theta_a = 104°$, then water should spontaneously advance over the post tops without any difficulty. However, the events during the receding movement of a drop is different: The droplet is at $\theta_r = 156°$ on the staggered rhombus posts and the neighbor post tops exhibit $\theta_r = 103°$, so the discontinuous contact line cannot recede across the post tops and must disjoin from entire post tops in concerted events in order to move. This receding contact line pinning causes to the 20° hysteresis observed due to the disjoining pressure.

On the other hand, when we consider the drop advancing and receding on the third topography having two length scales with $\theta_a/\theta_r > 176°/> 176°$ then the kinetics of contact line recession is also affected by lowering the transition state energy between metastable states. Gao and McCarthy pointed out that there was a thermodynamical effect where the Laplace pressure at which water intrudes between the posts was only a function of the advancing contact angle ($-\cos\theta_a$) and increasing the contact angle of the post tops from 104° to $> 176°$ increases the Laplace pressure by a factor greater than four times allowing spacing the posts at greater distances and taking greater advantage of the "apparent slip" on the air between posts that yields drag reduction [157].

In the second paper, Gao and McCarthy criticized that the citations given to and also the use of the Wenzel and Cassie

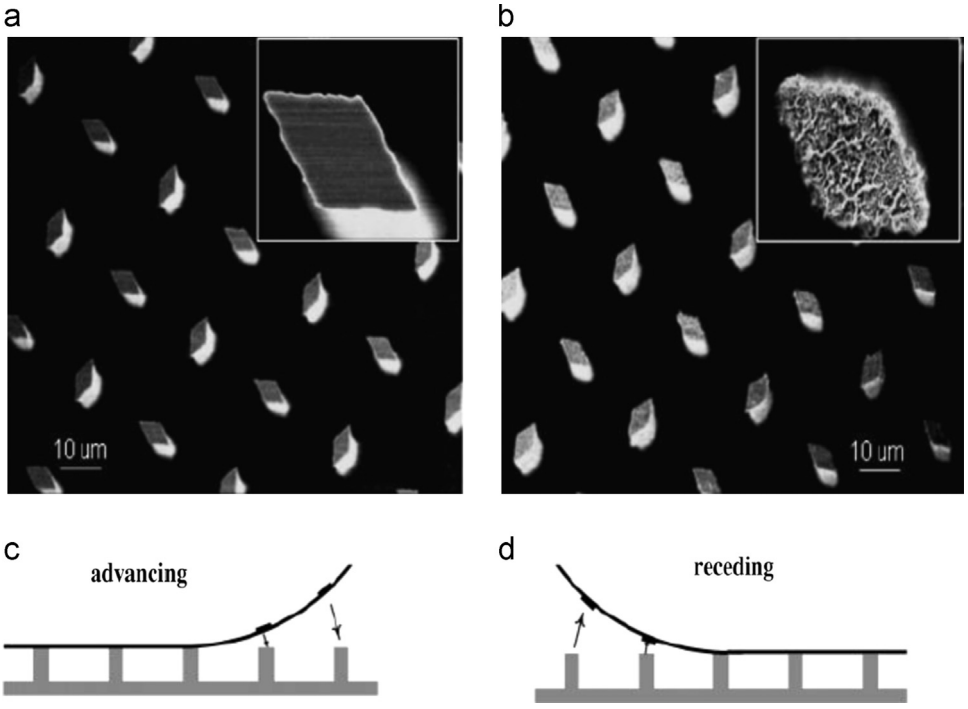

Fig. 5. (a) Scanning electron microscopy (SEM) image of the surface containing staggered $4 \times 8 \times 40$ μm^3 rhombus posts. (b) SEM image of the surface shown in panel a after being coated with a cross-linked hydrophobic polymer network. (c) Contact line events upon advancing. (d) Contact line events upon receding. Reprinted with permission from Ref. [157] Copyright (2006) American Chemical Society.

theories (which involve areas and not lines) which have grown in numbers at a very high rate in contrast with the fact that the paper of Pease [11] on three-phase contact lines has been completely ignored for long time by the surface scientists [158]. They pointed out that when a droplet moves horizontally from one to another equivalent contact area, much of the molecules which are present at the liquid/solid interface do not move due to the no-slip boundary condition of fluid mechanics. The only interfacial water molecules that move during this movement are those that wet new surfaces and dewet previously wetted surfaces. Thus, for the limiting case of a very small movement the only interfacial water molecules that move are those on the three-phase contact line. Consequently, no events occur over the area between the liquid and the solid away from the contact line and the structure of the three-phase contact line is thus central to the movement process and only the molecules on the contact line can contribute to hysteresis. Such an explanation invalidates the Wenzel and Cassie theories. They also suggested that the advancing and receding events can be very different processes (not the reverse of one another) with very different activation energies. Contact angle hysteresis can be related with the activation energy required for the movement of a droplet from one metastable state to another on a solid surface [158].

Meanwhile, Bormashenko and co-workers used an environmental scanning electron microscopy (ESEM) in the wet mode for the close inspection of the triple line of a sessile water droplet on micrometrically scaled honeycomb polystyrene templates which were fixed on a Peltier stage held at a temperature of 2 °C in the real time regime in 2007 [159]. The triple line was found to be meandering and grasps at roughly circular polymer islands. A water precursor rim of 1–5 μm surrounding the drop has been observed in the vicinity of the drop edge. In the same year, Bormashenko and co-workers investigated the Cassie–Wenzel wetting transition in vibrating drops [160]. Water drops were exposed to the vertical vibrations of the increased amplitude (0.02–2 mm) at various constant frequencies of 30–50 Hz until the wetting transition took place. Water penetrates into the pores of polystyrene pattern since the internal pressure in the drop increases due to the inertia force in the course of vibration. Internal pressure decreased with the increase in the drop volume as $V^{-1/3}$. They concluded that force per unit length of the triple line is the more important parameter and thus the dynamic Cassie–Wenzel transition is more likely a 1D than a 2D affair and wetting regime changes when a certain threshold value of the force acting on the unit length of a triple line is exceeded [160].

3.2. After Gao and McCarthy publication in 2007

As given in Section 1.4, Gao and McCarthy published a very important paper to disproof the Wenzel and Cassie equations experimentally, entitled "*How Wenzel and Cassie were wrong*" showing that three-phase contact lines and not contact areas are operative in determining the advancing and receding contact angle values in 2007 [13]. However, a hot debate started after this publication, where we will examine the publications supporting Gao–McCarthy paper after 2007 till 2014 in Section 3.2. The publications supporting the contact area approach (against Gao–McCarthy paper) will be given in Section 4.

Extrand demonstrated that it is possible to improve the apparent hydrophilicity of an oxidized graphite surface by introducing square textures in 2007. Hydrophilic liquids spread over these surfaces to produce noncircular wetting areas. If the channels between the features were made shallower or narrower, liquids wicked more and spread over a larger area. He stated that the use of the Wenzel equation should generally be avoided, as it is built upon a false premise that the apparent liquid–solid interfacial area drives wetting, but this is not true. Rather, interactions at the contact line control wetting of smooth and structured surfaces [161]. Stafford and co-workers probe the wetting of liquids on anisotropic micro-wrinkled features that exhibit well-defined aspect ratios. They found that the change of contact angles on a real rough surface is significantly affected by the nature of the three-phase contact-line structure, rather than by simply increasing the surface roughness [162].

On the other hand, Gao and McCarthy replied [163] the criticism of Panchagnula and Vedantam [214] (see Section 4.2) entitled "*Comment on How Wenzel and Cassie were Wrong by Gao and McCarthy*" [13] and pointed out that they prepared surfaces with "spots" that were either smoother or rougher or had different chemistry than the "field" surface and measured contact angles in two ways, one within the spot with small drops and the other with larger drops so that the spot was within the contact line. Then, they demonstrated that the area or presence of the spots within the contact line have no effect on the final contact angle. They stated that their results point blank disprove Wenzel's and Cassie's theories. They also pointed out that they were precise with their use of the word "lines", and specifically did not use the word "near" (to lines) and deliberately discounted areas. Gao and McCarthy added that many scientists, however, would not have anticipated the results since the Wenzel and Cassie equations have contributed to their faulty intuition. They stated that they submitted their paper, "*How Wenzel and Cassie were Wrong*" with the objective of correcting misconceptions that are held by the majority of students learning surface science and the majority of researchers publishing in the area of "superhydrophobicity". They also stated that the experimental findings of Panchagnula and Vedantam [214] on the contact line continuity had been reported by them before. Finally, Gao and McCarthy also stated that there is another group of people who look at this issue as one of semantics (without citing any publication, see Section 4.2) and they are wrong too [163].

Dorrer and Rühe coated micromachined silicon post surfaces with thin films of poly(ethylene glycol methyl ether methacrylate) layer having a contact angle of 70° on the smooth material and tested the validity of the Wenzel equation [164]. They found that, for surfaces where the degree of roughness and the hysteresis is high, this approach is questionable. On rough materials, the advancing and receding

contact angles cannot be computed from an averaged quantity such as the Wenzel roughness factor, but depend on the local shape and topography of the roughness features the moving meniscus is interacting with at a given moment. They proposed a model for the motion of the meniscus on the post structure where the advancing meniscus remains pinned on a row of posts, then bulging forward to make contact with the neighboring row of posts from above. Dorrer and Rühe reported that the force with which the meniscus is pinned on an ensemble of defects was not the only factor that determines the contact angle for certain roughness geometries, but the process of contacting with the next row of roughness features was also important [164]. Vedantam and Panchagnula developed a theory using a two-dimensional non-conserved phase field variable to parametrize the Gibbs free energy of the three-dimensional system in 2008 [165]. They concluded that the behavior of a drop is determined by the material properties near the three-phase contact line in accord with the experimental observations of Extrand [12] and Gao and McCarthy [13] although they insisted that the disagreement between Cassie theory and Extrand's [12] experiment arises from an incorrect choice of surface area fractions [165]. However, it is important to realize that he size scales of surface roughness or surface heterogeneity was never mentioned in the original Wenzel and Cassie papers, and the choice of surface area fractions is not a subjective matter.

Spencer and co-workers carried out an important experimental study where the water contact angle measurements were performed systematically on a wide variety of rough surfaces with precisely controlled surface chemistry [166]. Four different surface topographies were examined: sandblasted glass microscope slides, replicas of acid-etched, sandblasted titanium; lotus leaves and photolithographically manufactured golf-tee-shaped micropillars of photoresist on a silicon wafer. They pointed out that all four surface topographies are uniformly rough, such that it does not make a difference where a drop is placed. This precondition, as emphasized by McHale [211] has to be met to be able to compare contact angle data with Wenzel and Cassie equations. Surfaces have been analyzed by SEM and roughness factors evaluated by means of white-light profilometry. Spencer and co-workers reported that the pinning strength of a surface was found to be independent of the surface chemistry, provided that neither capillary forces nor air enclosure are involved. They stated that the topographical influence on the contact angle cannot simply be predicted via a roughness factor. None of the measured contact angles could have been predicted by the Wenzel equation with the exception of the hydrophobic data in the case of the sandblasted glass surface [166].

Yamamato and Ogata reported a thermodynamic method depending on 3D analysis to calculate the contact angle on micropatterned superhydrophobic surfaces, by combining contact line approach with the Young's equation to derive novel expressions [167]. The authors stated that they did not use neither Wenzel's nor Cassie's approach in their thermodynamic derivation, since a question concerning their validity has been raised by Gao and McCarthy [13]. Their results indicate that the wider canal width (the separation distance between the pillars) causes θ_e^r to decrease when the pillar width and height was kept constant. However, in contrast to canal width, varying the pillar width has little effect on θ_e^r when the canal width and height was kept constant (θ_e^r decreases slowly and gradually with an increase in the pillar width). Increasing the pillar height also increases θ_e^r significantly, when the canal and pillar widths were kept constant. In addition, trapping the air between pillars increases θ_e^r and tall pillars are required to achieve superhydrophobicity [167]. Fang et al. investigated the thermodynamic mechanisms responsible for the droplet motion on micropatterned surfaces and concluded that the roughness in the vicinity of the triple line rather than the overall surface area within the contact perimeter determines the apparent contact angles [168].

Larsen and Taboryski pointed out that the Gao and McCarthy paper caused some debate on the correct interpretation of the Cassie and Wenzel laws, which calls for further experimental clarification and they used microengineered hydrophobic circular patches of hexagonal geometry on a hydrophilic background to measure maximum water θ_a's [169]. 4–8 μL drops of deionized water are placed on a SU-8 chemically micropatterned surface as seen in Fig. 6. All measured contact angles were advancing contact angles measured instantly after the drop inflation was stopped and the shape of the drop had come to a rest and drops tend to take hexagonal shapes due to the pinning forces of the hydrophobic lattice structure.

Their results clearly show that the simple application of Cassie's law based on area fractions fails in fitting the data for faceted droplets. Then they replaced the area fraction factors by local line fraction factors along the triple phase boundary line between solid, liquid, and air in the Cassie equation similar to the line average method proposed by Cubaud et al. [170]. This time, the “Cassie on line” approach fitted the experimental data remarkably well. Larsen and Taboryski concluded that advancing contact angles for chemically heterogeneous surfaces only depend on the surface properties along the triple phase boundary lines and not on the area fractions of already wetted surface area [169]. Yang et al. investigated the relation between the apparent contact angle and sliding angle in order to clarify whether or not the roughness of contact area or three-phase contact line is the true factor determining the sliding properties of hydrophobic surface [171]. They prepared micropatterned surfaces consisting cubic pillars with different pillar heights, side lengths and spaces which were fabricated by photolithography and subsequent hydrophobization with a silane. Yang et al. reported that the sliding angle was irrelevant to the state of interfacial contact area of water–solid and the length of lower contact line and it was merely determined by the length of upper three-phase contact line [171].

Gao and McCarthy published two papers to defend their disproving of the Wenzel and Cassie equations in 2009 [172,173]. In the first one, they pointed out that they disproved these equations in experiment-based way, however received criticisms from only theory-based arguments and replied the

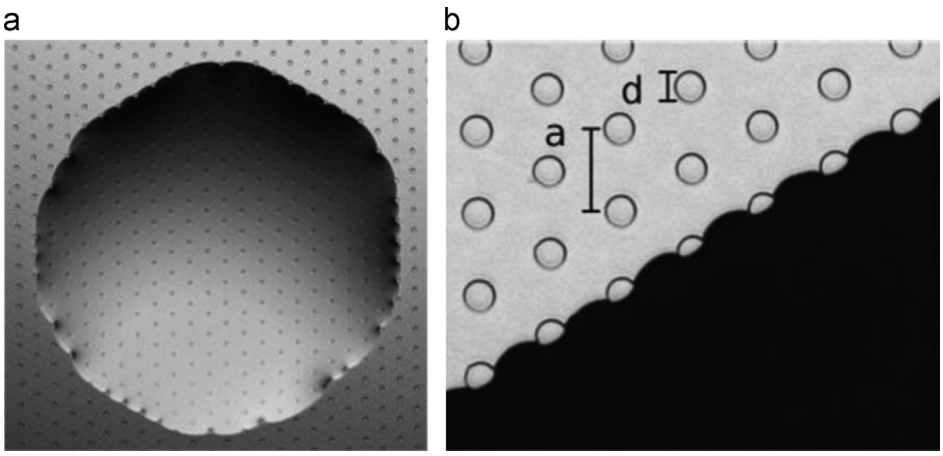

Fig. 6. (a) Microscope image of a water drop on a SU-8 chemically micropatterned surface. Drops tend to take hexagonal shapes due to the pinning forces of the hydrophobic lattice structure. (b) Straight drop edge showing maximum pinning force at the center of the straight drop edge line segment. *d* is the diameter of the hydrophobic circular patches, while *a* is the lattice constant of the hydrophobic lattice.
Reprinted with permission from Ref. [169] Copyright (2009) American Chemical Society.

main criticisms of Marmur and Bittoun [222] on four points [172]:

(1) "*The main problem with the above statement is that it stems from experiments performed with drops that were too small, ignoring the indications of existing theoretical understanding*". Gao and McCarthy replied that the drops that were used to measure contact angles were not too small, were much larger than the drops that Wenzel and Cassie used and were the same size used for over 99% of the sessile drop contact angle values ever reported. In addition, it can be pointed out that drop size is never an issue of the original Wenzel and Cassie–Baxter papers.

(2) "*It was rigorously proven and numerically demonstrated that the Wenzel and Cassie equations are approximations that become valid when the size ratio of the drop to the wavelength of roughness or chemical heterogeneity is sufficiently large*". Gao and McCarthy responded that all the scientists have made meaningful measurements of contact angle using small drops with no knowledge of or ability to control the wavelength of surface structure (chemistry or topography). It is well-known that researchers should not use larger drops, not be concerned with the wavelength of surface roughness or chemical heterogeneity, and not be concerned with the ratio of drop size to wavelength. They also pointed out a practical issue, that when the "wavelength of roughness or chemical heterogeneity" is too great, advancing and receding contact angles cannot be measured and stick-slip occurs. Increasing the drop volume does not help to overcome this problem. In addition, it can be pointed out that the size of the wavelength of roughness or chemical heterogeneity is never an issue of the original Wenzel and Cassie–Baxter papers.

(3) "*It may be more useful* (*though less provocative*) *to explain when and why the Wenzel and Cassie equations are right*". Gao and McCarthy replied that to use theory to explain "when and why…equations are right," is a wrong way in science, particularly when it leads to useless requirements of impractical drop size and surfaces of particular structural wavelength. They stated that experimentalists are forced to ignore these theoretical requirements because they do not apply to real analytical situations, for instance, actual raindrops or the multiple length scales of topography and leaf size of a pesticide-coated crop. If experimentalists obey the rules of theorists on the use of equations for only specific cases, then they would not be able to analyze many surfaces because the objects would be too small and the instruments would need to be replaced with those of different design.

(4) "*In addition it will be argued that meaningful measurement and definition of contact angles for a realistic, general case of roughness and chemical heterogeneity are possible only for relatively large drops. For such drops, the Wenzel and Cassie equations apply without any modification"*. Gao and McCarthy responded that this fourth statement claimed that essentially all of the contact angle data measured on earth are meaningless measurements, including Wenzel's and Cassie's since very large drops are required to apply Wenzel and Cassie equations without any modification. The authors advised using the well-known conventional experimental techniques and drop sizes that for decades have given insight into surfaces with all wavelengths of structure. They added that they forcefully advice the analysis of contact angle data from the perspective of the contact line and not the perspective of the contact area [172]. Gao and McCarthy also added that advancing and receding contact angles are the only meaningful contact angle values that can be measured and that CAH is a more meaningful measurement of shear hydrophobicity than any contact angle (CA) value. They pointed out Marmur et al. that criticizes their statement describes actual CA, Young CA, geometric CA, apparent (equilibrium) CA, Cassie CA, Wenzel CA, local Young CA, and most stable CA [222] but none of these contact angles can be measured, and none of them (as individual

values) are sufficient to describe water repellency. Gao and McCarthy proposed that the origin of faulty intuition is the confusion of force/per unit length based surface tension concepts with the energy per unit area based surface free energy concepts and stated that surface tension and surface free energy are discrete, distinct, and different quantities. However, people have regarded them as interchangeable since these quantities are mathematically equivalent at equilibrium but this conception is wrong and is the reason of the faulty intuition perpetuated by the Wenzel and Cassie theories [172].

In the second paper, Gao and McCarthy reviewed their 2006–2009 publications on wetting and superhydrophobicity [173]. They stated that the 1D (three-phase, solid/liquid/vapor) contact line perspective is more intuitive, more useful, and more consistent with facts than the disproved but widely held-to-be-correct area based 2D views and expressions. They proposed that advancing and receding contact angles are governed by events that occur at the three-phase contact line and needlessly complex theoretical understandings, incorrect models, and ill-defined terminology are not useful and can be destructive in the wetting field [173].

Bormashenko applied a variational approach to wetting of composite surfaces and reported that surface density of defects in the vicinity of the triple line dictates the apparent contact angle [174]. The physical and chemical heterogeneities located far from the three-phase line have no influence on the apparent contact angles for both Cassie and Wenzel wetting regimes. However, Bormashenko used a new term "the area adjacent to the triple line" which is defined to be less than 100 nm in thickness to exert an influence on the apparent contact angle [174]. This approach can be criticized from two points of view; one is the necessity of using the controversial solid/liquid interfacial area concept again, and the other is the selection of the arbitrary value of the thickness.

Erbil and Cansoy developed a test method on the applicability of Wenzel and Cassie equations for superhydrophobic surfaces [114]. They used the data of eight papers published from 2000 to 2008 for this test where water drops sit on micropatterned superhydrophobic surfaces containing both square and cylindrical pillars and evaluated the contact angle results of 166 micro-patterned samples with their simple method. They reported that the use of the Wenzel equation was found to be wrong for most of the samples and the deviations from the Wenzel theory were also high, and they finally concluded that the Wenzel equation cannot be used for superhydrophobic surfaces other than a few exceptions. The evaluation of Cassie equation is more difficult because two situations are possible for this approach: there may be only a partial contact of the drop with the top solid surface, or the penetration of the drop in between the pillars is also possible, however it was determined that large deviations of experimental water contact angles were found from the values calculated when Cassie equation is applied and 65% of the samples containing cylindrical pillars and 44% of the samples containing square pillars did not fit with the Cassie equation, indicating that the Cassie approach should be applied to superhydrophobic surfaces with caution [114].

Cannon and King developed a direct method to visualize three-phase contact line of a droplet on microstructured surfaces [175]. They formed a heated liquid metal droplet (CerroLow alloy which has a melting temperature of 47 °C and a contact angle of 110° on the smooth silicone surface) on a micropatterned polydimethylsiloxane surface at 80 °C and then cool the metal droplet to solidify to preserve the microstructure impressions onto the metal surface. After removing the solidified droplets, their bottom area was investigated by SEM to determine the contact line geometry. The authors successfully characterized how the three-phase contact line of a droplet changed with the microstructure geometry, however they did not provide any information on the effect of contact line length to the drop contact angles [175]. Nevertheless, this method seems to be useful to determine the contour of droplet three-phase contact lines for some cases. Bormashenko published a review entitled "*Wetting transitions on biomimetic surfaces*" and stated that the apparent contact angle is dictated by the area adjacent to the triple line and not by the total area underneath the droplet [176], citing Gao and McCarthy's paper [13]. Yang et al. tested Wenzel and Cassie equations by measuring the apparent contact angles of water droplets on micro-structured hydrophobic surfaces consisting of cubic pillars. Silicon surface with pillars of different dimensions is obtained by the photolithography and these pillars were later hydrophobized. The authors concluded that their experimental data showed that the state of outermost three-phase contact line plays an important role in determining the apparent contact angle and that the contact area within outermost three-phase contact lines is irrelevant to the apparent contact angle [177]. Liu et al. developed a new model based upon the three-phase contact line pinning, suggesting that the effective volume of a droplet on a micropatterned surface is a monotonic function of the macroscopic contact angle when the triple contact line is pinned and concluded that the triple contact line rather than the contact area that dominates the contact angle and the new model can predict the macroscopic contact angle in a wider range more accurately, which is quantitatively consistent with the experimental results [178].

Cheng and McCarthy demonstrated that the pinning of sessile water drops by hydrophilic features depends on the linear shape of the portion of the feature that interacts with the receding contact line [179]. They prepared different and unusually shaped puddles of water on water repellent surfaces using only thin hydrophilic contact lines of the desired shape. The volume of water that could be pinned depends on the linear shape of the portion of the feature that interacts with the receding contact line and not on the feature area. Unusual shapes for liquids to take can be designed and prepared. Hydrophilic arcs (sections of circles), short wedges (pointed to the center of the circle), long wedges (pointed to the opposite side of the circle) hydrophilic patterns were prepared and pinning of water drops inside these patterns were studied. The authors concluded that the pinning of water puddles by

hydrophilic contact lines can be used to control the 2D and 3D shape of the water puddles [179].

Nakajima and co-workers investigated the sliding of water droplets on hydrophobic surfaces having hydrophilic regions of varying sizes [180]. The hydrophilic area on the surfaces was aligned hexagonally with a constant area fraction. The sliding angle and contact angle hysteresis of the water droplets for these surfaces increased simultaneously with the increasing pattern size, showing that resistance for the sliding is correlated with the pattern distance. The authors concluded that the sliding behavior of water droplets is related with the contact line distortion between each defect at the receding side [180]. Erbil and co-workers prepared 36 micropattern samples made of square and 24 of cylindrical pillars were prepared by applying the DRIE technique on Si-wafers and tested the validity of Cassie equation [181]. Large positive deviations from the Cassie equation were found for square (up to 88%) and cylindrical (up to 76%) pillar samples. In order to obtain a maximum deviation from the Cassie equation, the patterns should contain square rather than the cylindrical pillars and the separation distance between the pillars should be smaller than the pillar diameter [181].

Shirtcliffe et al. published a review on the superhydrophobicity of polymer surfaces in 2011 where they reminded that the structures in the immediate vicinity of the contact line determine the wetting of liquid drops, not the average across the entire surface or under the droplet [182]. Dubov et al. [183] investigated the issue of the pinning of the triple line on hydrophobic surfaces textured with cylindrical pillars both experimentally and theoretically and showed that the dependences of both advancing and receding contact angles upon spacing are well accounted for by a simple model of the instability of the triple line given by Joanny and de Gennes [116]. Dubov et al. stated that both the typical Cassie model and the Joanny–de Gennes approach cannot account for the experimental results. They noted that the Joanny–de Gennes equation was obtained by summation over independent pinning sites, a process which is expected to be valid for only low densities. However, their experimental result differs from the Joanny–de Gennes approach because the distribution of pillars on their surfaces is periodic. Later they assigned two parameters, stiffness constant (κ) which is a fraction the surface energy and the displacement parameter (λ) depending on geometrical and physical parameters and assigned numerical values to these experimental findings and showed that the deformation occurs at a fixed displacement for an advancing triple line, and the line deformation is of the order of the pillar spacing, resulting in a nearly constant (and small) work of adhesion. In contrast, line deformation proceeds at a fixed force for a receding triple line (a peel force), giving a pronounced decrease of the work of adhesion as the pillar spacing increases and these opposite types of boundary conditions result in a strong contrast in energy barriers for advancing and receding triple lines [183].

Drop evaporation experiments were also used to monitor the transition of so called "Cassie state" to "Wenzel state" on superhydrophobic surfaces where a drop sitting on top of the microstructures plus air pockets collapsed down into the microstructures filling the space between the pillars [184–186]. McHale and co-workers followed the evaporation process for small water droplets from patterned polymer surfaces consist of circular pillars arranged in square lattice patterns [184]. Water droplets sitting upon the tops of the pillars initially evaporated in a pinned contact line mode, before the contact line recedes in a stepwise fashion jumping from pillar to pillar which mirrors the underlying lattice structure of the patterned substrate. In some cases, but not all, a collapse of the droplet into the pillar structure occurs abruptly. For these collapsed droplets, further evaporation occurs with a completely pinned contact area. A model depending of the diffusion of vapor into the surrounding atmosphere was used to describe the initial pinned contact line phase of evaporation quantitatively and fits the experimental points well [184].

Later, van Houselt and co-workers fabricated "omniphobic" surfaces by photolithography exhibiting high equilibrium contact angles ($\theta > 150^\circ$) for water, n-octane and olive oil and investigated the stability of droplets against wetting transitions during evaporation by systematically varying the shape and surface roughness of the micro-pillars on the surface [185]. They found that the apparent equilibrium contact angle of the droplets was not affected by increasing the roughness of the micropillars. van Houselt and co-workers concluded that the edge-curvature was the physical origin of an energy barrier and neither a Laplace-pressure driven mechanism nor a global interfacial energy argument describes the transition on these surfaces correctly, since they are not able to estimate the energy barrier that separates these states. They added new models are needed which include the hurdle of an energy barrier for the wetting transition [185]. Erbil reviewed the drop evaporation results in relation with the substrate effects [186].

Thormann and co-workers used the AFM colloidal probe technique to measure interactions between hydrophobized silicone pore array surfaces with two different pore spacings and a hydrophobic colloidal probe [187]. They found that neither the Wenzel nor the Cassier model could describe the wetting behavior of water contact angles which were not affected by the pore depth. The authors concluded that the position of the three-phase contact line, and not the interactions underneath the droplet, determines the contact angle. This contact line avoids the pores, creating a jagged line which explains the higher contact angle for the pore array surfaces compared to a chemically similar flat surface. Confocal Raman microscopy images demonstrated that water penetrated into the pores, but not necessarily filling them completely and some air pockets are present within the pores [187].

Extrand and Moon examined the relative importance of the contact line and interfacial areas in the capillary rise inside small diameter glass tubes with an intention that to compare the contact line/contact area controversy in a broader perspective by looking at other wetting geometries to gain better insight of the physical phenomena [188]. They showed that the increase in the wetted area within the tube did not affect the height of the meniscus. Then they coated lower part of the capillary tube with hydrophobic polystyrene (PS) and

immersed it into water and no water rose when water contacted with the PS surface only. However when they lowered the capillary tube farther into water down to a level until water contacted with the bare uncoated glass surface then water rose to the same height as the uncoated glass tubes and thus, it was shown that the change in liquid – solid interfacial area did not influence the height of capillary rise. Extrand and Moon concluded that the capillary rise phenomenon is only controlled by interactions in the vicinity of the three-phase contact line [188].

Wang and co-workers visualized the contact line distortion on heterogeneous and superhydrophobic surfaces and developed a unified model for CAH on these surfaces using a thermodynamic approach accounting for the effect of local energy barriers [189]. θ_a was found to be independent of the defect fractions on a surface for a low energy surface with high energy defects and matched the corresponding value on the homogeneous low energy surface. On the other hand, θ_r was influenced by the contact line distortion and depended on the relative fraction of the contact line. The fraction of the contact line on each surface was modeled and found to be a function of area fraction of the respective surfaces. The developed model showed good agreement with the experimental advancing and receding contact angles, both at low and high solid fractions [189]. Lv and Hao investigated the transportation mechanism of a water droplet on a microstructured hydrophobic surface experimentally and theoretically where the water droplet was driven by scale effect under disturbance and vibration [190]. When additional water is introduced to a drop or horizontal vibration is applied, the original water droplet could move unidirectionally in the direction from the small scale to the large scale on the microstructured hydrophobic surface in which the area fraction was kept constant, but the scales of the micropillars were monotonically changed. The authors stated that the Cassie model did not take into consideration the influences of topology and scale-effect on the wetting properties of a rough surface, so it could not be applied directly to predict apparent contact angle and droplet transportation behaviors in their experiments. In addition, Lv and Hao can successfully estimated the droplet transportation velocity by using the line tension on the solid–liquid contact boundary [190].

Nguyen and co-workers defined the center-to-center offset distance between successive square pillars in a column as eccentricity and determined that contact angles decreased with increasing eccentricity and increasing relative spacing between the pillars as seen in Fig. 7 and as the pillar relative spacing decreases, the effect of eccentricity on contact angles becomes more pronounced [191].

The authors reported that the dependency of contact angles as well as CAH on pillar eccentricity cannot be explained by the original form of the Cassie equation and they attributed the dependence of the contact angles on the pillar eccentricity to the contact line deformation resulting from the changed orientation of the pillars. It was shown that the length of the three-phase contact line increases with the decrease of the eccentricity value. At lower pillar spacing, contact line tends to pin to the pillars and the order of line tension becomes more significant [191]. Later, Nguyen and co-workers presented different techniques to describe the tortuosity of the three-phase contact line between the water droplet and microstructured surfaces [192]. Contact angles were measured by gradually rotating the sample at different viewing angles and it was found that the effect of changing the micro-pillar eccentricity on contact angles was much more pronounced. The authors reconstructed the corrugated shapes of the three-phase contact lines using the measured droplet aspect ratio (contact radius/height), and concluded that the noncircular corrugated shape of the three-phase contact line determines the energy barriers which is directly proportional with the degrees of anisotropic wetting and droplet distortion [192].

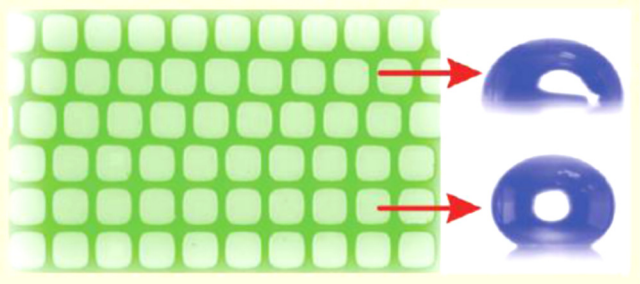

Fig. 7. Square micro-patterns having the same size and separation distance but different center-to-center offset distance (eccentricity) resulted in different contact angles.
Reprinted with permission from Ref. [191] Copyright (2012) American Chemical Society.

Olin et al. prepared three different superhydrophobic surfaces and investigated the water drop friction monitoring the motion of water drops during sliding down an incline using high-speed video and determined that the energy dissipation is dominated by intermittent pinning–depinning transitions at microscopic pinning sites along the trailing contact line of the drop for small capillary numbers [193]. Kim and co-workers derived modified forms of the Cassie and the Wenzel equations using energy minimization with simple mathematics and concluded that a contact angle on a real surface is only related to the infinitesimal region in the vicinity of contact line, not internal area surrounded by the contact line [194]. For this purpose, they re-defined the roughness factor which is related to only local region near contact line and area fractions in the vicinity of contact line. They also proposed that the area inside the contact line affects the total energy of the system, but not the contact angle and the contact angle is independent of the absolute value of the total energy since the contact angle satisfying the lowest energy is not changed [194]. Katariya and Ng examined discrete drop delivery from a continuous flow through an inclined superhydrophobic surface and found that the rear pinning of the three-phase contact line was strongly influential in drop retention, without any daughter droplet formation [195].

Bormashenko and co-workers published two papers in 2013 on contact line approach [196,197]. In the first one, they investigated the fine structure of the triple line for water droplets deposited on porous polymer substrates having

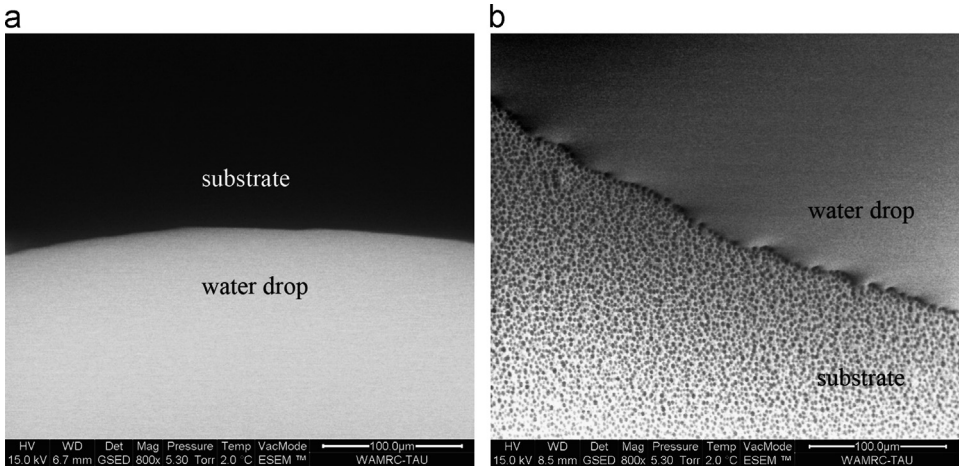

Fig. 8. ESEM images of the three-phase contact line on a (a) smooth and (b) heterogeneous polycarbonate surface. Reprinted with permission from Ref. [196] Copyright (2013) American Chemical Society.

honeycomb reliefs which were formed by the application of the breath-figures method [196]. The triple line was imaged with environmental scanning electron microscopy (ESEM) as seen in Fig. 8. The roughness exponent of a triple line was characterized with its averaged root-mean-square (rms) width $w(L)$, and its scaling experimental dependence upon the length L of the triple line, and the roughness exponent was found to be in the range of 0.60–063 indicating that the elastic potential of the triple line contains only even powers of the displacement [196].

In the second paper, Bormashenko and co-workers suggested that apparent contact angles are totally governed by the area of the solid surface adjacent to the three-phase contact line but the wetting regime is characterized by both apparent contact angle and the energy of adhesion and the energy of adhesion depends on the physical and chemical properties of the entire area underneath the droplet [197]. They deposited a droplet axisymmetrically on a superhydrophobic surface comprising a non-superhydrophobic spot to hold the drop strongly although the drop has a high apparent contact angle. The authors prepared rough surfaces by the hot embossing of low density polyethylene films where a microscaled stainless steel wire gauze was pressed with a manually operated hydraulic press at 105 °C forming hairy superhydrophobic LDPE reliefs. This patterned surface exhibited high apparent contact angles for water droplets (around 150°). Then, non-superhydrophobic spots with a characteristic size of 500 μm were formed on the "hairy" surfaces by pressing with a metallic needle at ambient conditions to destroy these "hairy" structures. Large area non-superhydrophobic rough surfaces had apparent contact angles of $120 \pm 5^{\circ}$ and high contact angle hysteresis. A water droplet of 4 μL remained attached to this surface even when they were turned upside down. The authors deposited a droplet axisymmetrically on the superhydrophobic surface comprising the non-superhydrophobic central spot and measured again high apparent contact angles of $150 \pm 3^{\circ}$ and a 2 μL droplet remained adhered to the surfaces even when they turned upside down which is an example of "rose petal effect". Then, the authors applied Dupré's "work of adhesion" equations to explain the drop adhesion situation. They finally suggested that not only apparent contact angle but also energy of adhesion are important for the correct characterization of the wetting situation and the energy of adhesion in turn is dictated by the total area of the solid surface wetted by a droplet. They also added that the apparent contact angles close to the triple line may lead to the misleading conclusion that wetting of a composite or rough surface is exhaustively characterized by considering the solid area in the nearest vicinity of the triple line which is a physical object, having a certain thickness and width; the last was estimated experimentally 2–5 μm [197]. This paper will be discussed in Section 5.

Amirfazli and co-workers developed a model to find the summation of surface tension forces along the three-phase contact line by integration along the contact line in order to calculate the drop adhesion force on smooth solid surfaces in the direction parallel to the substrate, for drops of arbitrary shape. The developed model was proposed to correct the perspective errors for any drop and contact line shape as long as there is no concave region on the contact line [198]. Gauthier et al. monitored the evaporation of liquid droplets on textured surfaces by measuring the evolution of the contact radius, drop height, and contact angle on both an axisymmetric surface (dartboard) and a periodic (square or checkerboard) surface as seen in Fig. 9 [199]. The authors also introduced a primitive 3D visualization of the drop shape near the edge by combining side and bottom views of the drop. The apparent contact angle was found to oscillate when the triple line recedes in all cases.

The authors determined that the triple line is pinned on a row of posts and the contact angle decreased as the drop evaporates for the axisymmetric surface and depinning occurs at the threshold angle, affecting the full contact line simultaneously where the intrinsic receding contact angle is the minimum contact angle, for which the tension applied to the triple line is maximum. However, the things are different for a drop evaporating on a periodic texture so that the protrusion on the edge interferes with contact angle in the opposite manner to reduce the contact angle by an amount which is inversely

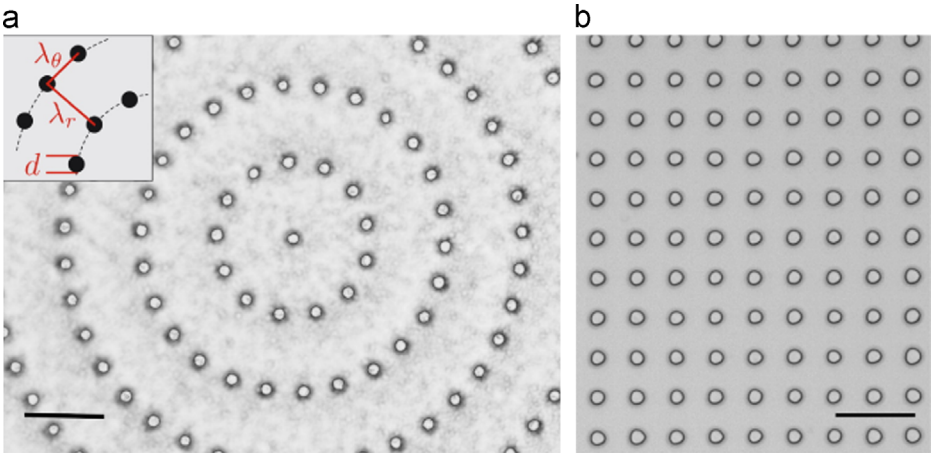

Fig. 9. Textures and geometrical parameters for (a) an axisymmetric surface (dartboard) with radial period $\lambda_r = 60$ μm and tangential period $\lambda_\theta = 30$ μm, (b) a periodic surface (checkerboard) with period $\lambda = 30$ μm. The pillar diameter is $d = 10$ μm, and the scale bar is 60 μm for both surfaces.
Reprinted with permission from Ref. [199] Copyright (2014) American Chemical Society.

proportional to the protrusion width and it is the maximum contact angle which is closest to the intrinsic contact angle [199].

4. Publications directly supporting interfacial contact area approach

4.1. Before Gao and McCarthy publication in 2007

Wenzel [14] the length of the asperity perimeter per unit area than the plan surface area if the surface of a substrate is rough and then related the contact angles with the geometric roughness factor, r^W, as given in Eq. (14) by comparing the actual liquid/solid interfacial area with the plan area in 1936. Wenzel assumed that the drop liquid fills up the grooves completely on a rough surface and a greater amount of actual surface is wetted under it if the surface of the solid is rough than if it is smooth. Consequently, for the process involving the rough surface, there is a greater net energy decrease to induce spreading, and the rough surface is wetted the more rapidly [14]. Cassie and Baxter considered the interfacial area fractions of solid and air pockets on a solid contacting with the drop liquid and derived an equation to calculate the apparent contact angle on a porous surface from these area fractions in 1944 [16]. Later, Cassie extended this analysis to rough and chemically heterogeneous surfaces using the same interfacial area fraction approach in 1948 [17]. Good derived a thermodynamic form of the Young's equation using surface free energy approach by using the Wenzel's equation [69].

Johnson and Dettre investigated contact angle hysteresis on idealized sinusoidal rough [72], and idealized heterogeneous surfaces by applying free energy approach [51,72–74]. They used idealized heterogeneous surfaces by postulating that a liquid drop is at rest on a solid surface consisting of alternating circular bands of different surface energy (concentric ring model) where the boundary is assumed to contribute no surface energy to the system and there is an energy barrier between each two positions of metastable equilibrium. The drop periphery moves over the barrier regions and this model provides for an infinitely sharp transition between regions of different surface tensions. The values of these free energies and free energy barriers control the contact angle hysteresis of the system. Free energy barriers hinder the attainment of a minimum free energy. They concluded that the contact angle which will actually be observed in a real system will depend on the energy barrier heights and on the ability of a drop to cross over these barriers [51].

On the other hand, Cassie and Wenzel equations were used to derive new terms such as “Cassie state” and “Wenzel state”. “Cassie state” term was used especially for patterned surfaces having micromachined posts as where drops suspended on top of roughness features and “Wenzel state” where drops impaled on roughness features [200–206]. The wetting transition from the Cassie to the Wenzel states has been studied both experimentally and theoretically. Marmur combined contact area based Cassie and Wenzel equations into a more general form and investigated the conditions for determining the transition between the homogeneous and heterogeneous wetting regimes [200]. Later, Marmur proposed that both the Cassie and Wenzel models are approximations that become better in predicting contact angles as the drop size increases compared to the size scales of the features and recommended to use large drops in order to assure the validity of the Wenzel and Cassie equations, enables axisymmetry, and minimizes the dependence of the advancing and receding angles on the drop volume. Marmur also advised that vibrations should be applied, either to overcome energy barriers and get to the most stable state [201]. These views was replied by Gao and McCarthy [172,173] and will be discussed in Section 5.

On the other hand, the occurrence of the so called “Cassie state” and “Wenzel state” can be possible simultaneously on the same superhydrophobic surface depending on how drops are deposited and some researchers investigated the method of drop deposition on the superhydrophobic surfaces, such as drops are dropped from some height or mechanically pressed on these surfaces [202–207]. Quere and co-workers proposed

that the main parameter that determines the contact angle of a drop on a hydrophobic rough surface is the fraction of solid actually in contact with the liquid and not the surface roughness [202]. The thermodynamic stability of these states was also investigated in detail by using Cassie and Wenzel equations and specific plots were drawn for this purpose [203–205]. Patankar stressed that it is not guaranteed for a drop that it will always exist in the lower energy state; rather, the state in which a drop will settle depends on how the drop is formed. Water may fill the grooves below the contact area of a Cassie drop but the liquid–solid contact is yet to be formed at the bottom of the valleys. Even, if the Wenzel state is at a lower energy, it does not necessarily mean that a drop must transform into that state. It will do so only if it can overcome the energy barrier for this transition [206]. Dorrer and Rühe studied the transition of Wenzel state to the Cassie state on microstructured post surfaces coated with a hydrophobic fluoropolymer by applying drop condensation using a Peltier cooling stage [207]. The condensation of water leads to the formation of small droplets in between and on top of the posts. These drops grow and coalesce over time, leading to the formation of drops that are in the Wenzel state and also partially in the Cassie and partially in the Wenzel state. Drops in the Wenzel state are energetically metastable and Wenzel-to-Cassie transitions are possible in principle but dewetting from the Wenzel state does not happen quantitatively. For example, Wenzel drops in contact with more than four square posts experience stronger pinning and do not transition to the Cassie state. But if microscopic droplets are in contact with four posts only then these droplets grow upward through continued water vapor condensation until they have filled the entire volume between the four posts. If, at this stage, the drop comes into contact with a Cassie drop, coalescence occurs, and the pinning forces are overcome, resulting in a drop that is in the Cassie state [207].

Bhusan et al. investigated the transition from the Cassie state to the Wenzel state and pointed out that the transition occurs at a critical value of a non-dimensional spacing factor parameter which is independent of the actual size of the roughness [208]. The spacing factor is equal to the cylindrical pillar diameter divided by the pitch (the distance between the centers of the posts). They stated that this result is different from the energy minimum criterion proposed by Lafuma and Quere earlier [205]. Bhusan et al. reported that the contact angle hysteresis on these micropatterned surfaces also depends upon this non-dimensional spacing factor and was found to be independent of the actual size of roughness [208]. Wang and Jiang defined a new state named "Gecko state" where the air pockets are sealed beneath the droplet [209]. This is different from the Cassie state where the air pockets below the drop are connected to the atmosphere. The sealed air pockets in the Gecko state introduce high adhesive properties to the substrates such as superhydrophobic aligned polystyrene [210].

4.2. After Gao and McCarthy publication in 2007

After Gao and McCarthy published their important paper entitled "*How Wenzel and Cassie were Wrong*" [13] and claimed to disprove these two equations in 2007, stating that "*all of the data presented in this paper indicate that contact angle behavior* (*advancing, receding, and hysteresis*) *is determined by interactions of the liquid and the solid at the three-phase contact line alone and that the interfacial area within the contact perimeter is irrelevant*"; contrary to the expectations of approval of these new findings, some of the scientists working in the contact angle field responded to and defended the use of Cassie and Wenzel equations.

McHale published a paper entitled "*Cassie and Wenzel: Were They Really So Wrong*?" in 2007 [211]. He mainly suggested that the Cassie surface fraction and Wenzel roughness parameter should be viewed as global properties of the surfaces rather than properties of the surfaces defined by the contact area of a droplet, and yet the surfaces can be described by these equations provided the surface fraction and roughness parameters are reinterpreted to take local values appropriate to the droplet perimeter. McHale reviewed the theoretical basis of the Cassie and Wenzel equations and proposed that these models are not so much wrong as have assumptions that define the limitations on their applicability. He derived versions of the Cassie and Wenzel equations involving roughness (r^W) and Cassie solid fraction (f_i) functions local to the three-phase contact line on the assumption that the droplet retains an average axisymmetry shape. After applying the well-known liquid/solid contact area approach, he emphasized that the original Cassie surface fraction and Wenzel roughness parameter should be viewed as global properties of the surfaces rather than properties of the surfaces defined by the contact area of a droplet.

McHale discriminated between the single defect experiment as presented by Gao and McCarthy and possible polydefect experiments and stated that a single small circular area (referred to a "defect" in McHale's article) within a larger area do not satisfy the assumption of "everywhere similar and isotropic" surface and so Cassie fractions cannot be used for comparison and disproof in the Gao–McCarthy paper. McHale stated that one could randomly choose a small part of the surface and would not be able to identify where on the surface the location was or identify an orientation simply by looking at the structure of the chosen small surface area in order to obey the "everywhere similar and isotropic" conditions. He proposed that a surface with small randomly placed defects, chemical or topographic, satisfies this assumption, but one with a single defect does not. He suggested that the original Wenzel and Cassie equations based on surface areas under a droplet are restricted in applicability to quite specific types of surfaces. These should be surfaces for which the roughness and surface fraction parameters are everywhere constant and which do not have values dependent on the location of the droplet or the size of the droplet contact area. McHale agreed with Gao–McCarthy [13] and also with Extrand [12] that it is the interactions at the three-phase contact lines that determines the contact angle for the cases where a drop sits on a single defect area. He pointed out, it is not appropriate to claim that the original Wenzel and Cassie equations are wrong, but one would say the experimental situation does not match the assumptions of the models [211].

On the other hand, McHale also indicated that the definition of droplet perimeter does not necessarily coincide with the three-phase contact line for superhydrophobic surfaces and the three-phase contact lines within the contact perimeter beneath the droplet can be important in determining the observed contact angle on superhydrophobic surfaces [211]. When a set of separated micro- and nanofabricated posts are used to form a superhydrophobic surface, it is possible to imagine an idealized "contact" perimeter to the droplet, but in doing so it is not a continuously connected three-phase contact line because there is a closed three-phase contact line at the top of each of these posts in the "contact" area under the droplet and this idealized circular contact perimeter does not include the entire set of three-phase contact lines. Without these contributions, the droplet would not remain in a suspended state, but would collapse into the surface structure under the weight of the droplet. When we minimize the surface free energy of a droplet, we assume that no change in penetration into the surface occurs (i.e., that no displacement of these interior three-phase contact lines occurs), but this is not true for many experimental cases such as evaporatively induced change of state which cause the transition to a Wenzel state [184]. Some of the views of McHale were replied by Gao and McCarthy [172,173].

Nosonovsky proposed that the Wenzel equation is valid for uniformly rough surfaces, that is, surfaces with r^W=constant, whereas for non-uniformly rough surfaces which was used by Gao and McCarthy, another form of Wenzel equation generalized by assuming that r^W is a function of coordinates, x and y [$r(x, y)$] should be used to determine the contact angle with a rough surfaces at the triple line [212]. Nosonovsky recalled that the forces in physics are defined as derivatives of the energy by corresponding generalized coordinates, so the question of whether the forces or the energy governs a physical phenomenon is similar to the chicken and egg problem and the concepts of the surface energy and the surface tension are, in a sense, equivalent. By using the liquid front advance on a rough surface on a 2D sketch, Nosonovsky showed that the derivative $r^W = dt/dx$ is equal to Wenzel's roughness factor (dt is equal to the distance along the curved surface and dx to the distance along the horizontal surface) in the case when the roughness factor is constant throughout the surface. However, Nosonovsky did not compare his $r^W = dt/dx$ with the original Wenzel $r = A_{actual}/A_{plan}$ ratio in his analysis. He also derived a generalized Cassie equation by the same manner that Cassie area fractions, f_1 and f_2 can be described as $f_1(x,y)$ and $f_2(x,y)$ by introducing the local densities of the two components that compose the heterogeneous surface. Nosonovsky proposed that these generalized equations can be used for the more complicated case of non-uniformly rough surfaces and assumed that the work reported by Gao and McCarthy was an example of this case [212].

Nosonovsky also discussed the size of roughness and heterogeneity for the use of these generalized equations. He proposed that the triple-line zone has two characteristic dimensions: the thickness (on the order of molecular dimensions) and the length (on the order of the droplet size) and the apparent contact angle may be viewed as the result of averaging the local contact angle at the triple line by its length, and thus the size of the roughness/heterogeneity details should be small compared to the length (and not the thickness) of the triple line. He stated that the generalized Wenzel and Cassie equations can be used on the scale when the sizes of the solid surface roughness/heterogeneity details are small compared with the size of the liquid–vapor interface, which is on the same order as the size of the droplet [212]. Some of the views of Nosonovsky were replied by Gao and McCarthy [172,173].

Panchagnula and co-workers pointed out that the three-phase contact line on square pillars (poles) are different than that of on surfaces where square holes (cavities) are present in 2007 [213]. These patterned substrates were both created using silicon wafers by a wet-etching process. In the case of pillars, three-phase contact line of a drop suspended on the surface is discontinuous and in the form of square loops around the tops and edges of the wetted pillars and only an apparent two-phase contact line is formed as a crease on the continuous liquid–vapor surface as it is folded between the pillars. However, the three-phase contact line is a real, continuous line on the solid parts in the case of a drop placed on a surface containing holes. They found that, advancing contact angle of the water drop increases linearly with an increase in the area void fraction for surfaces with periodically placed pillars indicating that the Cassie theory predictions fit the experimental results well. However, the contact angle is seen to be independent of the area void fraction for the cases where a drop is located on the surface with square cavities. Furthermore, it was found that the contact angles for the specimens with square cavities are greater than those of pillars over the range of area void fractions investigated. Panchagnula and co-workers attributed this violation from the Cassie theory to the fundamental difference in the three-phase contact line topology-continuous for cavities and discontinuous for pillars. They pointed out that they provided experimental evidence of a failure of Cassie theory even with surfaces whose heterogeneity length scale is much smaller than the length scale associated with the drop [213].

Later Panchagnula and Vedantam directly criticized the comments of Gao and McCarthy [13] on their "*How Wenzel and Cassie were Wrong*" paper suggesting that both Gao and McCarthy and also Extrand [12] wrongly used the Cassie's equation in their analysis [214]. They proposed that in order to apply the Cassie's equation, the surface area fractions, f_1 and f_2, of the solid heterogeneous surface that is about to be wetted by the advancing three-phase contact line as inputs and not those of the entire drop footprint and the disagreement between Cassie theory and Gao–McCarthy and Extrand's experiment does not arise from a fault with Cassie theory but from an incorrect choice of surface area fractions [214]. Gao and McCarthy replied these unjustified attack to their former papers findings in a new paper published in Langmuir (in the same issue) and pointed out that this important subject is not a matter of semantics and wrong misconceptions and their results point blank disprove Wenzel's and Cassie's theories as

given in Section 3.2 [163]. Panchagnula and Vedantam's views were further replied by Gao and McCarthy in 2009 [172,173].

Bormashenko published a paper entitled "*Why does the Cassie–Baxter equation apply*?" in 2008 [215]. He proposed that a drop can sit on the air pocket but the three-phase contact line cannot and the same is true for the situation when air pockets are filled with water where the contact line can only sit on solid area. Bormashenko also assumed that the drop is surrounded by a thin precursor film of liquid which diminishes the energy excess connected with the triple line bending. He added that the presence of a thin precursor film on the hydrophilic and pseudo-partially wetted surfaces is thermodynamically favorable. This precursor film advances for a distance of *dx* forming an effective surface area around the triple contact line according to the virtual work principle. Bormashenko stated that the drop radius should be much larger than the characteristic dimension of the interface heterogeneities and the substrate area adjacent to the triple line and located under the precursor film exerts an influence on the apparent contact angles. In addition, this effective area should be much larger than the cross-section of one pocket or spot of solid. The author concluded that if these limitations are fulfilled, the Cassie equation may be applied for calculation of apparent contact angles [215]. Bormashenko and co-workers published the rigorous derivation of Young, Cassie–Baxter and Wenzel equations by assuming the liquid/solid contact area under the drop is operative and the analyzed the contact angle hysteresis phenomenon in a second publication in the same year [216]. There are contradictions in the insights of these two publications and unfortunately no conceptual comparisons were made between them.

Nosonovsky and Bhushan claimed that Wenzel and Cassie equations fit the experimental data well and the only question remains as to under what circumstances the Wenzel and Cassie equations can be used and also the stability, and transitions between these states are important [217]. This paper is somewhat a continuation of Nosonovsky's 2007 paper [212]. The authors suggested that Wenzel and Cassie equations relate the local contact angle with the apparent contact angle of a rough/heterogeneous surface by averaging the former. They stated that the triple contact line has two very different length scales: its width is on the molecular size scale and its length is on the order of micrometers or millimeters and the roughness details should be small compared to the size of the droplet (and not on the order of the molecular size). They concluded that normal Wenzel and Cassie equations can be used for the cases where uniform roughness/heterogeneity is present and when a more complicated case of nonuniform heterogeneity is present, then the "generalized" Wenzel and Cassie equations should be used [217].

Chen and co-workers fabricated a series of square pillar patterns using silicon wafers and modified by a self-assembled fluorosilanated monolayer and reported that the dynamic contact angles of water on these patterns were found to be consistent with the theoretical predictions of the Cassie and the Wenzel model [218].

Marmur extended his previous analysis [200] where he combined the Cassie and Wenzel equations into a more general form to investigate the possibility of making high-contact-angle, rough surfaces from low-contact-angle materials in 2008 [219]. He proposed that it is possible to make a superhygrophobic (very high contact angle) surface from a hygrophilic (low contact angle) material if the roughness topography is multi-valued. The hygrophobicity in such situations is based on the heterogeneous wetting regime, where air is trapped beneath the liquid inside the roughness valleys. However, this is only possible for the cases where the feasibility condition is fulfilled, which means that the Gibbs energy does not have a saddle point [219]. In 2009, Marmur published two new papers both defending the contact area approach [220,221]. The first one is a review on the solid surface characterization by wetting with the objective of reporting the current status of the theories that are required for the correct measurement and interpretation of equilibrium contact angles [220]. Marmur commented that the validity of the Wenzel and Cassie equations has been challenged recently [12,13] but the experimental data to disprove these equations were based on experiments employing only a very limited range of drop volumes and the size of the drop was bigger than the heterogeneity scale by a relatively small factor of at most 2.5 (he means that the drops were too small). Then, Marmur claimed that the initial experiments done with bigger drops [222] seem to confirm the theoretical validity of these equations for large volume drops. He suggested the drop becomes more axisymmetric as its size increases and when the drop is not sufficiently large, the deviations from the shape it would have had on an ideal surface (e.g., a spherical shape when gravity is negligible) may be major. Marmur also proposed that the main experimental challenge is the measuring of the apparent contact angle that can yield the Young contact angle and the best option is to measure the "most stable contact angle" of a large drop because there are theories to calculate the Young contact angle from the "most stable contact angle". But experimental determination of the "most stable contact angle" is still under development and some promising experiments have attempted to reach the most stable CA by applying vibrations [220]. Marmur's comments were thoroughly replied by Gao and McCarthy [172,173].

In the second paper of 2009 entitled "*When Wenzel and Cassie Are Right*: *Reconciling Local and Global Considerations*", Marmur and Bittoun directly commented on the contact line/contact area problem [221]. They stated that local conditions at the contact line determine the actual contact angles, and global considerations regarding the solid–liquid interfacial area determine the "*most stable contact angle*" which is the one predicted by the Wenzel or Cassie equation if the drop is sufficiently large compared with the wavelength of roughness or chemical heterogeneity. They criticized that the experiments [12,13] were performed only for drops of sizes similar in order of magnitude to the wavelength of roughness or chemical heterogeneity and the Wenzel and Cassie equations are a priori not expected to be valid under such conditions [222]. Gao and McCarthy also replied these objections as given in Section 3.2 [172,173].

Choi et al. fabricated a range of model superoleophobic surfaces with controlled surface topography and deposited

uncured 30–50 μL polydimethysiloxane (PDMS) drops having high viscosity (μ=5500 mPa s), on these hoodoo surfaces that had previously been dip-coated with low surface energy fluorinated molecules. The stage was tilted by 10–30° to force the PDMS drops to advance or recede along the inclined hoodoo surface. The PDMS drops were then thermally cured at 85 °C for 30 min to obtain the profile of three-phase contact line, however the long equilibration time of the uncured PDMS droplets, resulting from their high viscosity makes them unsuitable for contact angle measurements. Therefore, another organic liquid, decane on a fluoro-POSS dip-coated smooth silicon wafer was chosen for the contact angle measurements because it possesses a surface tension and equilibrium contact angle that are similar to the values of the PDMS oil used in our imaging. (This indicates that contact angle results of decane drops were compared with the three-phase contact line profile of PDMS drops in this work, a method which is very unusual.) The authors reported that their experimental studies of both the local distortion of the three-phase contact line at the micron scale, as well as the measurement of the apparent contact angles at the macroscopic scale, clearly illustrates that the distortion of the three-phase contact line per se was not the key factor that leads to differences between the predictions from the Cassie equation and the measured values of the apparent advancing or receding contact angles. Instead, they claimed to show that the differential areal fraction of solid substrate which the three-phase contact line encounters as it is displaced across the surface is the most important factor in determining the apparent advancing and receding contact angles. Choi et al. proposed a modified Cassie equation which was claimed to predict more accurately the apparent advancing and receding contact angles [223].

Spencer and co-workers fabricated randomly placed holes and pillars by means of photolithography using four different surface chemistries: native PDMS, perfluorosilanized PDMS, epoxy, and CH3-terminated thiols on gold and measured contact angles in order to investigate the solid area fraction (f_1) and air area fraction (f_2) with the contact angles [224]. They determined that the static contact angles increase more or less linearly with f_2, indicating the importance of f_1 and f_2 for the wetting behavior of a drop in the Cassie state. Since the topographical structures here are small compared to the drop diameter, the area parameters f_1 and f_2 can also be considered as line parameters influencing the contact line [224].

Patankar and coworkers checked experimentally the applicability of the Cassie equation to predict the apparent contact angle of a drop on rough hydrophobic surfaces [225]. Square pillar and hole arrays were fabricated on a silicon surface by using deep reactive ion etching technique and coated with a fluorosilane. The authors reported that the Cassie formula was found to be relevant in general to model the apparent contact angle on rough surfaces. The method based on minimization of interfacial energy is not incorrect but is in fact formally equivalent to force-balance-based approach. Cassie equation is an approximation and does not represent the actual contact line configuration during advancing or receding if pinning occurs. However, it is improper to consider the Cassie formula to be unrelated to contact line configuration. Deviations of the apparent contact angle from the Cassie angle were seen for the advancing front on pillar type roughness and can be correlated with distortions of the actual contact line, due to pinning [225].

Milne and Amirfazli discussed the correct use of Cassie equation and pointed out that the majority of papers cite a potentially incorrect form of the Cassie equation to interpret or predict contact angle data [226]. They suggested that for micro-patterned rough surfaces, the commonly applied form of the Cassie equation, $\cos\theta_c = f\cos\theta - (1-f)$ can be only used for the special case of flat topped pillar geometry without any penetration of the liquid. However, the liquid–vapor interface can contain appreciable corrugations (i.e. roughness) of its own by means of excessive curvature of the interface due hydrostatic pressure or exposure of the drop to pillars of different heights, or penetration into the larger scale of a dual scale structure and regardless of cause, the air surface area fraction, f_a, cannot be calculated by $f_a = (1-f)$, since $f_a \neq (1-f)$ is a general statement and therefore, $(f_a + f \geq 1)$ should be used. The differences between the two equations were discussed in the text and the errors involved in using the incorrect equation were estimated to be between ~3° and 13° for superhydrophobic surfaces [226].

5. Discussions and comments on some important papers

5.1. Experimental use of contact angles

An ideal solid surface is assumed to be atomically flat and chemically homogenous by definition however, in reality there is no such an ideal solid surface, and all the real solid surfaces are often very uneven and thus the contact angle characterization is usually a difficult task. As seen in the brief history (Section 1.1) and contact angle measurement sections (Section 1.2), contact angles are determined by industrial and academic researchers, analytical personnel, and production line workers for mainly practical purposes, such as investigating new surfaces, quality control during a production etc. and the applications of contact angles in the academic or industrial research are very wide (see Section 1.3). It was recommended that advancing, receding and static apparent contact angles must be measured all together in order to determine the properties of the surface under investigation [3–5,18,59]. Contact angle hysteresis must also be reported along with these contact angles since it is a meaningful measurement of surface roughness, chemical heterogeneity [4,18,116–118], shear hydrophobicity, drop rolling, fouling-release properties for cells and biomaterials such as sporelings of the green alga *Ulva* [227], blood platelets and some proteins [228]. Meanwhile, we should avoid incorrect models, and ill-defined terminology which are confusing and can be destructive in the contact angle field [173].

At present, it is clear that the advancing and receding contact angles are governed by events that occur at the three-phase contact line [11–13,114,172–174,177,182,183,187,190–197]. On the other hand, we should be careful that the apparent contact angles are not equal to neither advancing nor receding

contact angles, and usually much different than that of the sometimes measured local contact angles formed by the precursor liquid films on a surface. However, we also need the apparent contact angle values for the surface free energy calculations (see Section 2.4) especially for applied research purposes and if we have only advancing or receding contact angle values at hand, then the most practical way is to use the advancing contact angle value instead of the apparent contact angle value for further calculations.

Theoreticians in the surface science are free to invent new contact angle types in order to explain the various complex problems of wetting. However, these contact angles must be measurable, and the novel theories must be testable by the experimentalists. As pointed out by Gao and McCarthy [172], none of the various contact angles defined by Marmur [222] namely, actual CA, Young CA, geometric CA, apparent (equilibrium) CA, Cassie CA, Wenzel CA, local Young CA, and most stable CA can be measured without special instruments (and some cannot be measured at all) and none of them (as individual values) are sufficient to describe the water repellency. It is also nearly impossible for any experimental surface scientist to be concerned with the wavelength of surface roughness or chemical heterogeneity, and not be concerned with the ratio of drop size to wavelength before any contact angle measurement.

Researchers or technical personnel should avoid using large drops in order to prevent the introduction of the gravity effects which will flatten the drop (drop volumes of 2–8 μL are generally used in contact angle practice). It is well known that when surface roughness or chemical heterogeneity is too large, stick-slip movement of drops generally occurs and θ_a and θ_r cannot be measured properly and increasing the drop volume does not help to overcome this problem [115,172,230]. The claim of the "*Wenzel and Cassie equations become valid with very large drops and small-wavelength roughness or chemical heterogeneity*" is meaningless from this point of view. It should be remembered that the size of the drop and the wavelength of roughness or chemical heterogeneity was never an issue of the original Wenzel and Cassie–Baxter papers. We agree with the statements of Gao and McCarthy that "*If experimentalists obey the rules of theorists on the use of equations for only specific cases, then they would not be able to analyze many surfaces because the objects would be too small and the instruments would need to be replaced with those of different design*" [172]. The use of drops having 2–8 μL volumes is suitable us to characterize the surfaces with all wavelengths of structures for our research or industrial needs in the well-known conventional contact angle measurement techniques. In addition, the contact angle measurements with the application of horizontal and vertical vibrations should not be used for practical purposes and can be only used to investigate the dynamics of drops on surfaces when required.

On the other hand, new microscopic techniques such as environmental scanning electron microscopy (ESEM), atomic force microscopy (AFM), interference microscopy and confocal microscopy are under use especially in the last decade to measure contact angles of very small droplets and provide more inside into contact line pinning [196,217,231–249]. ESEM technique can be used to obtain images even under liquids and was applied in the contact angle field several times [196,217,232–237]. The use of AFM in the contact angle field for ultra small droplets has a long history [238–245]. Confocal microscopy is preferably applied for droplets having a contact angle range of 30–90° thus allowing the collection of a larger number of image slices from which the drop profile can be reconstructed [246,247]. Interference microscopy is generally used for droplets having low contact angles less than 30° where the fringe patterns formed by the interfering beams reflected from the solid–liquid and the liquid–vapor interfaces are used to calculate the contact angle value [248,249]. Confocal and interference microscopy methods are mostly used for droplets with diameters of about 10 to 100 μm. A combination of interference microscopy and confocal fluorescence microscopy is offered to study the contact angles of micrometer-sized water droplets [247]. It is possible that the information obtained by using these new microscopic techniques would help for the better understanding of the contact angle phenomena.

5.2. Problems related with the solid surface area minimization

A liquid surface attains equilibrium almost as soon as it is formed because of the mobility of surface molecules. Contrary to the behavior of liquid molecules, the surface molecules of solids are practically fixed in position and they cannot move to any other place. Individual atoms and molecules are only able to vibrate around their mean position. Thus, most solids are incapable of displaying faces demanded by the macroscopic minimizing of surface free energy [4,63] and they are incapable of adjusting to such equilibrium conformations and in practice their surface structure will be largely a frozen-in record of an arbitrary past history where some imperfections, humps and cracks are present [4,62]. Consequently, solid surfaces cannot spontaneously contract to minimize their surface area and a non-equilibrium surface structure forms. However, this does not mean that the surface tension is absent in solids: In principle, the surface tension also exists in all solids and the inward pull on the solid surface atoms are always present, due the cohesion between molecules similar to liquids; nevertheless the changes of surface shape due to the surface tension in solids are very much slower (if not completely prevented) in solids than in liquids; this is not due to the cohesion forces being absent, but the mobility of surface molecules (or atoms) being very much less.

In addition, when the surface area of a liquid decreases, then the number of surface molecules (or atoms) decreases in proportion according to the Gibbs equation, whereas for solids such a spontaneous decrease in surface molecules is very limited. Instead, when the surface area of a solid is decreased by compressing it mechanically, then the distance between neighboring surface molecules (or atoms) changes with the decrease in the area, while the number of surface atoms remains constant, in most cases. Thus, it is convenient to

define "*surface tension of solids*" in terms of restoring force necessary to bring the freshly exposed surface to its equilibrium state. However, the definition of "*surface free energy of solids*" is equal what we said for the liquids, it is the work spent in forming unit area of a solid surface. It is clear from the above argument that the surface tension ≠ the surface free energy for solids. Thus, the laws of capillarity of liquids cannot be applied to solids. These fundamental points are recently revisited by Snoeijer and Andreotti [250,251]. The authors concluded that for liquid surfaces, the absence of liquid above the liquid–vapor interface creates an attractive anisotropic force within a few molecular lengths from the interface, but the repulsion scales with the local density of the fluid since it remains isotropic. Then, the strong surface tension force which is parallel to the interface is formed due to the attractive anisotropy. It is suggested that this anisotropy and corresponding tangential force occurs at liquid–solid interfaces as well, whereas the half-space of liquid missing and the surface tensions γ_{SL} and γ_{SV} do not pull on the solid however the resultant force on the liquid near the contact line does involve the surface tensions γ_{LV}, γ_{SL}, and γ_{SV} [250].

Interfacial tension between two liquids is defined as the force that operates inwards from a surface perpendicular to each phase tending to minimize the area of the interface since the liquid molecules at the interphase are mobile. However, for a liquid–solid surface, the solid molecules at the interface are not mobile and cannot contribute to the area minimization process as given above. But a local equilibrium forms between a solid and an adjacent liquid phase at the three-phase contact line (even though non-equilibrium in larger sense) in terms of van der Waals, polar and hydrogen bonding interactions [62]. However, we also do not know the extent of mobility of the liquid molecules at the solid–liquid interphase. Thus, it is most probable that the area minimization process never occurs and the usual contact area based thermodynamical equations for the interfacial free energy ($-\Delta G^a_{SL} = W^a_{SL}$) are not valid including Young–Dupré's [Eq. (12)], Wenzel's [Eq. (14)] and Cassie's equations [Eqs. (15)–(17)] for the interactions at the solid/liquid contact area underneath the drop.

Meanwhile, Young's equation is valid locally because its derivation via the force based vectorial summation on a line does not have such a default. However, the apparent contact angles on a surface cannot be assumed as the arithmetic average of all the local Young angles on the three-phase contact line on a rough and heterogenous surface. The reasons are given below: If the solid surface is largely heterogeneous, or rough then the local contact angles obeying Young's equation will be local equilibrium ones and different in quantity on various parts of the surface. Consequently, varying local curvatures will exist on the drop and there will a natural tendency for the liquid drop to extend over low contact angle regions and to retreat from high contact angle ones. The average contact angle will then reflect both the surface forces of the solid and the topology of surface heterogeneities and surface free energy based thermodynamic equations cannot be successfully applied for such a case [62]. On the other hand, if the solid surface is considerably flat and homogeneous, the average apparent contact angle measured on this surface represents all the possible local contact angles on this solid surface much better than that of a heterogeneous and rough one. Although not very consistent scientifically, the solid free energy calculation methods given in Section 2.4 can be used for such considerably flat and homogeneous surfaces especially to provide solutions for research and practical industrial needs.

Recently, Bormashenko and co-workers published a paper suggesting that apparent contact angles are totally governed by the area of the solid surface adjacent to the three-phase contact line but the wetting regime is characterized by both apparent contact angle and the energy of adhesion and the energy of adhesion depends on the physical and chemical properties of the entire area underneath the droplet [197]. This paper mixes two contradicting concepts in a single conclusion and must be read with caution. When we examine their experimental part, we understand that the authors prepared rough surfaces by the hot embossing of low density polyethylene films where a microscaled stainless steel wire gauze was pressed with a manually operated hydraulic press at a high temperature forming hairy superhydrophobic polyethylene reliefs. This patterned surface exhibited high apparent contact angles for water droplets (around 150°). Then, non-superhydrophobic spots with a characteristic size of 500 μm were formed on the "hairy" surfaces by pressing with a metallic needle manually at ambient conditions to destroy these "hairy" structures. Large area non-superhydrophobic rough surfaces had apparent contact angles of $120 \pm 5^\circ$ and high contact angle hysteresis. A water droplet of 4 μL remained attached to this surface even when they were turned upside down. The authors deposited a droplet axisymmetrically on the superhydrophobic surface comprising the non-superhydrophobic central spot and measured again high apparent contact angles of $150 \pm 3^\circ$ and a 2 μL droplet remained adhered to the surfaces even when they turned upside down which is an example of "rose petal effect". Then, the authors applied Dupré's well-known "work of adhesion" equations to explain the drop adhesion to solid. They finally suggested that not only apparent contact angle but also energy of adhesion are important for the correct characterization of the wetting situation and the energy of adhesion in turn is dictated by the total area of the solid surface wetted by a droplet. They also added that the apparent contact angles close to the triple line may lead to the misleading conclusion that wetting of a composite or rough surface is exhaustively characterized by considering the solid area in the nearest vicinity of the triple line which is a physical object, having a certain thickness and width; the last was estimated experimentally 2–5 μm [197].

We will discuss the problems related with the width of the three-phase contact line as a separate section given below. Here, we have to point out that some level of experimental standards are required to define flat spots by destroying "hairy" structures with a needle manually where the spot was somewhat flattened by the pressure of a needle in a very rough way. The authors could not measure the area beneath the droplet and they do not know the fractional areas of water/solid and water/

air pockets on these needle-made complex polymer surfaces. They assumed that there was a complete liquid/solid interfacial contact beneath the droplet and used well known contact area based Young–Dupré's work of adhesion equations to develop a new theory. At the end, the final conclusions regarding to the energy of adhesion in turn is dictated by the total area of the solid surface wetted by a droplet are drawn from the ill-prepared and ill-defined spots under the drops. Such an approach introduces new confusion to this highly debatable contact angle field. More carefully planned and executed experiments are needed to investigate the "rose petal effect" and to make such very important conclusions.

5.3. Problems related with the free energy calculations from lines

From elementary physics and thermodynamics, we know that the work function can be calculated by using forces and distance as $[dW = Fdx]$. Pease proposed that the line of junction can occupy various possible parallel positions on the plane of the solid surface, and different positions allow different mean works of adhesion depending upon the configuration of the different chemical groups exposed on the solid surface [11]. A large apparent water contact angle can be obtained when the three-phase junction line passes across the largest possible number of non-polar groups (or air) and avoids as many hydrophilic groups as possible. The physical system that determines the apparent contact angle is the mean work of adhesion that can be calculated from all the configurations that the three-phase junction line can assume. However, regarding to advancing contact angles, greatest work must be applied to overcome the greatest possible resistance created by the structures and chemical heterogeneities on the surface, and the mean work of adhesion between the drop and the surface is minimal for this case. On the other hand, regarding to receding contact angles, we are dealing with the drop removal process from a wet surface where there is a strong work of adhesion is already present at this time, and we must apply a work which will overcome the maximum mean work of adhesion. At present, we know that three-phase contact line can occupy various positions on the rough micro-patterned surfaces in the 3D space rather than residing on a 2D plane since the tortuosity of the contact line between neighbor pillars do not allow it to reside only in a horizontal 2D plane located between the drop and solid. Kim and co-workers derived modified forms of the Cassie and the Wenzel equations using energy minimization with simple mathematics and concluded that a contact angle on a real surface is only related to the infinitesimal region in the vicinity of contact line, not internal area surrounded by the contact line [194]. For this purpose, they re-defined the roughness factor which is related to only local region near contact line and area fractions in the vicinity of contact line. They also proposed that the area inside the contact line affects the total energy of the system, but not the contact angle and the contact angle is independent of the absolute value of the total energy since the contact angle satisfying the lowest energy is not changed [194]. Some other attempts to calculate works from the lines had already been carried out before [116,183]. These points need to be clarified in the future. However, there is no adequate theory that connects the length, tortuousness, and continuity of three-phase contact line, or chemical composition on the contact line with the magnitude of contact angles measured on this surface at present.

5.4. Problems related with the width of the three-phase contact line

Gao and McCarthy [163] also pointed out that they were precise with their use of the word "lines", and specifically did not use the word "near" (to lines) and deliberately discounted areas. However, Bormashenko later used a new term "the area adjacent to the triple line" which is defined to be less than 100 nm in thickness to exert an influence on the apparent contact angle [174,176,196,197,215]. This approach may be criticized from two points of view; one is the reason of the necessity of using the controversial solid/liquid interfacial contact area concept again although we know that the solid surfaces cannot minimize their contacting areas; and the second point is the selection of the arbitrary value of the width of the three-phase contact line. The quantification of this width seems very difficult, if not impossible. When we examine Fig. 10, we can see that local contact angles may be larger or smaller than the apparent contact angles depending on the strength of the intermolecular interactions between solid and liquid. A precursor film may be present in some cases as seen for the case of the right image, but calculating its width along the length of the three-phase contact line seems to be impossible on a chemically heterogenous and rough surface. In addition, why do we force ourselves for such a task? A line can be used in calculus and physics much more easily if it has no width or thickness. It is clear that the term "the area adjacent to the triple line" cannot be assumed as a general

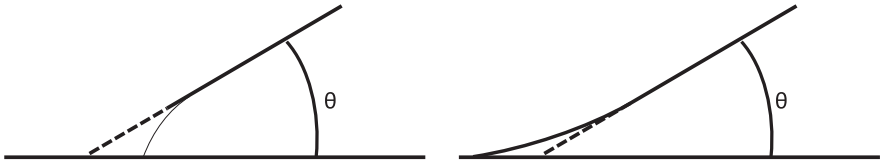

Fig. 10. Liquid/vapor interface deviates from the apparent contact angle near the three-phase contact line due to the presence or absence of long and short range molecular interactions.

approach in the contact angle field and can be used for special cases where the formation of the precursor film is important.

5.5. Effect of the length, density and shape of three-phase contact line to apparent contact angles

At present, there is no adequate theory on the effect of the length, density and shape of three-phase contact lines to apparent contact angles. However, we know some experimental facts, especially the effect of triple contact line on the receding contact angles: θ_r's are higher for the cases where the three-phase contact lines are longer and more contorted. For example, when the spacings between the posts were increased on micropatterned surfaces, then the receding contact angles also increased [153]. θ_r was influenced by the contact line distortion and depended on the relative fraction of the contact line [189]. Regarding to the receding movement of a drop, the discontinuous contact line cannot recede across the post tops and must disjoin from entire post tops in concerted events in order to move the contact line from a pinned position because the droplet is at a very high receding contact angle value ($\theta_r = 156^\circ$) on the post and the neighbor post tops exhibit only a low receding contact angle value ($\theta_r = 103^\circ$) [157]. The force with which the meniscus is pinned on an ensemble of defects was not the only factor that determines the contact angle for certain roughness geometries, but the process of contacting with the next row of roughness features was also important [164]. The events happening during the advancement of a droplet is different than that of a receding droplet and the discontinuous contact line does not move during drop advancement on a micro-patterned surface but, instead, sections of the liquid–vapor interface descend onto the next posts [157]. These findings are important to understand the physical mechanism of droplet rolling and pinning on a micro-patterned surface.

Meanwhile, Extrand developed a new approach on the contact line density criterion which is successful to estimate the suspension or collapse of liquid drops on patterned rough surfaces [154–156]. Although, it is original and useful, this approach takes into account of the solid/liquid interactions of all the asperities beneath the droplet through the asperity perimeters, however it is better to count only the solid/liquid interactions for the asperities present on the three-phase contact line of drop on the solid alone. We know that this task seems very difficult especially when the asperities are small and having sharp edges and this point awaiting to be solved by a new approach in the future.

5.6. Validity of the Wenzel equation

Wenzel equation was proven to be incorrect by Gao and McCarthy experimentally [13] and was found to be invalid for the majority of publications investigating its use [73,114,161,164,166,177]. Data of eight papers published from 2000 to 2008 was used where water drops sit on micro-patterned superhydrophobic surfaces containing both square and cylindrical pillars and the contact angle results of 166 micro-patterned samples were evaluated by applying a simple test method using Wenzel roughness factor, pattern areas and reported contact angles and the use of the Wenzel equation was found to be wrong for most of the samples and the deviations from the Wenzel theory were also high, and finally it was concluded that the Wenzel equation cannot be used for superhydrophobic surfaces other than a few exceptions [114]. It is interesting to note that, since the experimental surface area determination was a difficult task in the old days, some comments in some papers on surface roughness was very inadequate: Johnson and Dettre prepared rough surfaces by spraying paraffin and fluorocarbon wax onto glass slides and these surfaces were made progressively smoother by heating in an oven. They stated that the theoretical derivation for an idealized rough surface agrees well with that of real surfaces. However, the reasoning for this conclusion is questionable because they did not measure the roughness factor of their samples and reported only the number of heat treatments (!) in their plots [73]. In conclusion, Wenzel equation must be abandoned and "Wenzel state" term can be exchanged with another term such as "complete liquid/solid contact state" or any other in order to prevent giving the feel of the Wenzel equation as a valid one, to the newcomers to the contact angle field.

5.7. Validity of the Cassie equation

Initially, we must discriminate between the area based original Cassie's equation [Eqs. (15)–(17)] and the other modified Cassie equations. Original contact area based Cassie's equation was proven to be incorrect by Extrand [12] and Gao–McCarthy experimentally [13] and was found to be invalid according to many publications investigating its use [114,157,158,169,172,173,177,181,187,190,191]. Data of eight papers containing both square and cylindrical pillars and the contact angle results of 166 micro-patterned samples were evaluated by applying a simple test method using Cassie area fraction factors and reported contact angles and it was reported that large deviations of experimental water contact angles were found from the values calculated when the original Cassie equation is applied and 65% of the samples containing cylindrical pillars and 44% of the samples containing square pillars did not fit with the Cassie equation, indicating that the Cassie approach should be applied to superhydrophobic surfaces with caution [114].

In reality, Cassie's equation is a standard mixing equation of the physical chemistry when more than one components are present and the area fractions of Cassie (f_i) may be replaced with other quantities such as density of three-phase contact line and other similarly selected properties. Then the modified form of Cassie's equation may be useful to describe the effects arising from each component to the solid surface which are determined by contact angles. For example, the area fraction factors were replaced by the local line fraction factors along the triple phase boundary line and the new "Cassie on line" approach fitted the experimental data remarkably well [169,170,229].

6. Conclusions and perspectives

In this review, we presented the views on the dependence of apparent contact angles on liquid/solid contact area beneath the drop or three-phase contact line. We summarized the important points of the published articles of both the three-phase contact line and interfacial contact area approach defenders after presenting a brief history of the contact angles and their measurement methods. We stressed the experimental importance of contact angles both in academia and industry and suggested that new contact angle types can be offered by surface scientists as long as these can be measurable, and the related novel theories can be testable by the experimentalists.

It was found that much of the data in the literature are inconsistent with the Wenzel and Cassie theories, and the experiments designed to test the theories by Extrand in 2003 and Gao and McCarthy in 2007 and 2009 have disproved them. It is concluded that advancing, receding contact angles, and contact angle hysteresis of rough and chemically heterogeneous surfaces are determined by interactions of the liquid and the solid at the three-phase contact line alone and the interfacial area within the contact perimeter is irrelevant. Consequently, the well-known Wenzel (1934) and Cassie (1945) equations which have been used for long time and were derived by using the liquid/solid contact area approach should be invalid and should be abandoned. However, it is possible that "modified forms" of Cassie's equations can be used in the future since it resembles to the standard mixing equations of the physical chemistry and can be applied if the fractions of the triple line on different parts of a heterogeneous surface can be experimentally determined. On the other hand, there is a problem with the use of Cassie and Wenzel "state" terms. "Cassie state" describes the drops suspended on top of roughness features and "Wenzel state" drops impaled on roughness features. At present, these terms are the words that have evolved in the language to give visual insight for the scientists that encounters with these issues and used in many publications. Although these terms should also be left in strict scientific terms after Wenzel and Cassie equations are abandoned, it would be difficult to disuse them rapidly in the contact angle field and we will see the persistence of these terms in the contact angle literature in the future.

We related the inconsistencies of the liquid/solid contact area based equations to the surface area minimization problems of solids. The solid molecules at the interface are not mobile and solid surfaces cannot spontaneously contract to minimize their surface area and a non-equilibrium surface structure forms. Thus, surface tension $\neq$ the surface free energy for solids, and the laws of capillarity of liquids cannot be applied to solids. This is the main reason of the invalidity of contact area based Wenzel and Cassie's equations. However, a local equilibrium forms between a solid and an adjacent liquid phase at the three-phase contact line (even though non-equilibrium in larger sense) in terms of van de Waals, polar and hydrogen bonding interactions. Unfortunately, we also do not know the extent of mobility of the liquid molecules at the solid–liquid interphase with the effect of solid molecules on the surface and contact angle measurements reflect some part of this information too.

Work of adhesion can be calculated from contact lines by using forces and distance and some scientist already carried this approach before. However, at present, there is no adequate theory that connects the length, tortuousness, and continuity of three-phase contact line, or chemical composition on the contact line with the magnitude of contact angles measured on this surface and this is an important field awaiting the contribution of both experimentalists and theoreticians.

We also checked the validity of the presence of the width of the three-phase contact line since a new concept named "the area adjacent to the triple line" was in use in the literature in previous years. We criticized this approach from two points of view; one is the unknown reason of the necessity of re-creating the controversial solid/liquid contact area concept again, since we know that the solid surfaces cannot minimize their contacting areas; and secondly, the selection of the arbitrary value of the width of the three-phase contact line seems to be very difficult task and unnecessary. We prefer to use the three-phase contact line concept having no width (or any other dimensions) instead of "the area adjacent to the triple line" concept for all the general contact angle cases, unless for the special cases where the formation of the precursor film on the solid surface is important.

We also pointed out that there is no adequate theory at present, on the effect of the length, density and shape of three-phase contact lines to apparent contact angles although we know the general trends affecting especially receding contact angles. Although these experimental findings are important to understand the physical mechanism of droplet rolling and pinning on a micro-patterned surface, we need new models to explain these relationships and this field also awaiting the contribution of both contact angle experimentalists and theoreticians.

Appendix A. List of acronyms and abbreviations

θ	contact angle
θ_e	equilibrium contact angle
θ_a	advancing contact angle
θ_r	receding contact angle
$\mathrm{CAH} \equiv \theta_a - \theta_r$	contact angle hysteresis
θ_e^r	equilibrium contact angle on a rough surface
θ_e^s	equilibrium contact angle on a flat surface
γ_{LV}	interfacial tensions between liquid and vapor
γ_{SL}	interfacial tensions between solid and liquid
γ_{SV}	interfacial tension between solid and vapor
γ_{S^o}	solid surface tension under vacuum
γ_c	critical surface tension of a solid
h	height of a drop
r_b	base radius of a drop
R	radius of the spherical drop
A_{SL}	solid/liquid contact area
A_{LV}	liquid/vapor contact area
A^r	actual area of liquid/solid contact
A^s	plan area of liquid/solid contact
V	volume of drop
G	Gibbs free energy
W_{SL}^a	work of adhesion between solid and liquid
W_c	work of cohesion

r^W	Wenzel geometric roughness factor (the ratio of actual area to the plan area)
f_1	area fraction of component 1 on a composite surface
f_2	area fraction of component 2 on a composite surface
f_S	area fraction of the solid component on a solid/air composite surface
a	capillary constant of a liquid
k	spring constant of the contact line for localized perturbations
ρ_L	liquid density
g	earth's gravity
π_e	equilibrium film pressure (or spreading pressure)
ζ_{SL}	superficial interfacial tension between solid and liquid
β	a constant in Zisman's equation, Eq. (18)
ψ	a constant in Neumann's equation, Eq. (30)
γ_{SV}^d	dispersion component of interfacial free energy between solid and vapor
γ_{LV}^d	dispersion component of interfacial free energy between liquid and vapor
γ_{SV}^p	polar component of interfacial free energy between solid and vapor
γ_{LV}^p	polar component of interfacial free energy between liquid and vapor
γ_{SV}^{Tot}	total interfacial free energy between solid and vapor
γ_{LV}^{Tot}	total interfacial free energy between liquid and vapor
γ_{SL}^{LW}	Lifshitz–van der Waals component of interfacial free energy between solid and liquid
γ_S^{LW}	Lifshitz–van der Waals component of surface free energy of solid
γ_L^{LW}	Lifshitz–van der Waals component of surface free energy of liquid
γ_{SL}^{AB}	acid–base component of interfacial free energy between solid and liquid
γ_S^{AB}	acid–base component of surface free energy of solid
γ_L^{AB}	acid–base component of surface free energy of liquid
γ_S^+	Lewis acid component of solid surface tension
γ_S^-	Lewis base component of solid surface tension
γ_L^+	Lewis acid component of liquid surface tension
γ_L^-	Lewis base component of liquid surface tension
γ_{SLV}	line tension
γ_{SLV}^*	pseudo-line tension
K_{gs}	geodesic curvature of the three-phase contact line
Λ	contact line density
p	length of the asperity perimeter per unit area
ζ	area density of asperities
κ	stiffness constant
λ	displacement parameter
$w(L)$	root-mean-square (rms) width
L	length of triple line

References

[1] N.K. Adam, The Physics and Chemistry of Surfaces, Dover Publications Inc., New York, 1968.
[2] P.G. de Gennes, F.B. Wyart, D. Quere, Capillarity and Wetting Phenomena: Drops, Bubles, Pearls, Waves, Springer, New York, 2004.
[3] H.J. Butt, K. Graf, M. Kappl, Physics and Chemistry of Interfaces, Wiley-VCH, Weinheim, 2003.
[4] H.Y. Erbil, Surface Chemistry of Solid and Liquid Interfaces, Blackwell Publishing, Oxford, 2006.
[5] E.Y. Bormashenko, Wetting of Real Surfaces, De Gruyter, Berlin, 2013.
[6] T. Young, Philos. Trans. R. Soc. Lond. 95 (1805) 65–87.
[7] M.A. Dupré, Théorie Mécanique de la Chaleur (Chapter 9), Gauthier-Villars, Paris, 1869.
[8] Lord Rayleigh, Philos. Mag. 30 (1890)(pp. 285–298, 456–475).
[9] L. Boltzmann, Pogg. Ann. 141 (1870) 582–590.
[10] W. Thompson, Proc. R. Inst. 11 (1886) 483–507.
[11] D.C. Pease, J. Phys. Chem. 49 (1945) 107–110.
[12] C.W. Extrand, Langmuir 19 (2003) 3793–3896.
[13] L. Gao, T.J. McCarthy, Langmuir 23 (2007) 3762–3765.
[14] R.N. Wenzel, Ind. Eng. Chem. 28 (1936) 988–994.
[15] R.N. Wenzel, J. Phys. Colloid Chem. 53 (1949) 1466–1467.
[16] A.B.D. Cassie, S. Baxter, Trans. Faraday Soc. 40 (1944) 546–551.
[17] A.B.D. Cassie, Discuss. Faraday Soc. 3 (1948) 11–16.
[18] R.J. Good, J. Adhes. Sci. Technol. 6 (1992) 1269–1302.
[19] A.M. Worthington, R. Soc. Lond. 32 (1881) 362–377.
[20] F. Guthrie, Proc. R. Soc. Lond. 13 (1864) 444–483.
[21] G.H. Quincke, Wied. Ann. 2 (1877) 145;
G.H. Quincke, Wied. Ann. 27 (1886) 219;
G.H. Quincke, Wied. Ann. 52 (1894) 1;
G.H. Quincke, Wied. Ann. 61 (1897) 257;
G.H. Quincke, Wied. Ann. 64 (1898) 618.
[22] A.K. Huntington, Trans. Faraday Soc. 1 (1906) 345–355.
[23] C.H. Bosanquet, H. Hartley, Philos. Mag. 42 (1921) 456–462.
[24] N.K. Adam, G. Jessop, J. Chem. Soc. 127 (1925) 1863–1868.
[25] A.H. Nietz, J. Phys. Chem. 32 (1928) 255–269.
[26] E.L. Green, J. Phys. Chem. 33 (1929) 921–935.
[27] H.L. Sulman, Trans. Inst. Min. Metall. 39 (1920) 44–204.
[28] I.W. Wark, J. Phys. Chem. 37 (1933) 623–644.
[29] A.F. Taggart, T.C. Taylor, C.R. Ince, Am. Inst. Min. Met. Eng. Tech. Publ. 204 (1929) 1–17.
[30] I.W.C. O'Kane, W.A. Westgate, L.C. Glover, P.R. Lowry, New Hamps. Agric. Exp. Stn. Tech. Bull. 39 (1930) 1–44.
[31] F.E. Bartell, E.J. Merrill, J. Phys. Chem. Soc. 55 (1932) 1178–1190.
[32] F.E. Bartell, G.B. Hatch, J. Phys. Chem. 39 (1935) 11–24.
[33] G.L. Mack, J. Phys. Chem. 40 (1936) 159–167.
[34] E. Kneen, W.W. Benton, J. Phys. Chem. 41 (1937) 1195–1203.
[35] D.H. Bangham, R.I. Razouk, Trans. Faraday Soc. 33 (1937) 1459–1472.
[36] R.J. Good, J. Colloid Interface Sci. 52 (1975) 308–313.
[37] F.M. Fowkes, D.C. McCarthy, M.A. Moustafa, J. Colloid Interface Sci. 78 (1980) 200–206.
[38] G.E. Boyd, H.K. Livingston, J. Am. Chem. Soc. 64 (1942) 2383–2388.
[39] W.D. Harkins, H.K. Livingston, J. Chem. Phys. 10 (1942) 342–356.
[40] H.K. Livingston, J. Phys. Chem. 48 (1944) 120–124.
[41] N.K. Adam, H.K. Livingston, Nature 182 (1958) 128.
[42] J.R. Dann, J. Colloid Interface Sci. 32 (1970) 302–319.
[43] M.E. Tadros, P. Hu, A.W. Adamson, J. Colloid Interface Sci. 49 (1974) 184–195.
[44] J. Tse, A.W. Adamson, J. Colloid Interface Sci. 72 (1979) 515–523.
[45] H.J. Busscher, G.A.M. Kip, A. Van Silfhout, J.J. Arends, J. Colloid Interface Sci. 114 (1986) 307–313.
[46] M.E. Schrader, Langmuir 9 (1993) 1959–1961.
[47] L.J.M. Schlangen, L.K. Koopal, M.A. Cohen-Stuart, J. Lyklema, Colloids Surf. 89 (1994) 157–167.
[48] H.Y. Erbil, Langmuir 10 (1994) 2006–2009.
[49] L.H. Lee, J. Colloid Interface Sci. 214 (1999) 64–78.
[50] J. Skvarla, M. Nagy, J. Phys. Chem. C 115 (2011) 18670–18682.
[51] R.E. Johnson, R.H. Dettre, J. Phys. Chem. 68 (1964) 1744–1750.
[52] C.W. Extrand, Y. Kumagai, J. Colloid Interface Sci. 191 (1997) 378–383.
[53] W.C. Bigelow, D.L. Pickett, W.A. Zisman, J. Colloid Sci. 1 (1946) 513–538.
[54] H.W. Fox, W.A. Zisman, J. Colloid Sci. 5 (1950) 514–531.

[55] H.W. Fox, W.A. Zisman, J. Colloid Sci. 7 (1952) 109–121.
[56] E.G. Shafrin, W.A. Zisman, J. Colloid Sci. 7 (1952) 166–177.
[57] A.H. Ellison, W.A. Zisman, J. Phys. Chem. 58 (1954) 503–506.
[58] T. Fort, H.T. Patterson, J. Colloid Sci. 18 (1963) 217–222.
[59] A.W. Neumann, R.J. Good, in: R.J. Good, R.R. Stromberg (Eds.), Surface and Colloid Science, vol. 11, Plenum Press, New York, 1979.
[60] R.E. Johnson, J. Phys. Chem. 63 (1959) 1655–1659.
[61] Contact Angle, Wettability, and Adhesion, Advanced Chemical Series, in: F.M. Fowkes (Ed.), American Chemical Society, Washington DC, 1964.
[62] A.W. Adamson, I. Ling, Contact Angle, Wettability, and Adhesion, Advanced Chemical Series, in: F.M. Fowkes (Ed.), American Chemical Society, Washington DC, 1964, pp. 57–73.
[63] C. Herring, Phys. Rev. 82 (1951) 87–93.
[64] J.J. Bikerman, Physical Surfaces, Academic Press, New York, 1970, p. 240–242.
[65] A.W. Neumann, R.J. Good, J. Colloid Interface Sci. 38 (1972) 341–358.
[66] J.D. Eick, R.J. Good, A.W. Neumann, J. Colloid Interface Sci. 53 (1975) 235–248.
[67] G.J. Jameson, M.C.G. del Cerro, J. Chem. Faraday Trans. 72 (1976) 883–895.
[68] J.J. Bikerman, J. Colloid Sci. 5 (1950) 349–359.
[69] R.J. Good, J. Am. Chem. Soc. 74 (1952) 5041–5042.
[70] F.E. Bartell, J.W. Shepard, J. Phys. Chem. 57 (1953) 211–215.
[71] F.E. Bartell, J.W. Shepard, J. Phys. Chem. 57 (1953) 455–458.
[72] R.E. Johnson, R.H. Dettre, Contact Angle, Wettability, and Adhesion, Advanced Chemical Series, in: F.M. Fowkes (Ed.), American Chemical Society, Washington DC, 1964, pp. 112–135.
[73] R.E. Johnson, R.H. Dettre, Contact Angle, Wettability, and Adhesion, Advanced Chemical Series, in: F.M. Fowkes (Ed.), American Chemical Society, Washington DC, 1964, pp. 136–144.
[74] R.E. Johnson, R.H. Dettre, J. Phys. Chem. 69 (1965) 1507–1515.
[75] C. Huh, S.G. Mason, J. Colloid Interface Sci. 60 (1977) 11–38.
[76] L.W. Schwartz, S. Garoff, Langmuir 1 (1985) 219–230.
[77] J.N. Israelachvili, M.L. Gee, Langmuir 5 (1989) 288–289.
[78] A. Marmur, J. Colloid Interface Sci. 168 (1994) 40–46.
[79] P.S. Swain, R. Lipowsky, Langmuir 14 (1998) 6772–6780.
[80] D.N. Staicopolus, J. Colloid Interface Sci. 17 (1962) 439–447.
[81] L.R. Fisher, J. Colloid Interface Sci. 72 (1979) 200–205.
[82] G.W. Longman, R.P. Palmer, J. Colloid Interface Sci. 29 (1967) 185–188.
[83] W. Funke, G.E.H. Hellwig, A.W. Neumann, Angew. Makromol. Chem. 8 (1969) 185–193.
[84] A.W. Neumann, Adv. Colloid Interface Sci. 4 (1974) 105–191.
[85] I. Langmuir, V.J. Schaeffer, J. Am. Chem. Soc. 59 (1937) 2400–2414.
[86] C.J. Budziak, A.W. Neumann, Colloids Surf. 43 (1990) 279–293.
[87] D.Y. Kwok, C.J. Budziak, A.W. Neumann, J. Colloid Interface Sci. 173 (1995) 143–150.
[88] A.F. Taggart, T.C. Taylor, C.R. Ince, Trans. Am. Inst. Min. Met. Eng. 87 (1930) 285–386.
[89] Y. Rotenberg, L. Boruvka, A.W. Neumann, J. Colloid Interface Sci. 93 (1983) 169–183.
[90] J.K. Spelt, Y. Rotenberg, D.R. Absolom, A.W. Neumann, Colloids Surf. 24 (1987) 127–137.
[91] P. Cheng, D. Li, L. Boruvka, Y. Rotenberg, A.W. Neumann, Colloids Surf. 43 (1990) 151–167.
[92] O.I. del Rio, A.W. Neumann, J. Colloid Interface Sci. 196 (1997) 136–147.
[93] J.M. Alvarez, A. Amirfazli, A.W. Neumann, Colloids Surf. A: Physicochem. Eng. Asp. 206 (2002) 485–495.
[94] M.A. Rodriguez-Valverde, M.A. Cabrerizo-Vilchez, P. Rosales-Lopez, A. Paez-Duenas, R. Hidalgo-Alvarez, Colloids Surf. A: Physicochem. Eng. Asp. 156 (1999) 163–176.
[95] R.L. Bendure, J. Colloid Interface Sci. 42 (1973) 137–144.
[96] P. Somasundaran, M. Danitz, K.J. Mysels, J. Colloid Interface Sci. 48 (1974) 410–416.
[97] T.S. Jiang, S.G. Oh, J.C. Slattery, J. Colloid Interface Sci. 69 (1979) 74–77.
[98] Y. Uyama, H. Inoue, K. Ito, A. Kishida, Y. Ikada, J. Colloid Interface Sci. 141 (1991) 275–279.
[99] L.M. Lander, L.M. Siewıerskı, W.J. Brittain, E.A. Vogler, Langmuir 9 (1993) 2237–2239.
[100] M. Miyama, Y.X. Yang, T. Yasuda, T. Okuno, H.K. Yasuda, Langmuir 13 (1997) 5494–5503.
[101] E. Rame, J. Colloid Interface Sci. 185 (1997) 245–251.
[102] A. Krishnan, Y.H. Liu, P. Cha, R. Woodward, D. Allara, E.A. Vogler, Colloids Surf. B: Biointerfaces 43 (2005) 95–98.
[103] M. Strobel, C.S. Lyons, Plasma Processes Polym. 8 (2011) 8–13.
[104] H.Y. Erbil, G. McHale, S.M. Rowan, M.I. Newton, Langmuir 15 (1999) 7378–7385.
[105] G. McHale, H.Y. Erbil, M.I. Newton, S. Natterer, Langmuir 17 (2001) 6995–6998.
[106] M.A. Fortes, J. Colloid Interface Sci. 100 (1984) 17–26.
[107] A. Carre, J.C. Gastel, M.E.R. Shanahan, Nature 379 (1996) 432–434.
[108] C.W. Extrand, Y. Kumagai, J. Colloid Interface Sci. 184 (1996) 191–200.
[109] R. Pericet-Camara, A. Best, H.J. Butt, E. Bonaccurso, Langmuir 24 (2008) 10565–10568.
[110] R. Pericet-Camara, G.K. Auernhammer, K. Koynov, S. Lorenzoni, R. Raiteri, E. Bonaccurso, Soft Matter 5 (2009) 3611–3617.
[111] Y.S. Yu, Y.P. Zhao, J. Colloid Interface Sci. 339 (2009) 489–494.
[112] E.R. Jerison, Y. Xu, L.A. Wilen, E.R. Dufresne, Phys. Rev. Lett. 106 (2011) 186103.
[113] J.D. Andrade, L.M. Smith, D.E. Gregonis, in: J.D. Andrade (Ed.), Surface and Interfacial Aspects of Biomedical Polymers, vol. 1, Plenum Press, New York, 1985, pp. 249–292.
[114] H.Y. Erbil, C.E. Cansoy, Langmuir 25 (2009) 14135–14145.
[115] M.E.R. Shanahan, Langmuir 11 (1995) 1041–1043.
[116] J.F. Joanny, P.G. de Gennes, J. Chem. Phys. 81 (1984) 552–562.
[117] H.B. Eral, D.J.C.M. 't Mannetje, J.M. Oh, Colloid Polym. Sci. 291 (2013) 247–260.
[118] E. Bormashenko, Y. Bormashenko, G. Whyman, R. Pogreb, A. Musin, R. Jager, Z. Barkay, Langmuir 24 (2008) 4020–4025.
[119] H.W. Fox, W.A. Zisman, J. Colloid Sci. 7 (1952) 428–442.
[120] A.W. Zisman, Contact Angle, Wettability, and Adhesion, Advanced Chemical Series, in: F.M. Fowkes (Ed.), American Chemical Society, Washington DC, 1964, pp. 1–51.
[121] F.M. Fowkes, J. Phys. Chem. 66 (1962) 382.
[122] F.M. Fowkes, Ind. Eng. Chem. 56 (1964) 40–52.
[123] F.M. Fowkes, J. Colloid Interface Sci. 28 (1968) 493–505.
[124] D.K. Owens, R.C. Wendt, J. Appl. Polym. Sci. 13 (1969) 1741–1747.
[125] H.Y. Erbil, J. Appl. Polym. Sci. 33 (1987) 1397–1412.
[126] D.H. Kaelble, J. Adhes. 2 (1970) 66–81.
[127] H.Y. Erbil, R.A. Meric, Colloids Surf. 33 (1988) 85–97.
[128] H.Y. Erbil, R.A. Meric, Angew. Makromol. Chem. 163 (1988) 101–114.
[129] J.M. Park, J.H. Kim, J. Colloid Interface Sci. 168 (1994) 103–110.
[130] F.M. Fowkes, F.L. Riddle, W.E. Pastore, A.A. Weber, Colloids Surf. 43 (1990) 367–387.
[131] A.W. Neumann, J.K. Spelt, R.P. Smith, D.W. Francis, Y. Rotenberg, D.R. Absolom, J. Colloid Interface Sci. 102 (1984) 278–284.
[132] D. Li, A.W. Neumann, Adv. Colloid Interface Sci. 39 (1992) 299–345.
[133] D. Li, A.W. Neumann, J. Colloid Interface Sci. 148 (1992) 190–200.
[134] I.D. Morrison, Langmuir 5 (1989) 540–543.
[135] M. Morra, E. Occhiello, F. Garbassi, Adv. Colloid Interface Sci. 32 (1990) 79–116.
[136] L.H. Lee, Langmuir 9 (1993) 1898–1905.
[137] L.H. Lee, Langmuir 10 (1994) 3368.
[138] C.J. van Oss, M.K. Chaudhury, R.J. Good, Chem. Rev. 88 (1988) 927–941.
[139] C.J. van Oss, Interfacial Forces in Aqueous Media, Marcel Dekker, New York, 1994.
[140] P.A. Small, J. Appl. Chem. 3 (1953) 71–80.
[141] H.Y. Erbil, Polymer 37 (1996) 5483–5491.
[142] R.J. Good, M.N. Koo, J. Colloid Interface Sci. 71 (1979) 283–292.
[143] W.J. Herzberg, J.E. Marian, J. Colloid Interface Sci. 33 (1970) 161–163.

[144] B.A. Pethica, J. Colloid Interface Sci. 62 (1977) 567–569.
[145] J. Gaydos, A.W. Neumann, J. Colloid Interface Sci. 120 (1987) 76–86.
[146] M. Yekta-Fard, A.B. Ponter, J. Colloid Interface Sci. 126 (1988) 134–140.
[147] L. Boruvka, J. Gaydos, A.W. Neumann, Colloids Surf. 43 (1990) 307–326.
[148] J. Drelich, J.D. Miller, J. Hupka, J. Colloid Interface Sci. 155 (1993) 379–385.
[149] J. Drelich, J.D. Miller, A. Kumar, G.M. Whitesides, Colloids Surf. 93 (1994) 1–13.
[150] J. Drelich, J.D. Miller, J. Hupka, J. Colloid Interface Sci. 164 (1994) 252–259.
[151] A.W. Adamson, A.P. Gast, Physical Chemistry of Surfaces, 6th ed., John Wiley & Sons, Inc., New York, 1997.
[152] J.E. McNutt, G.M. Andes, J. Chem. Phys. 30 (1959) 1300–1303.
[153] D. Oner, T.J. McCarthy, Langmuir 16 (2000) 7777–7782.
[154] C.W. Extrand, Langmuir 18 (2002) 7991–7999.
[155] C.W. Extrand, Langmuir 20 (2004) 5013–5018.
[156] C.W. Extrand, Langmuir 22 (2006) 1711–1714.
[157] L. Gao, T.J. McCarthy, Langmuir 22 (2006) 2966–2967.
[158] L. Gao, T.J. McCarthy, Langmuir 22 (2006) 6234–6237.
[159] E. Bormashenko, Y. Bormashenko, T. Stein, G. Whyman, R. Pogreb, Langmuir 23 (2007) 4378–4382.
[160] E. Bormashenko, R. Pogreb, G. Whyman, M. Erlich, Langmuir 23 (2007) 65016503.
[161] C.W. Extrand, S.I. Moon, P. Hall, Langmuir 23 (2007) 8882–8890.
[162] J.Y. Chung, J.P. Youngblood, C.M. Stafford, Soft Matter 3 (2007) 1163–1169.
[163] L. Gao, T.J. McCarthy, Langmuir 23 (2007) 13243.
[164] C. Dorrer, J. Rühe, Langmuir 24 (2008) 1959–1964.
[165] S. Vedantam, M.V. Panchagnula, J. Colloid Interface Sci. 321 (2008) 393–400.
[166] D.M. Spori, T. Drobek, S. Zürcher, M. Ochsner, C. Sprecher, A. Mühlebach, N.D. Spencer, Langmuir 24 (2008) 5411–5417.
[167] K. Yamamoto, S. Ogata, J. Colloid Interface Sci. 326 (2008) 471–477.
[168] G. Fang, W. Li, X. Wang, G. Qiao, Langmuir 24 (2008) 11651–11660.
[169] S.T. Larsen, R. Taboryski, Langmuir 25 (2009) 1282–1284.
[170] T. Cubaud, M.M. Fermigier, J. Colloid Interface Sci. 269 (2004) 171–177.
[171] C.W. Yang, P.F. Hao, F. He, Chin. Sci. Bull. 54 (2009) 727–731.
[172] L. Gao, T.J. McCarthy, Langmuir 25 (2009) 7249–7255.
[173] L. Gao, T.J. McCarthy, Langmuir 25 (2009) 14105–14115.
[174] E. Bormashenko, Langmuir 25 (2009) 10451–10454.
[175] A.H. Cannon, W.P. King, J. Vac. Sci. Technol. B 28 (2010) L21–L24.
[176] E. Bormashenko, Philos. Trans. R. Soc. A – Math. Phys. Eng. Sci. 368 (2010) 4695–4711.
[177] C.W. Yang, F. He, P.F. Hao, Sci. China Chem. 53 (2010) 912–916.
[178] J. Liu, Y. Mei, R. Xia, Langmuir 27 (2011) 196–200.
[179] D.F. Cheng, T.J. McCarthy, Langmuir 27 (2011) 36933697.
[180] T. Furuta, M. Sakai, T. Isobe, S. Matsushita, A. Nakajima, Langmuir 27 (2011) 7307–7313.
[181] C.E. Cansoy, H.Y. Erbil, O. Akar, T. Akin, Colloids Surf. A: Physicochem. Eng. Asp. 386 (2011) 116–124.
[182] N.J. Shirtcliffe, G. McHale, M.I. Newton, J. Polym. Sci. Part B – Polym. Phys. 49 (2011) 1203–1217.
[183] A.L. Dubov, J. Teisseire, E. Barthel, Europhys. Lett. 97 (2012) 26003.
[184] G. McHale, S. Aqil, N.J. Shirtcliffe, M.I. Newton, H.Y. Erbil, Langmuir 21 (2005) 11053–11060.
[185] A. Susarrey-Arce, A.G. Marin, H. Nair, L. Lefferts, J.G.E. Gardeniers, D. Lohse, A. van Houselt, Soft Matter 8 (2012) 9765–9770.
[186] H.Y. Erbil, Adv. Colloid Interface Sci. 170 (2012) 67–86.
[187] P.M. Hansson, Y. Hormozan, B.D. Brandner, J. Linnros, P.M. Claesson, A. Swerin, J. Schoelkopf, P.A.C. Gane, E. Thormann, Langmuir 28 (2012) 11121–11130.
[188] C.W. Extrand, S.I. Moon, Langmuir 28 (2012) 15629–15633.
[189] R. Raj, R. Enright, Y. Zhu, S. Adera, E.N. Wang, Langmuir 28 (2012) 15777–15788.
[190] C. Lv, P. Hao, Langmuir 28 (2012) 16958–16965.
[191] N. Kashaninejad, W.K. Chan, N.-T. Nguyen, Langmuir 28 (2012) 4793–4799.
[192] N. Kashaninejad, N.T. Nguyen, W.K. Chan, Soft Matter 9 (2013) 527–535.
[193] P. Olin, S.B. Lindström, T. Pettersson, L. Wågberg, Langmuir 29 (2013) 9079–9089.
[194] K. Seo, M. Kim, D.H. Kim, Korea–Aust. Rheol. J. 25 (2013) 175–180.
[195] M. Katariya, T.W. Ng, J. Phys. D: Appl. Phys. 46 (2013) 345302.
[196] E. Bormashenko, A. Musin, G. Whyman, Z. Barkay, M. Zinigrad, Langmuir 29 (2013) 14163–14167.
[197] E. Bormashenko, Y. Bormashenko, J. Phys. Chem. C 117 (2013) 19552–19557.
[198] S.F. Chini, V. Bertola, A. Amirfazli, Colloids Surf. A: Physicochem. Eng. Asp. 436 (2013) 425.
[199] A. Gauthier, M. Rivetti, J. Teisseire, E. Barthel, Langmuir 30 (2014) 1544–1549.
[200] A. Marmur, Langmuir 19 (2003) 8343–8348.
[201] A. Marmur, Soft Matter 2 (2006) 12–17.
[202] J. Bico, C. Marzolin, D. Quere, Europhys. Lett. 47 (1999) 220–226.
[203] B. He, N.A. Patankar, J. Lee, Langmuir 19 (2003) 4999–5003.
[204] D. Quere, A. Lafuma, J. Bico, Nanotechnology 14 (2003) 1109–1112.
[205] A. Lafuma, D. Quere, Nat. Mater. 2 (2003) 457–460.
[206] N.A. Patankar, Langmuir 20 (2004) 7097–7102.
[207] C. Dorrer, J. Rühe, Langmuir 23 (2007) 3820–3824.
[208] B. Bhusan, M. Nosonovsky, Y.C. Jung, J. R. Soc. Interface 4 (2007) 643–648.
[209] S. Wang, L. Jiang, Adv. Mater. 19 (2007) 3423–3424.
[210] M. Jin, X. Feng, L. Feng, T. Sun, J. Zhai, T. Li, L. Jiang, Adv. Mater. 17 (2005) 1977–1981.
[211] G. McHale, Langmuir 23 (2007) 8200–8205.
[212] M. Nosonovsky, Langmuir 23 (2007) 9919–9920.
[213] N. Anantharaju, M.V. Panchagnula, S. Vedantam, S. Neti, S. Tatic-Lucic, Langmuir 23 (2007) 11673–11676.
[214] M.V. Panchagnula, S. Vedantam, Langmuir 23 (2007) 13242.
[215] E. Bormashenko, Colloids Surf. A: Physicochem. Eng. Asp. 324 (2008) 47–50.
[216] G. Whyman, E. Bormashenko, T. Stein, Chem. Phys. Lett. 450 (2008) 355–359.
[217] M. Nosonovsky, B. Bhushan, Langmuir 24 (2008) 1525–1533.
[218] K.Y. Yeh, L.J. Chen, J.Y. Chang, Langmuir 24 (2008) 245–251.
[219] A. Marmur, Langmuir 24 (2008) 7573–7579.
[220] A. Marmur, Annu. Rev. Mater. Res. 39 (2009) 473–489.
[221] A. Marmur, E. Bittoun, Langmuir 25 (2009) 1277–1281.
[222] T.S. Meiron, A. Marmur, I.S. Saguy, J. Colloid Interface Sci. 274 (2004) 637–644.
[223] W. Choi, A. Tuteja, J.M. Mabry, R.E. Cohen, G.H. McKinley, J. Colloid Interface Sci. 339 (2009) 208–216.
[224] D.M. Spori, T. Drobek, S. Zürcher, N.D. Spencer, Langmuir 26 (2010) 9465–9473.
[225] Y. Kwon, S. Choi, N. Anantharaju, J. Lee, M.V. Panchagnula, N.A. Patankar, Langmuir 26 (2010) 17528–17531.
[226] A.J.B. Milne, A. Amirfazli, Adv. Colloid Interface Sci. 170 (2012) 48–55.
[227] I.O. Ucar, C.E. Cansoy, H.Y. Erbil, M.E. Pettitt, M.E. Callow, J.A. Callow, Biointerphases 5 (2010) 75–84.
[228] H.Y. Erbil, Colloid Polym. Sci. 291 (2013) 355–360.
[229] X. Xu, X. Wang, Colloid Polym. Sci. 291 (2013) 299–306.
[230] M. Oksuz, H.Y. Erbil, J. Phys. Chem. C 118 (2014) 9228–9238.
[231] C. Neto, D.R. Evans, E. Bonaccurso, H.J. Butt, V.S.J. Craig, Rep. Prog. Phys. 68 (2005) 2859–2897.
[232] N.A. Stelmashenko, J.P. Craven, A.M. Donald, E.M. Terentjev, B.L. Thiel, J. Microsc. 204 (2001) 172–183.
[233] M.P. Rossi, H.H. Ye, Y. Gogotsi, S. Babu, P. Ndungu, J.C. Bradley, Nano Lett. 4 (2004) 989–993.
[234] Y.T. Cheng, D.E. Rodak, A. Angelopoulos, T. Gacek, Appl. Phys. Lett. 87 (2005) 194112.
[235] M. Brugnara, C. Della Volpe, S. Siboni, D. Zeni, Scanning 28 (2006) 267–273.

[236] Y.C. Jung, B. Bhushan, J. Microsc. 229 (2008) 127–140.
[237] A. Jansson, A. Nafari, A. Sanz-Velasco, K. Svensson, S. Gustafsson, A.M. Hermansson, E. Olsson, Microsc. Microanal. 19 (2013) 30–37.
[238] M. Preuss, H.J. Butt, Langmuir 14 (1998) 3164–3174.
[239] R. Wang, L. Cong, M. Kido, Appl. Surf. Sci. 191 (2002) 74–84.
[240] A. Checco, P. Guenoun, J. Daillant, Phys. Rev. Lett. 91 (2003) 186101.
[241] A.V. Nguyen, J. Nalaskowski, J.D. Miller, J. Colloid Interface Sci. 262 (2003) 303–306.
[242] R. Seemann, M. Brinkmann, E.J. Kramer, F.F. Lange, R. Lipowsky, Proc. Natl. Acad. Sci. 102 (2005) 1848–1852.
[243] Y.C. Jung, B. Bhushan, Nanotechnology 17 (2006) 4970–4980.
[244] Y.C. Jung, B.J. Bhushan, Vac. Sci. Technol. A 26 (2008) 777.
[245] B. Bhushan, H. Lee, Faraday Discuss. 156 (2012) 235–241.
[246] D.G. Fischer, B. Ovryn, Opt. Lett. 25 (2000) 478–480.
[247] M. Sundberg, A. Mansson, S. Tagerud, J. Colloid Interface Sci. 313 (2007) 454–460.
[248] A. Dimitrov, P.A. Kralchevsky, A.D. Nikolov, D.T. Wasan, Colloids Surf. 47 (1990) 299–321.
[249] K.W. Stockelhuber, B. Radoev, H.J. Schulze, Colloids Surf. A 156 (1999) 323–333.
[250] A. Marchand, J.H. Weijs, J.H. Snoeijer, B. Andreotti, Am. J. Phys. 79 (2011) 999–1008.
[251] J.H. Snoeijer, B. Andreotti, Annu. Rev. Fluid Mech. 45 (2013) 269–292.